AFRL-HE-WP-TR-2003-0154

United States Air Force
Research Laboratory

DARPA

INVESTIGATIONS OF OPERATIONAL LIFETIME AND MODES OF FAILURE OF ORGANIC LIGHT EMITTING DEVICES

Stephen R. Forrest
PRINCETON UNIVERSITY
PRINCETON NJ 08544

Mark Thompson
UNIVERSITY OF SOUTHERN CALIFORNIA
LOS ANGELES CA 90089

Paul Barbara
UNIVERSITY OF TEXAS
AUSTIN TX 78712

Julia J. Brown
UNIVERSAL DISPLAY CORPORATION
EWING NJ 08618

FEBRUARY 2004

FINAL REPORT FOR THE PERIOD 1 JUNE 2001 TO 30 MAY 2003

Human Effectiveness Directorate
Warfighter Interface Division
2255 H Street
Wright-Patterson AFB OH 45433-7022

NOTICES

When US Government drawings, specifications, or other data are used for any purpose other than a definitely related Government procurement operation, the Government thereby incurs no responsibility nor any obligation whatsoever, and the fact that the Government may have formulated, furnished, or in any way supplied the said drawings, specifications, or other data, is not to be regarded by implication or otherwise, as in any manner licensing the holder or any other person or corporation, or conveying any rights or permission to manufacture, use, or sell any patented invention that may in any way be related thereto.

Please do not request copies of this report from the Air Force Research Laboratory. Additional copies may be purchased from:

National Technical Information Service
5285 Port Royal Road
Springfield, Virginia 22161

Federal Government agencies and their contractors registered with the Defense Technical Information Center should direct requests for copies of this report to:

Defense Technical Information Center
8725 John J. Kingman Road, Suite 0944
Ft. Belvoir, Virginia 22060-6218

TECHNICAL REVIEW AND APPROVAL

AFRL-HE-WP-TR-2003-0154

This report has been reviewed by the Office of Public Affairs (PA) and is releasable to the National Technical Information Service (NTIS). At NTIS, it will be available to the general public.

This technical report has been reviewed and is approved for publication.

FOR THE COMMANDER

//Signed//

BRIAN P. DONNELLY, Lt Col, USAF
Deputy Chief, Warfighter Interface Division
Air Force Research Laboratory

REPORT DOCUMENTATION PAGE

Form Approved
OMB No. 0704-0188

1. AGENCY USE ONLY (Leave blank)	2. REPORT DATE	3. REPORT TYPE AND DATES COVERED
	February 2004	Final Report 1 June 2001 - 30 May 2003

4. TITLE AND SUBTITLE

"Investigations of Operational Lifetime and Modes of Failure of Organic Light Emitting Devices"

5. FUNDING NUMBERS

C: MDA 972-01-1-0032
PE: 62708E
PR: H731
TA: 14
WU: 71841103

6. AUTHOR(S)

Stephen R. Forrest (a), Mark Thompson (b), Paul Barbara (c), Julia J. Brown (d)

7. PERFORMING ORGANIZATION NAME(S) AND ADDRESS(ES)

(a) Princeton University, Princeton NJ 08544
(b) University of Southern California, Los Angeles, CA 90089
(c) University of Texas, Austin TX 78712
(d) Universal Display Corporation, Ewing NJ 08618

8. PERFORMING ORGANIZATION

9. SPONSORING/MONITORING AGENCY NAME(S) AND ADDRESS(ES)

Air Force Research Laboratory (AFMC)
Human Effectiveness Directorate
Warfighter Interface Division
Air Force Materiel Command
Wright-Patterson AFB OH 45433-7022

10. SPONSORING/MONITORING

AFRL-HE-WP-TR-2003-0154

11. SUPPLEMENTARY NOTES

12a. DISTRIBUTION/AVAILABILITY STATEMENT

Approved for public release, distribution is unlimited.

12b. DISTRIBUTION CODE

13. ABSTRACT *(Maximum 200 words)*

Reliability limitations of organic light emitting devices (OLEDs) were explored in a joint effort project lead by Princeton University, with subcontracting efforts by the University of Southern California, the University of Texas and Universal Display Corporation. Methodologies and protocols for screening of device structures and materials were developed. Extended lifetimes of red, green and blue phosphorescent OLEDs were achieved. For example, lifetimes of over 50,000 hours were obtained for both red and green devices. Blue device lifetimes observed were still less than 1000 hours. This difference in blue lifetime was studied using through both photo- and electro-luminescence methods, and was determined to be due, in part, to the high energies needed to excite the blue lumophores, which results in charge imbalance in the emission layers of the OLEDs. Contact degradation was also studied at the microscopic scale using near-field scanning optical microscopy (NSOM) in concert with our transparent OLED structure (TOLED). It was found that defects introduced during processing are largely responsible for the formation and growth of dark spots.

14. SUBJECT TERMS

Organic light emitting devices (OLED) structures and materials, transparent OLED, TOLED, reliability, failure modes, dark spots, plastic flexible displays, organic vapor phase vacuum deposition, near-field scanning optical microscopy, NSOM, atomic force microscopy, AFM

15. NUMBER OF PAGES

85

16. PRICE CODE

17. SECURITY CLASSIFICATION OF REPORT	18. SECURITY CLASSIFICATION OF THIS PAGE	19. SECURITY CLASSIFICATION OF ABSTRACT	20. LIMITATION OF ABSTRACT
Unclassified	Unclassified	Unclassified	Unlimited

This page intentionally left blank.

CONTENTS

LIST OF FIGURE CAPTIONS.....iv
LIST OF TABLE CAPTIONS.....v
FOREWORD.....vi
PREFACE.....vii
ACKNOWLEDGEMENTS.....vii

1. SUMMARY.....1

2. INTRODUCTION.....2

3. METHODOLOGY AND RESULTS.....3
   3.1 Phosphorescent Blue Reliability.....3
      3.1.1 Photophysical Degradation.....4
      3.1.2 Lifetime.....8
      3.1.3 Hole Blocking Layer.....9
   3.2 Extrinsic Degradation of OLEDs.....10
   3.3 Singlet Oxygen Generation by Phosphor Dopants.....14
   3.4 Overcoating OLEDs to Retard Dark Spot Growth.....18
   3.5 NSOM Studies of OLED Failure.....19
   3.6 Electrophosphorescent Device Stability.....22
      3.6.1 Bottom-Emission PHOLEDs on Glass Substrates.....22
      3.6.2 Transparent Top-Emitting PHOLEDs on Glass Substrates.....27
      3.6.3 Bottom Emission PHOLEDs on Flexible Plastic Substrates.....30

4. DISCUSSION AND CONCLUSIONS.....33

5. RECOMMENDATIONS.....35

6. SYMBOLS, ABBREVIATIONS, AND ACRONYMS.....36

APPENDICES
A. LIST OF PATENTS.....40
B. LIST OF TECHNICAL JOURNAL PUBLICATIONS.....41
C. LIST OF PROFESSIONAL PERSONNEL.....42
D. LIST OF ADVANCED DEGREES AWARDED.....43
E. JUNE 11, 2003 FINAL REVIEW MATERIALS.....44

LIST OF FIGURE CAPTIONS

Figure 1(a-c): Types of organic light emitting diode (OLED) displays.....1

Figure 1(d): Schematic diagram of a simple, conventional OLED display device.....2

Figure 2: Photophysical decay of Firpic.....4

Figure 3: FIrpic spectra taken both prior to and following aging studies.....7

Figure 4: Controlled environment chamber.....11

Figure 5: Initial and final images of a device during degradation; line scans are shown at 20 min time intervals.....12

Figure 6: Dark spot growth rates.....12

Figure 7: Growth rates of dark pixels (left) and dark area (right).....13

Figure 8: C_{60} thickness dependence for dark spot growth in devices.....14

Figure 9: Structures of phosphor dopants used in $^1O_2$ generation study.....15

Figure 10: $^1O_2$ luminescence intensity (arbitrary units) vs. absorbance optical density at 355 nm for BT, BT-py and TPP.....17

Figure 11: Relative dark spot growth rates for various OLED overcoatings.....18

Figure 12: TOLED Structure.....20

Figure 13: Topographic image of the TOLED device.....20

Figure 14: NSOM experiment on dark spot formed by damage of electrode induced by an NSOM tip.....21

Figure 15: Extreme device damage that occurs when darks spots continue to develop.....21

Figure 16: Lifetime of the $Ir(ppy)_3$ and Green 2 PHOLEDs at L_0=600 cd/m^2 (CIE coordinates of each device are in parentheses).....23

Figure 17: Luminous efficiency *vs* Luminance of the Red 1, Red 2, and Red 3 PHOLEDs (CIE coordinates of each device are in parentheses).....25

Figure 18: Lifetime of the Red 1 and Red 2, and Red 3 PHOLEDs at L_0=300 cd/m^2 (CIE coordinates of each device are in parentheses).....26

Figure 19: Comparison of J-V-L curves of top-emitting, transparent, and bottom-emitting OLEDs (top-emitting luminance measured through the cover glass).....28

Figure 20: Photon radiation *vs* far-field angle; all data was taken at J = 10 mA/cm^2.....29

Figure 21: Lifetime of a bottom-emitting and transparent Ir(ppy)$_3$ PHOLEDs with MgAg/ITO cathode.....30

Figure 22: Lifetimes of Ir(ppy)$_3$ PHOLEDs on barrier coated PET (driven at 2.5 mA/cm^2) and ITO coated glass (driven at 2.6 mA/cm^2).....32

LIST OF TABLE CAPTIONS

Table 1: Quantum yields for singlet oxygen generation (Φ_Δ) with 355 or 532 nm excitation (λ), rate constants for oxygen quenching of the phosphor excited state, determined by Stern-Volmer analysis ($k_{q,SV}$) and rate constants for singlet oxygen quenching by the Ir complex sensitizer [$k_q(^1O_2)$].....16

Table 2: Performance summary of Red 1, Red 2, and Red 3 PHOLEDs; efficiency and lifetime are recorded at L_0 =300 cd/m^2.....25

FOREWORD

This grant MDA 972-01-1-0032 was selected under Air Force Office of Scientific Research (AFOSR) Broad Agency Announcements BAA 2001-01. Proposal number 01-NL-113 entitled "Investigation of the Operational Lifetime and Modes of Failure of Organic Light Emitting Devices" was reviewed by an interagency panel of experts from the Air Force Research Laboratory Human Effectiveness Directorate (AFRL/HE), the Defense Advanced Research Projects Agency (DARPA), the Army Research Laboratory Sensors and Electron Devices Directorate (ARL/SEDD), and the Natick Soldier Center (NSC) led by Dr. Charles Y-C Lee of AFOSR/NL and found to be scientifically sound and acceptable for award consideration. Because of DARPA's interest in this area, AFOSR recommended the proposal to DARPA for funding consideration. The grant was issued from DARPA to the Princeton University and required the DARPA to provide 100% of the total project funding of $700,000 via ARPA Order No. H731/14. Dr. Hopper at AFRL was the DARPA Agent and was designated by DARPA as the government Contracting Officer's Technical Representative (COTR).

In addition to the body of the report, the results of this two-year project are documented in one patent listed in Appendix A and in 10 publications listed in Appendix B. Personnel involved and graduate degrees awarded with funding under this effort are listed in Appendices C and D. An extensive pictorial presentation of the results are available in the form of the 11 June 2003 final review presentation charts in Appendix E.

This project built on the foundation of a previous $5,438,957 DARPA-funded AFRL-managed grant F33615-94-1-1414 led by Princeton University from 13 June 1994 through 30 April 2002. Accomplishments on this earlier grant, funded under the DARPA High Definition Systems Program, have been published in two earlier technical reports, which are available from the National Technical Information Service:

> Stephen R. Forrest, Mark E. Thompson, and Juan Lam,
> "Novel, Full Color Flat Panel Display Technology Employing High Performance Crystalline Organic Semiconductor Light Emitting Diodes"
> AFRL-HE-WP-TR-1998-0098, 44 pages (May 1998).
>
> Stephen R. Forrest,
> "Vacuum Deposited Organic Light Emitting Devices on Flexible Substrates"
> AFRL-HE-WL-TR-2002-0147, 118 pages (August 2002).

This report AFRL-HE-WL-TR-2003-0154 has been formatted in accordance with a commercial standard, with tailoring from the AFRL Scientific Technical Information Office. This standard is as follows: "Scientific and Technical Reports—Elements, Organization, and Design," American National Standard ANSI/NISO Z39.18-1995 (NISO Press, Bethesda MD, 1995), which is available electronically via the following website address:
http://www.wrs.afrl.af.mil/library/sti-pubh.htm

The technical review of this document was accomplished by Dr. Darrel G. Hopper of AFRL.

PREFACE

The objective of this applied research program was to determine the physics, chemistry, and device engineering causes for the the short lifetime of organic light emitting diode devices and to determine methods to overcome these failure mechanisms.

Princeton University in Princeton NJ assembled a team comprising the University of Southern California (USC), the University of Texas at Austin (UTA), and the Universal Display Corporation. Princeton University provided program management and concentrated on device fabrication issues. The University of Southern California concentrated on materials issues. The University of Texas at Austin concentrated on special analytical techniques. The Universal Display Corporation concentrated on lifetime issues. All participants contributed to all issues, accomplished various tests, and collaborated in the analysis of one-another's results. The degree of integration of effort is illustrated by the creation of materials at USC, fabrication of devices at PU, and near-field scanning optical microscopy (NSOM) work at UTA.

Technology transition between Princeton University and the University of Southern California to Universal Display Corp. has been continuous throughout the course of the project. Specifically, tools and methods to monitor photophysical degradation, as well as numerous compounds for use in blue PHOLEDs have been transitioned during the project.

ACKNOWLEDGEMENTS

We gratefully acknowledge the financial support received from DARPA under grant number MDA 972-01-1-0032. We thank Dr. Robert W. Tulis of DARPA and Dr. Darrel G. Hopper of AFRL for their support throughout the project. Furthermore, the authors thank PPG Industries for their work on new materials, Vitex Systems and DoE Pacific Northwest National Laboratory for their work on barrier coated plastics, and Prof. C. Adachi of Chitose Institute of Science and Technology for helpful discussions.

This page intentionally left blank.

1. SUMMARY

The reliability limitations of organic light emitting diode (OLED) displays was explored in a joint effort lead by Princeton University, with subcontracting efforts by the University of Southern California (USC), the University of Texas at Austin (UTA), and Universal Display Corporation (UDC).

Methodologies and protocols for screening of device structures and materials were developed using each of three types of OLED structure shown in Figure 1(a-c).

Extended lifetimes of red, green and blue phosphorescent OLEDs were achieved. Lifetimes of >50,000 hours for both red and green OLED devices were obtained, with blue device lifetimes still less than 1000 hours observed. This difference in blue lifetime was studied through photo- and electro-luminescence methods, and was found to be due in part to the high energies needed to excite the blue lumophores, resulting in charge imbalance in the emission layers of the OLEDs.

Contact degradation was also studied at the microscopic scale using simultaneous near-field scanning optical microscopy (NSOM) and optical microscopy in experiments enabled by our transparent OLED (TOLED) structure. A key result from all of the experiments is that defects introduced during processing are largely responsible for the formation and growth of dark spots in OLEDs.

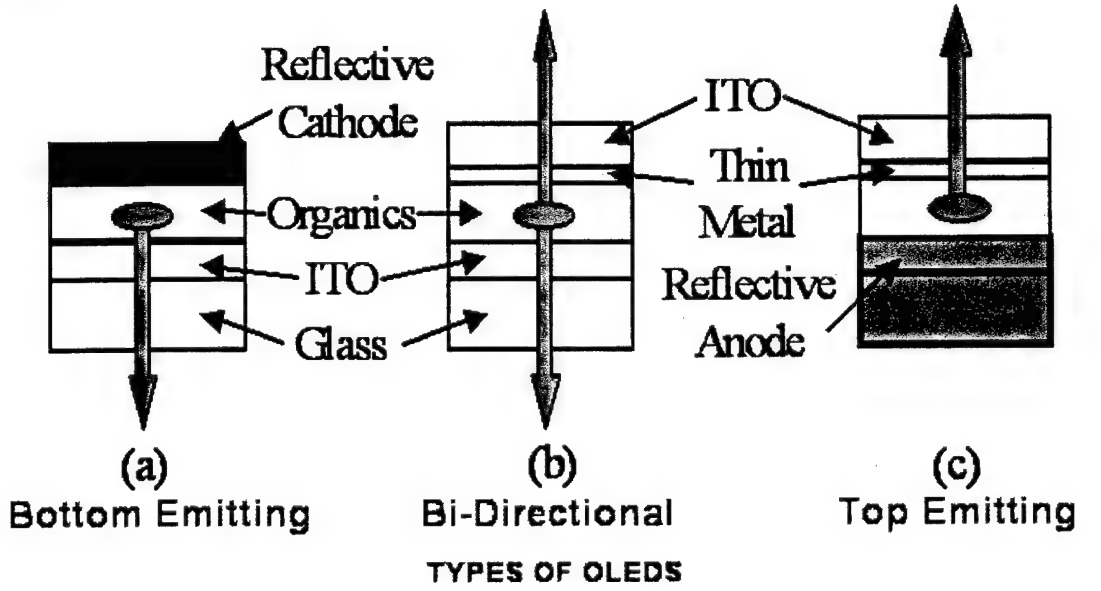

Figure 1 (a-c): Types of OLED display devices.

2. INTRODUCTION

The focus of this research was to understand failure modes in OLED display devices, develop protocols for the quantification of reliability, and improve the operational lifetime of these devices. Our technology platform is based on phosphorescent OLEDs (PHOLEDs) which have proven to be the highest efficiency emissive source yet developed for displays. In Figure 1(d) we show a typical test structure—the conventional PHOLED consisting of an indium tin oxide (ITO) anode, hole injection layer (HIL), hole transport layer (HTL), phosphor-doped emission layer (EML), hole and exciton blocking layer (HBL), electron transport layer (ETL), and metal cathode.

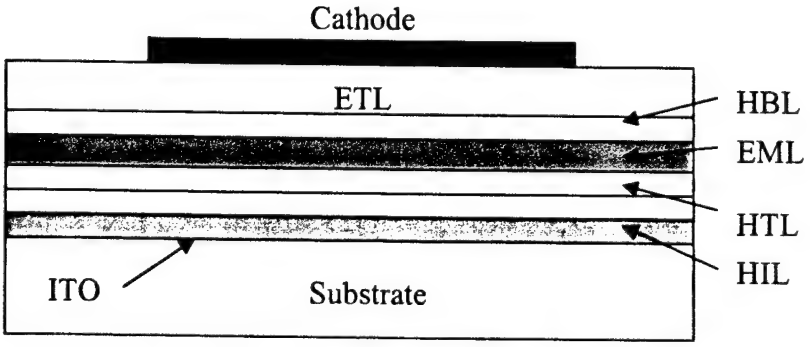

Figure 1(d): Schematic diagram of a simple, conventional OLED display device.

The complexity of the device provides some insight into the difficulties encountered in determining failure mechanisms in OLEDs. All adjacent layers, interfaces and dopants can chemically interact, and individually they can all lead to degradation of device performance over time. Hence, it is important to develop methodologies that can isolate separate modes effects arising from each of the layers and their interactions.

The specific research objectives were as follows: (a) establish protocols for accelerated aging of transparent, conventional and flexible organic light emitting device (FOLED) displays; (b) using NSOM and other analytical techniques, investigate the growth of dark spots on the above-noted displays, including the acceleration of this effect after flexing; (c) investigate effects of material grading of the organic/organic heterojunction and determine the dependence of long term stability on this factor; (d) investigate different encapsulation methods for both flexible and rigid display substrates; (e) develop models to understand results of long term aging studies; (f) continue studies and gathering data on contact, transport layer, doping, packaging, and flexing experiments; (g) accomplish detailed pre- and post-aging measurements of the energetics and operational characteristics (including photoelectron spectroscopy measurements of aged and aging interfaces) of the molecular devices grown by both organic vapor phase deposition (OVPD) and vacuum thermal deposition.

3. RESULTS AND DISCUSSION

3.1 Phosphorescent Blue Reliability

High-efficiency PHOLEDs have now been demonstrated in the red, green and blue portions of the visible spectrum. The single greatest obstacle remaining in the path to a full-color, long-lifetime OLED display is material and device reliability. Device lifetimes in the green and red portions of the spectrum are reaching the levels required for conventional display applications while lifetimes in the blue portion of the spectrum remain below the threshold for usability.

The question of blue reliability is not one that can be addressed in a single series of experiments, the solution to this problem needs to be attacked on a variety of fronts, by examining the materials themselves on both chemical and physical levels as well as considering the lifetime of given device structures and the susceptibility of such structures to certain conditions. These conditions include environmental (e.g. testing atmosphere) and operational (e.g. more sensitivity to one charge carrier—positive or negative—than another). Understanding the results of such experiments will prove critical to understanding the physical mechanism behind device degradation as well as the means to engineer materials and device structures which lend to greater overall operational stability.

The most successful (in terms of both quantum efficiency and operational stability) PHOLEDs demonstrated to date have employed either bis- or tris-cyclometallated Ir(III) compounds as the emissive material. Not surprisingly, the material under investigation for this particular study of phosphorescent blue reliability is iridium(III)bis[(4,6-di-fluorophenyl)-pyridinato-$N,C^{2'}$], which goes by the acronym "FIrpic." Since the operational stability of a device can often be the net result of a series of competing effects, it is typically instructive to try and reduce the number of variables under consideration for a given experiment. For an OLED, this can be accomplished by removing layers from the device structure to see the effect their omission has on the lifetime of the device. As a further simplification, one can go so far as to remove the "device" altogether and examine only the photostability of the host-guest emissive layer or further, the photostability of a neat film of the guest material. The path selected for this study of FIrpic involved examining first the operational lifetime of a completed device structure (to obtain a calibration point), and then continuing the study by examining the photostability of FIrpic in neat film. Then we examined the blue PHOLED material and the HBL.

3.1.1 Photophysical Degradation

Photophysical degradation of emissive phosphors was instituted as a primary screening method for determining the stability of dopants, as well as the stability of dopant/host systems. The principle of measuring photophysical degradation is that by observing the decrease in luminance of a film consisting of the dopant and host due to steady state excitation by a pump laser, one can infer the importance of excitons in the materials degradation process. That is, only neutral excited states are produced on optical excitation. Hence, if there is a loss of luminance over time incurred simply by optical pumping, we can eliminate, or at least ignore to first order, the role that charge plays in reducing system stability. This method, developed at Princeton University and then transferred during the program to Universal Display Corporation, was applied primarily to the study of blue phosphors such as FIrpic which are known to result in blue emitting PHOLEDs with only modest stabilities (100-1000 hours). An example decay curve for the luminescence of FIrpic due to optical pumping is shown in Figure 2.

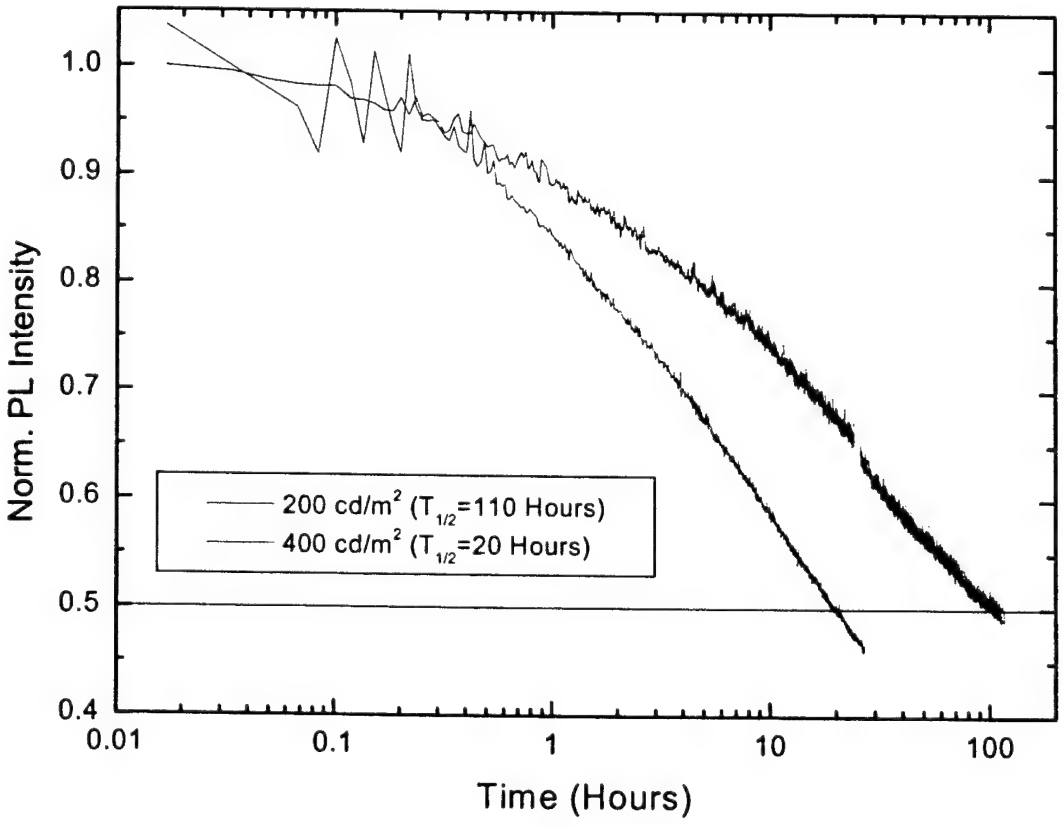

Figure 2: Photophysical decay of FIrpic

One generally observes that the operational lifetime of an OLED depends on the level of excitation (whether optical or electrical) to which the device is subjected. For the purposes of this study, the lifetime is defined as the point at which the initial device (or film) luminescence drops to one-half of its starting value. The structure used to examine the device operating lifetime under electrical excitation consisted of a 10-nm-thick copper phthalocyanine (CuPc) hole injection layer, a 30-nm-thick 4-4′-bis[*N*-(1-naphthyl)-*N*-phenyl-amino]biphenyl (α-NPD) HTL, a 30-nm-thick emissive layer consisting of 6% FIrpic (by weight) codeposited with either mCP (*N,N′*-dicarbazolyl-3,5-benzene), tCP (1,3,5-tri-(N-carbazolyl)benzene) or CBP (*N,N′*-dicarbazolyl-4-4′-biphenyl), followed finally by a 40-nm-thick ETL consisting of 4-biphenyloxolato aluminum(III)bis(2-methyl-8-quinolinato)4-phenylphenolate (BAlq). These devices were packaged with desiccant using a ultraviolet (UV)-curable epoxy, and then excited with a current density sufficient to generate a luminance of 100 cd/m^2 in the forward viewing direction. The lifetime does not vary significantly between all three devices (mCP:[123±12 hours], tCP:[190±12 hours]), CBP:[122±12 hours]), suggesting that the choice of host (at least between mCP, tCP and CBP) does not significantly affect overall device lifetime. This came as a sort of surprise as the authors expected the devices employing mCP and tCP as hosts to exhibit improved lifetimes as a result of improved energy transfer between mCP or tCP and FIrpic. As has been previously reported, transfer between the CBP and FIrpic triplet energy levels is strongly endothermic in nature, leaving the transfer mechanism very susceptible to trap states caused by defects or impurities introduced into the device during growth and processing. In comparison, devices based on mCP and tCP are exothermic, meaning the energy transfer from the host triplet energy level to the FIrpic triplet energy level is very favorable and efficient, presumably leading to a reduced sensitivity to trap states, allowing one to speculate that such devices should have improved lifetimes. The fact that this is not the case suggests that the poor reliability of devices based on FIrpic is not rooted in the efficiency of host-guest energy transfer and could instead be intrinsic to the chosen device structures or, to FIrpic itself.

Since investigations into device lifetime under electrical excitation suggested that FIrpic itself could be the source of poor overall device reliability, the next phase of this study was to focus on the photophysical stability of FIrpic in neat film. Films of FIrpic were grown on quartz and excited using a filtered mercury lamp (with wavelength about 366 nm). Characteristic photoluminescence (PL) from the film was collected with a Si-photodetector while spectra were collected using a fiber-coupled spectrometer. All experiments were performed with unpackaged films, enclosed in a vacuum tube pumped to a base pressure of about 10^{-7} Torr. The results of two of these experiments, for an initial luminance of 200 cd/m^2 and 400 cd/m^2 are depicted in Figure 2. A clear dependence on initial luminance is observed, with the film excited at 200 cd/m^2 (20 hours) having a lifetime 5-6 times greater than the film excited at 400 cd/m^2 (110 hours). Interesting to note is the fact that the lifetime under optical excitation (200 cd/m^2 photoluminescence) is on the same order as the lifetime under electrical excitation (100 cd/m^2 electroluminescence), which suggests that the stability of the film is increased under optical excitation. These results indicate that there may be intrinsic stability problems associated with the device structure previously discussed and possibly as well with the excitation of the molecule electrically versus optically.

In an attempt to better understand the results of the photodegradation experiments performed on FIrpic, the absorption and photoluminescence spectra of the tested sample were examined before and after testing. One would in general expect that if chemical bond breaking (for instance) was the source of film degradation, the accompanying absorption spectrum should change significantly (likely a decrease in absorption or, a shift in absorption to a different portion of the spectrum). In Figure 3, one notes that no such change in absorption (or photoluminescence shape for that matter) is observed. This result is very interesting as it suggests that molecules of FIrpic may not be destroyed during the photodegradation study. This data also suggests that the study may simply be introducing non-radiative, exciton quenching sites into the film which serve to reduce the overall photoluminescence efficiency of the film. We propose that such non-radiative quenching centers could actually be formed by the presence of oxygen in the film, either incorporated during growth, or leaked into the system during testing.

The sensitivity of the photoluminescence efficiency of cyclometallated Ir(III) complexes to oxygen, specifically triplet oxygen is well documented in solution. We carried out similar crude experiments involving the degassing of thin films of FIrpic with dry nitrogen and observed increases in film photoluminescence efficiency of more than 25% (depending on degassing pressure), presumably resulting from the displacement of oxygen from the film by the dry nitrogen, reducing any quenching effect the presence of oxygen may have on the luminescent properties of the film. This observed effect is reversible, meaning if the film is again permitted to sit undisturbed in room air, the photoluminescence from the sample is reduced, and then under flow of dry nitrogen, the photoluminescence again increases. It is conceivable that a similar effect could be present in our studies of the photodegradation of FIrpic, suggesting that the degradation in FIrpic may be partially reversible.

In summary, the primary focus of this study was an attempt to isolate the various causes of degradation in the cyclometallated Ir(III) complex FIrpic. It was determined that the overall device lifetime is the net result of intrinsic instabilities in the chosen device structure as well as intrinsic instabilities in FIrpic itself. Specifically, we investigated these instabilities in FIrpic by examining the photodegradation of FIrpic under intense illumination. Based on our preliminary findings, we suspect that the presence of oxygen is a likely culprit for the short lifetime of FIrpic under optical excitation. We further postulate that oxygen is likely playing a significant role in the degradation of devices which employ FIrpic as an emissive material. Experiments examining the photoluminescent lifetime as a function of the oxygen partial pressure in the testing atmosphere should help to clarify and confirm this theory.

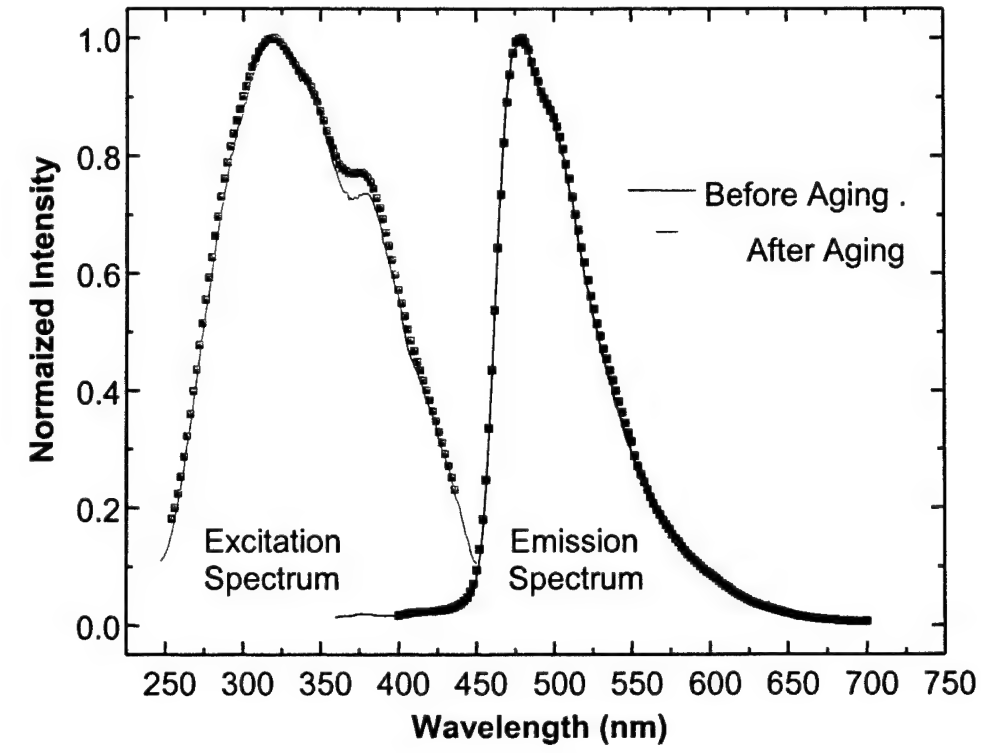

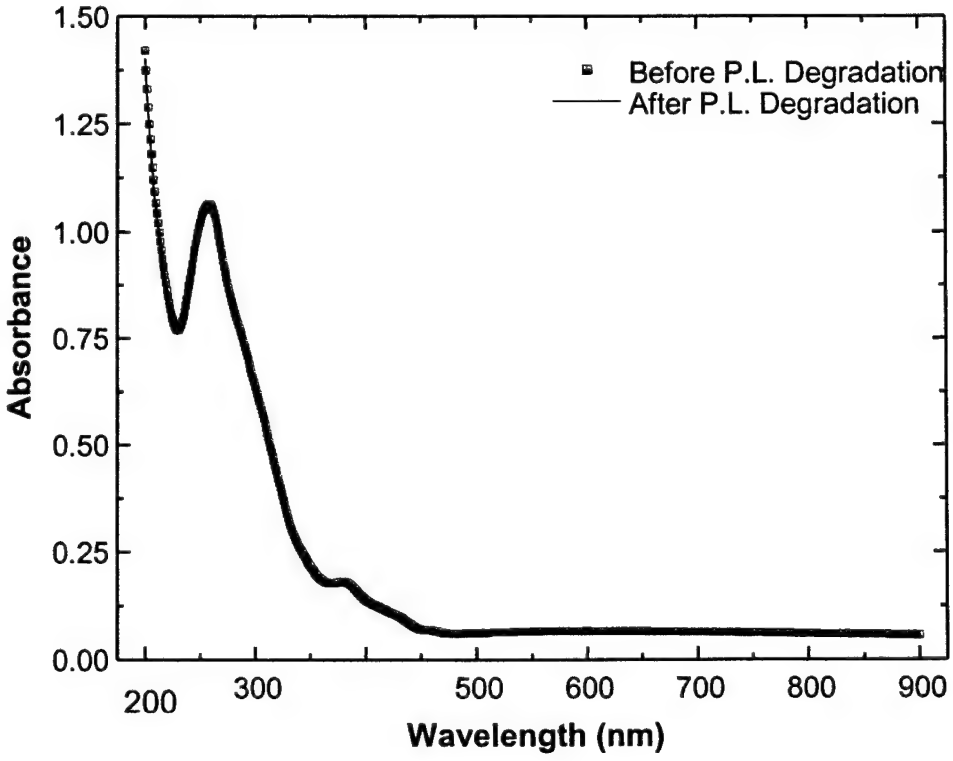

Figure 3: FIrpic spectra taken both prior to and following aging studies.

3.1.2 Lifetime

Long operational stability of blue OLEDs presents a particularly difficult problem to solve. In both fluorescent and phosphorescent OLEDs, blue emitters have dramatically shorter lifetimes than red and green devices. The problem is most severe in both triplet emitting devices and in polymers. We addressed this problem during the course of the program from a fundamental as well as "new chemistry" viewpoint. Specifically, blue triplet emitters have the problem of requiring energy transfer from a fluorescent host. Hence, an excess 0.7 to 1 eV exchange of energy is required to excite the host. At the already high energies of blue emission, this additional charge can result in accelerated degradation of the host. Hence, in our work, we have developed a new approach to blue emission: that of embedding the dopant directly in a "passive" ultrawide-energy gap host (UGH) series of compounds. Here, the blue phosphor (FIr6, etc) is directly excited by charge injection from the HBL and the HTL sides of the structure. Furthermore, the phosphor is responsible for charge conduction. The only purpose of the host is to "hold the dopant molecules in place," separated from each other such that concentration quenching is avoided. Using this method, 12% external quantum efficiencies are obtained for deep blue emitting devices. We have described this work in more detail in R. J. Holmes, et al. *Appl. Phys. Lett.*, **83**, 3818 (2003).

In conventional energy transfer systems there also are problems in the energetics of blue emission that impact device lifetime. That is, it is difficult to effect energy transfer from host to guest due to the very high triplet and singlet energies of the phosphor. Hence, in the first demonstrations of blue electrophosphorescence, the host-guest transfer process occurred by endothermic energy transfer, whereby the host energy was slightly less than the guest triplet energy. Impurities present in the host matrix thereby present a robust mechanism for energy loss and potentially lower device operational stability. Hence, during this program we developed large energy gap hosts, such as mCP, demonstrating to our knowledge the first exothermic energy transfer to occur in a blue emitting phosphor OLED. The guest in this case was FIrpic, and the efficiency of the blue device was significantly improved from that of the endothermic pair employing 4,4'-bis(N-carbazolyl)biphenyl (CBP) as a host. We have fully described this work in R. J. Holmes, et al., *Appl. Phys. Lett.*, **82**, 2422 (2003).

Finally, by continued improvement in the fabrication processes and purity of the source materials, during this program we were successful in vastly improving the reliability of red, green and blue PHOLEDs. Currently the blue lifetime stands at 1000 hours, green at 50,000 hours, and red at 50,000 hours when normalized to an initial display luminance of 100 cd/m^2. Indeed, the red and green PHOLED lifetimes are completely compatible with the most stringent demands of display lifetime, while the blue remains inadequate, with improvements of a factor of 10 still required. We continue, after the close of the program, to investigate the fundamental energetic limitations to blue PHOLED lifetime, and continue to expand our class of compounds that may lead to longer lived blue electrophosphorescent devices. We have provided a snap shot of PHOLED reliability at the end of this program in R. C. Kwong, et al. *Appl. Phys. Lett.*, **81**, 162 (2002).

3.1.3 Hole Blocking Layer (HBL)

We also investigated the operational lifetime limitations presented by the HBL. We found that the morphological instabilities of bathocuproine (BCP) were one of the predominant mechanisms leading to a reduction in operating lifetime of high efficiency PHOLEDs. Systematic studies indicated that doping of the HBL with a higher glass transition impurity could lead to improved morphological stability. This was an important finding, as it allowed us to employ an HBL that could provide high efficiency, and at the same time high PHOLED stability. In our case, we doped BCP with BAlq, an alternative hole blocker that gives high stability at reduced efficiency. This work has resulted in a patent disclosure, listed in Appendix A, and full details of our results are presented in B. W. D'Andrade, et al., *Appl. Phys. Lett.*, **83**, 3858 (2003).

3.2 Extrinsic Degradation of OLEDs

Extrinsic degradation of OLEDs is typically manifested in the growth of dark spots. The growth of these dark spots is tied to the environment that the devices are run in. Atmospheric exposure accelerates the growth of dark spots significantly.

We initially used atomic force microscopy (AFM) and optical microscopy to study the growth of dark spots in OLEDs in a collaborative effort between the groups at USC, U. Texas, and Princeton U (see Section 3.3). In order to be used in these studies the OLEDs needed to be transparent to obtain good registry between the AFM and optical images. The devices used for this study had Mg-Ag/ITO cathodes. From these devices we were able to draw a number of conclusions. We found that electroluminescent (EL) dark spots in OLEDs originate as non-conductive areas at the metal/organic interface, and rapidly grow as a result of atmospheric exposure. The dark spots are attributed to regions of poor electron injection formed by local oxidation. Continuous diffusion of oxygen and water into the device leads to growth of the oxidized region of the cathode, radially from the central defect. Significant structural changes in the cathodes occur well after initial formation and growth of the EL dark spots takes place. In contrast to the growth of dark spots, bubble formation was found to be enhanced at high current densities.

The next step of this study, conducted at USC, was to ascertain what factors are most important in determining the rate of growth of dark spots. If one can retard the growth of dark spots, the packaging requirements would be far less than for standard devices. For this work we needed an efficient method to evaluate the distribution of dark spots and their growth rate as a function of the environment, materials, device architecture, et cetera. The system shown in Figure 4 was built for this study. The environmental chamber was built of plexiglass. The OLED was placed inside the chamber and run. The digital camera sat outside the chamber and recorded the image of the degrading device as the dark spots grew. From the digital camera images, we determined the growth rate of the dark spots. The chamber was fitted with a humidity controller that controlled the relative humidity between 7 and 100% with an accuracy of ±2%. Using mass flow controllers the oxygen level was to be varied between 0 and 100%. This allowed us to independently vary the oxygen and water levels in the atmosphere and study their effects on dark spot growth independently. One may think that the lowest level of water and oxygen in the atmosphere would have been desirable for these studies, but this was not the case. If we had held the water and oxygen levels at very low levels we would have packaged devices and would not have been able to study dark spot growth easily. Our goal was to be able to monitor dark spot growth and collect all of the data that needed in a few hours. That way we could readily monitor a wide range of devices under a wide range of different conditions. We, thus, determined the effect of water and oxygen on the growth rate, and the best conditions for accelerating dark spot growth to a rate readily measured in a few hours of device operation.

The images shown in Figure 5 were taken of a standard OLED with a thin-layer structure as follows: [ITO/NPD(400Å)/Alq3(500Å)/LiF(10Å)/Al(1000Å)]. The device was operated at 80% relative humidity, under nitrogen. The device was run at a constant current, and the images shown are for t = 0 and t = 160 min. Images were taken at 20 minute intervals. The line scans of

one of the dark spots are shown to the right of the images. By plotting the width of the dark spot versus time we can get the rate of dark spot growth. This plot is shown in Figure 6 for this device, as well as for other devices. The linearity of these plots is quite good leading an accurate estimation of the dark spot growth rate. Both lithium fluoride/aluminum (LiF/Al) and magnesium-silver (Mg-Ag) cathode give the same rate of dark spot growth (0.28 μm/min) at 80% relative humidity and a lower rate (0.16 and 0.11 μm/min for LiF/Al and Mg-Ag cathodes respectively) as the humidity is decreased to 30%. This is consistent with the picture that water significantly accelerates dark spot growth. It is interesting that the rate of dark spot growth appears to be independent of the cathode material. These measurements have only been made for a few dark spots for each device at this point. We need to extend out analysis to a statistically significant number of dark spots. In addition, we need to analyze the dark spot density as a function of the humidity and oxygen levels.

Our original hypothesis for what caused dark spot growth in vacuum deposited OLEDs was oxidation of the ETL/cathode interface. If that were the case, one would expect the dark spot growth rate to be affected by the identity of the ETL material. In order to determine if ETL composition affected dark spot growth we prepared four different devices, with different materials at the ETL/cathode interface. The general device structure was ITO/NPD (400 Å)/Alq_3 (400 Å)/EIL (100 Å)/Mg-Ag, where EIL = electron injecting layer, which was varied amongst Alq_3 (reference), C_{60}, BCP (bathocuprione), and FIrpic (phosphorescent dopant). The growth rate of the dark spots is shown in Figure 7. The graph to the left shows the total number of dark pixels in the digital image and the right shows the normalized total dark area.

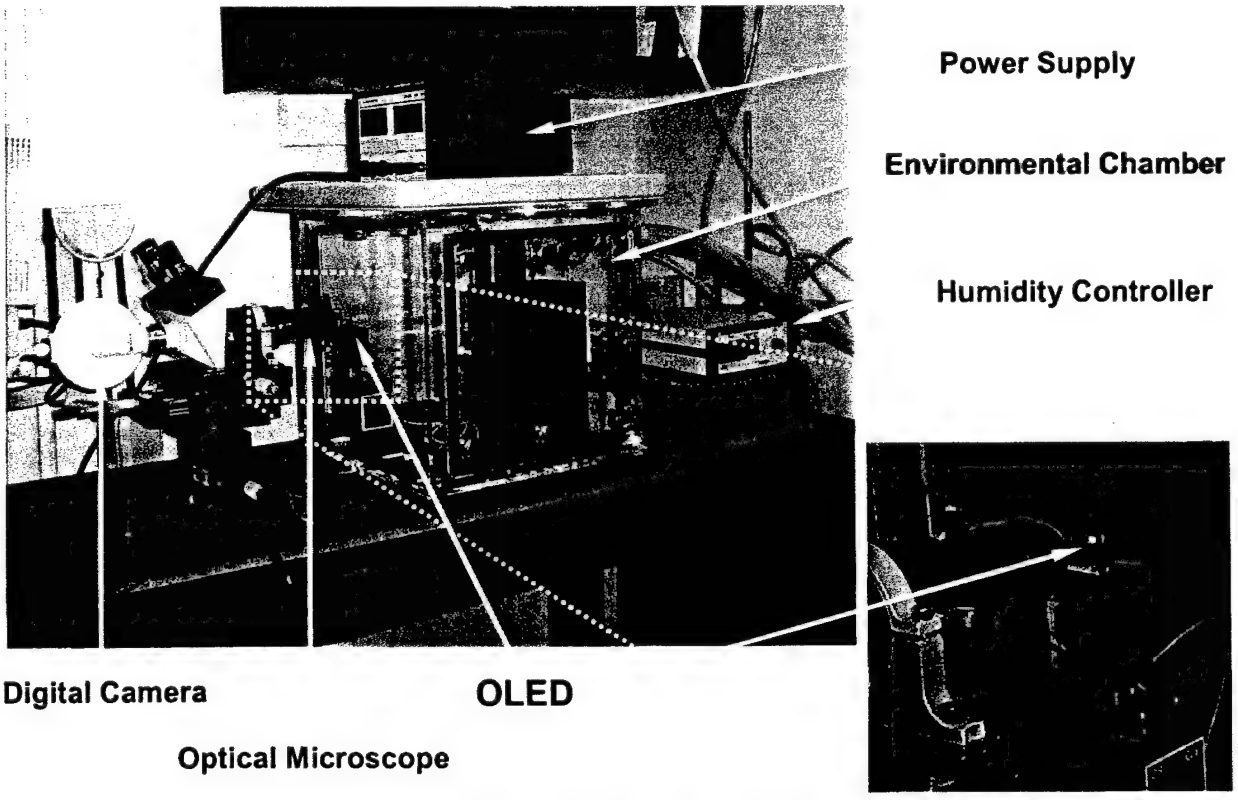

Figure 4: Controlled environment chamber

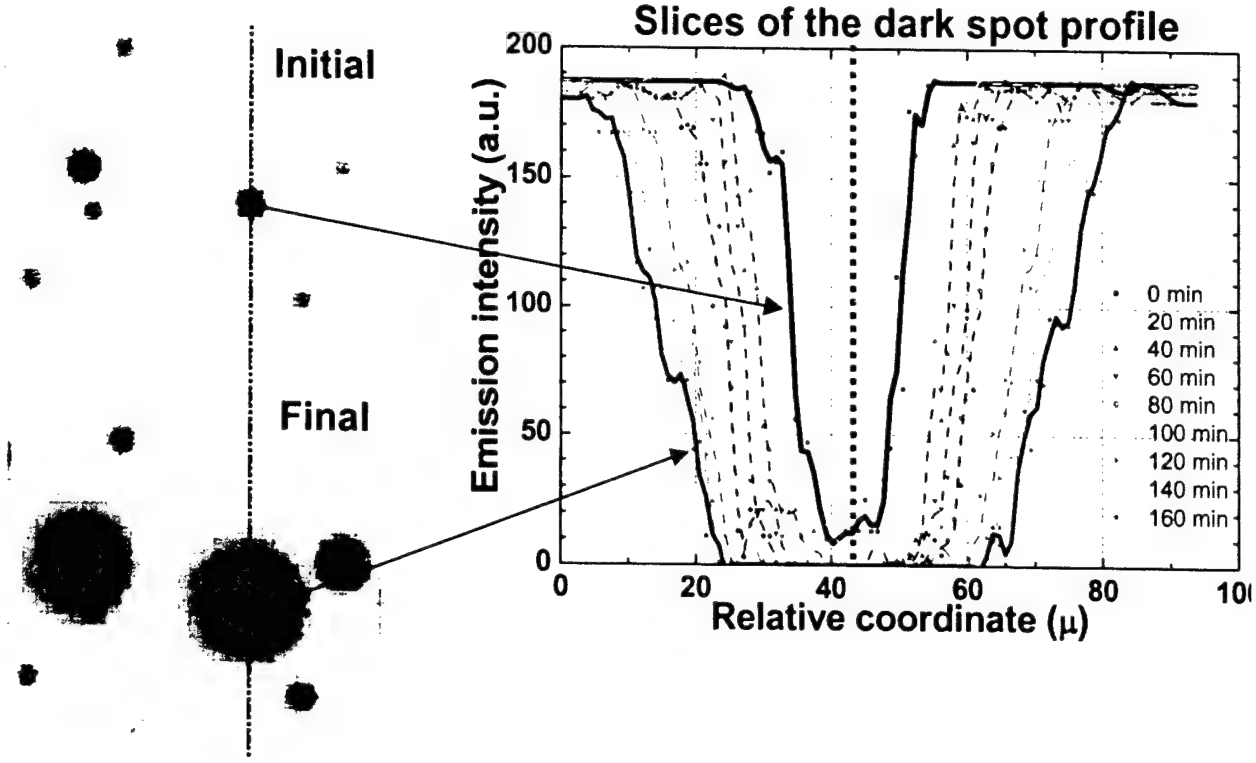

Figure 5: Initial and final images of a device during degradation. The line scans are shown at 20 min. intervals.

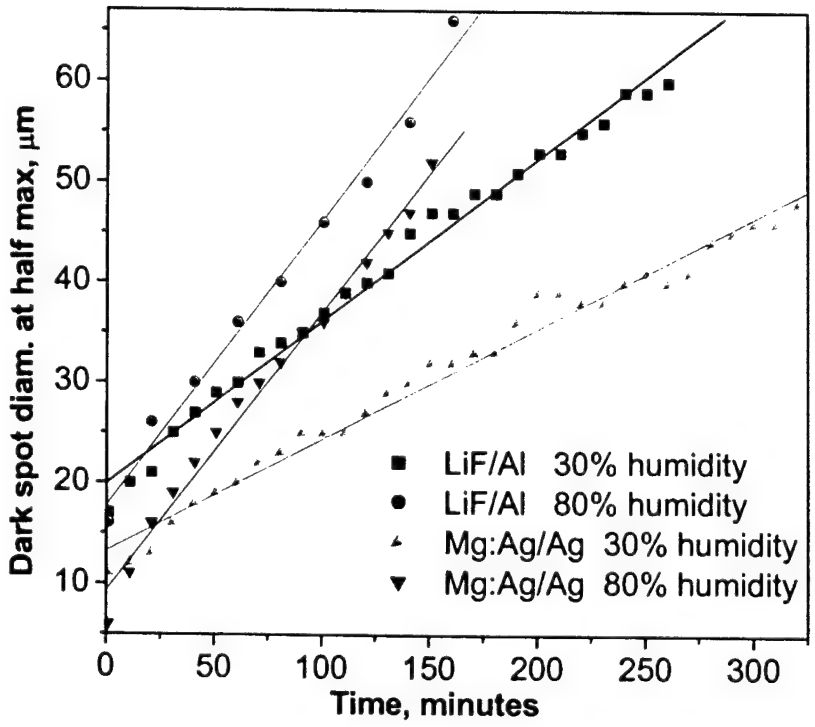

Figure 6: Dark spot growth rates.

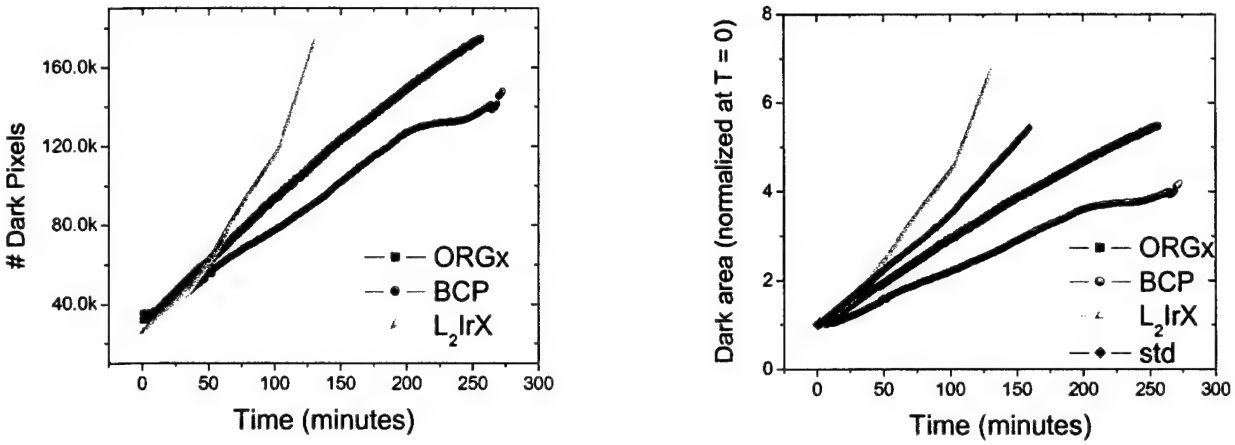

Figure 7: Growth rates of dark pixels (left) and dark area (right).

These data were compiled from 150 digital images. The EIL clearly affects the rate of growth of the dark spots in these devices. FIrpic is a well known blue emissive dopant in phosphorescent OLEDs. It has also been used as an electron transporting and injecting layer in OLEDs. While the use of FIrpic leads to efficient OLEDs, it significantly enhances the growth rate of dark spots. Both BCP and C_{60} interface layers apparently give markedly slower dark spot growth than the reference device, however, the BCP data is misleading. The BCP devices have darks spots grow by forming halos first and then expanding. Halo growth does not occur for the C_{60} based devices. The use of C_{60} as an EIL has not been reported previously. C_{60} is an efficient EIL for both retarding dark spot growth and efficiently injecting electrons from the Mg-Ag cathode and Alq_3. We have examined the C_{60} thickness dependence for dark spot growth in these devices, Figure 8. The most efficient device for retarding dark spots has a 100 Å C_{60} layer. The most important conclusion to take away from this data is that the organic/cathode interface is very important in controlling dark spot growth. This supports our original hypothesis that oxidation at this interface is the principal cause of dark spot growth.

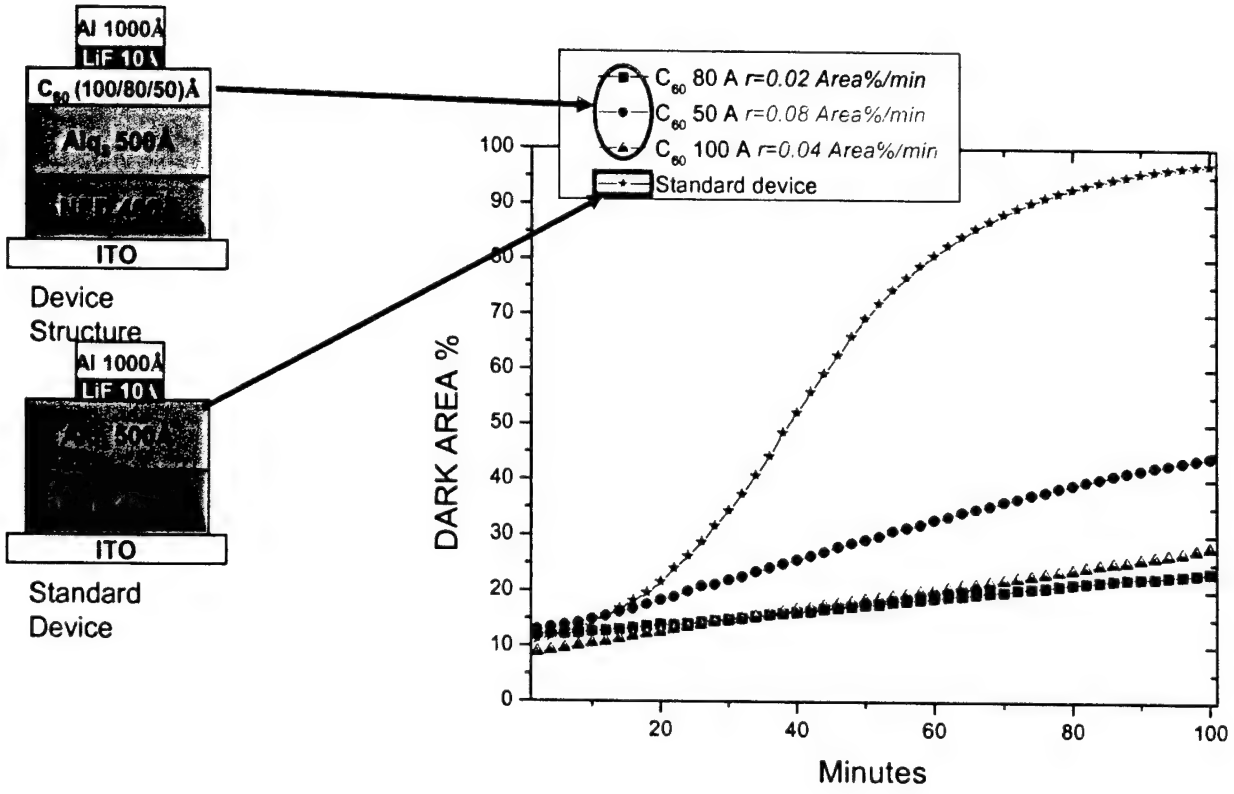

Figure 8: C_{60} thickness dependence for dark spot growth in devices.

3.3 Singlet Oxygen Generation by Phosphor Dopants

The chemistry of cyclometallated Ir(III) complexes has received a great deal of attention recently. These complexes have proven to be very efficient emissive dopants in molecular and polymeric light emitting diodes.[1] While studying the photophysical properties of these complexes, it was noticed that the quantum efficiencies, ϕ, and triplet lifetimes, τ, are severely reduced by oxygen,[1(a),2] only giving high values ($\phi > 0.5$ and $\tau > 2$ μs) for rigorously degassed samples. This observation prompted us to investigate these complexes as potential singlet oxygen ($^1O_2$) sensitizers, as singlet oxygen formation is a likely quenching process. We now report that a variety of bis-cyclometalated Ir(III) complexes are indeed useful photosensitzers for the production of $^1O_2$, with generally high quantum efficiencies and small concomitant physical quenching of singlet oxygen.

---

[1] (a) S. Lamansky, P. Djurovich, D. Murphy, F. Abdel-Razzaq, H.-E. Lee, C. Adachi, P. E. Burrows, S. R. Forrest, M. E. Thompson, *J. Am. Chem. Soc.*, **2001**, *123*, 4304-4312. (b) S. Lamansky, R. C. Kwong, M. Nugent, P. I. Djurovich, M. E. Thompson, *Org. Elect.*, **2001**, *2*, 53-62. (c) Ikai, M.; Tokito, S.; Sakamoto, Y.; Suzuki, T.; Taga, Y. *Appl. Phys. Lett.*, **2001**, *79*, 156-158. (d) Adachi, C.; Baldo, M. A.; Forrest, S. R.; Thompson, M. E. *J. Appl. Phys.*, **2001**, *90*, 4058. Yang, M.-J.; Tsutsui, T. *Jap. J. Appl. Phys.* **2000**, *39*, L828-L829.

[2] (a) K. K.-W. Lo; D. C.-M. Ng; C.-K Chung, *Organometallics* **2001**, *20*, 4999-5001. (b) G. Di Marco; M. Lanza; A. Mamo; I. Stefio; C. Di Pietro; G. Romeo, S. Campagna, *Anal. Chem.*, **1998** *70*, 5019-5023. (c) Y. Amao,; Y. Ishikawa; I. Okura, *Anal. Chim. Acta* **2001**, *445*, 177-182.

The Ir(III) complexes employed in this $^1O_2$ generation study are depicted in Figure 9. These complexes were prepared by literature procedures.[3] The lowest energy (emissive) excited state of these complexes is a mixture of metal-ligand charge transfer (MLCT) and $^3(\pi-\pi^*)$ states,[1(a)] composed principally of C^N ligand orbitals, with the β-diketonate ligand (Figure 6, L^X = D) acting as an ancillary ligand. Stern-Volmer analysis shows that phosphorescence from these complexes is efficiently quenched by triplet oxygen, at near diffusion controlled rates (Table 1).

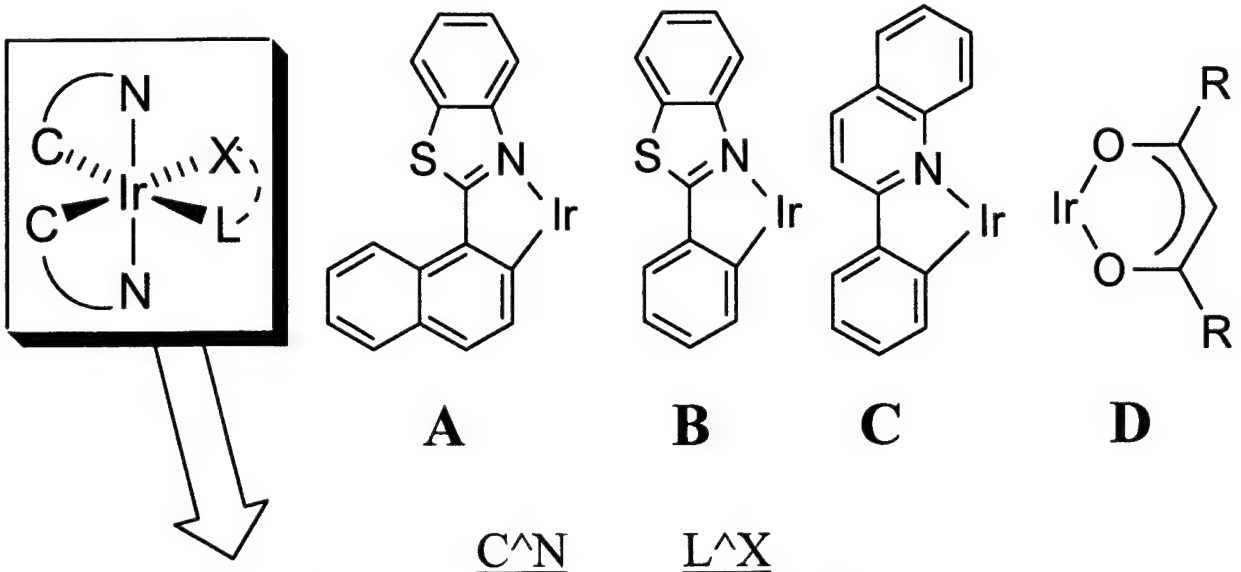

	C^N	L^X
BSN	A	D, R=Me
BSN*	A	D, R=*t*-Bu
PQ	C	D, R=Me
BT	B	D, R=Me

Figure 9: Structures of phosphor dopants used in $^1O_2$ generation study.

Oxygen quenching of the photoexcited Ir complexes does involve the formation of $^1O_2$, as all of the Ir complexes studied here proved to be excellent singlet oxygen sensitizers. The quantum yields for $^1O_2$ production (Φ_Δ) were obtained by measuring the intensity of the $^1O_2$ luminescence signal (λ_{max} = 1268 nm) and are listed in Table 1. Measurements were taken with 355 and 532 nm excitation, in air-saturated solutions. Triplet-triplet (T-T) annihilation was negligible at these concentrations, as evidenced by the fact that the $^1O_2$ intensity does not decrease as the sensitizer concentration is increased (see Figure 10), as it would if T-T annihilation were depleting the excited sensitizer. The $^1O_2$ quantum yields are very large and near unity for all of the β-diketonate complexes examined here. The Φ_Δ values are high for both ligand based excitation (355 nm) and direct excitation of the lowest energy excited state (MLCT+^{3}LC) at 532 nm.

[3] S. Lamansky, P. Djurovich, D. Murphy, F. Abdel-Razaq, R. Kwong, I. Tsyba, M. Bortz, B. Mui, R. Bau, M. E. Thompson, *Inorg. Chem.*, **2001**, *40(7)*, 1704-1711. The synthetic procedures and characterization data are given in the supplementary materials.

Table 1: Quantum yields for singlet oxygen generation (Φ_Δ) with 355 or 532 nm excitation (λ), rate constants for oxygen quenching of the phosphor excited state, determined by Stern-Volmer analysis ($k_{q,SV}$) and rate constants for singlet oxygen quenching by the Ir complex sensitizer [$k_q(^1O_2)$].

Sensitizer[a]	λ (nm)	Φ_Δ[b]	$k_{q,SV}$ (10^9 M^{-1} s^{-1})	$k_q(^1O_2)$ (10^6 M^{-1} s^{-1})
BSN	355 532	0.59±0.07 0.89±0.02		6.3 ± 0.2
BSN*	355 532	0.60±0.06 0.77±0.08	2.9 ± 0.1	4.0 ± 0.3
PQ	355 532	0.62±0.05 0.89±0.07	7.2 ± 0.3	1.0 ± 0.2
BT	355 532	0.86±0.07 1.00±0.07	5.9 ± 0.6	0.5 ± 0.2
BSN-G	355 532	0.54±0.02 0.81±0.06		1.7= 0.5
BT-G	355 532	0.72±0.08 0.77±0.04	3.5±0.2	2.6 ± 0.3
BT-py	355 532	0.95±0.09 0.97±0.14		None detected

a: Measurements were made in C_6H_6 solvent. b: The references for quantum yield measurements were C_{60} (0.76), TPP (0.62) and Perinaphthenone (0.95), at 355 nm and TPP (0.62) at 532 nm.

Other Ir complexes are known to form $^1O_2$ upon optical excitation (*e.g.* $[Ir(bpy)_3]^{3+}$ and $[Ir(phen)_3]^{3+}$);[4] however, they are also very efficiently $^1O_2$ quenchers.[4,5] Large $^1O_2$ quenching rates would severely limit potential applications of the bis-cyclometallated Ir complexes as photosensitizers. We therefore determined $^1O_2$ quenching rates for all of the Ir complexes reported here. These quenching rate constants [$k_q(^1O_2)$] are given in Table 1. The quenching rates for all of the complexes with β-diketonate ancillary ligand were found to be small, ranging from (10 ± 2) x 10^5 $M^{-1}sec^{-1}$ for PQ to (6 ± 0.2)x 10^6 $M^{-1}sec^{-1}$ for *Iridium (III) bis(2-(1-naphthyl)benzothiazolato-N,C2') acetylacetonate* (BSN). These $^1O_2$ quenching rates are roughly three orders of magnitude slower than the phosphorescence quenching rates (k_{qSV}), consistent with the high Φ_Δ values observed here. For the *Iridium (III) bis(2-phenyl benzothiozolato-N,C2') acetylacetonate* (BT) complex the singlet oxygen quenching rate is in fact smaller than those of many standard singlet oxygen sensitizers such as 5,10,15,20-tetraphenylporphyrin (TPP) [k_q = (6±2) x 10^7 $M^{-1}s^{-1}$],[6] while the quantum yield is near unity. Even though the three

[4] J. N. Demas, E. W. Harris, R. P. McBride, *J. Am. Chem. Soc.* **1977**, *99*, 3547-3551; J.N. Demas, E. W. Harris, C. M. Flynn, Diemente, D. *J. Am. Chem. Soc.* **1975**, *97*, 3838-3839.
[5] M. Selke, C. S. Foote, W. L. Karney, *Inorg. Chem.* **1995**, *34*, 5715-5720.
[6] P. R. Ogilby, C. S. Foote, *J. Am. Chem. Soc.* **1983**, *105*, 3423-3430.

cyclometalling ligands used here (A, B and C in Figure 6) give rise to very different absorption and emission energies,[1(a),3] their efficiencies for singlet oxygen production are very similar. Based on spectroscopic measurements for these four complexes,[1(a)] the orbital make-up for the triplet excited states are similar, and largely ligand based (*i.e.* π-π*). Hence, it is not too surprising that they have similar efficiencies for $^1O_2$ generation. The slight decrease of Φ_Δ of BSN at 532 nm relative to BSN* at 532 nm appears to be out of the error range and may be due to a steric blocking effect.

All of the phosphors are photostable under aerobic conditions, as we have not detected significant decomposition for irradiation times of up to 60 minutes. Thus, we expect that $^1O_2$ sensitization may only marginally affect the lifetimes of light emitting diodes doped with these Ir based emitters. Moreover, OLEDs must be packaged under anaerobic conditions to maintain long lifetime and prevent dark spot growth, which will prevent oxygen from reaching the sensitizer.

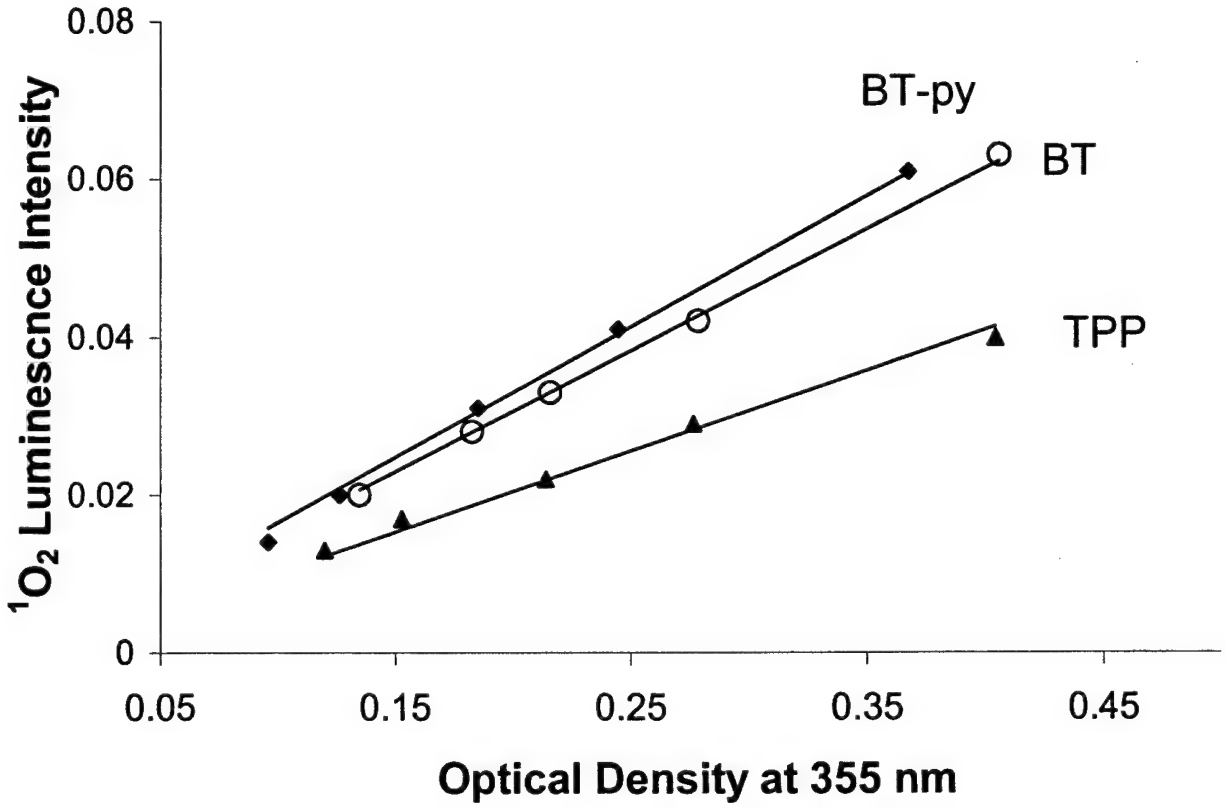

Figure 10: $^1O_2$ luminescence intensity (arbitrary units) vs. optical density at 355 nm for BT, BT-py and TPP.

3.4 Overcoating OLEDs to Retard Dark Spot Growth

Many, if not all, of the dark spots are the result of pinholes and particle related defects in the cathode. These cathode defects allow the ambient water and oxygen to access the cathode/organic interface, leading to dark spot growth. Changing the organic materials in contact with the cathode can affect the rate of dark spot growth, as discussed above, but we chose to investigate an alternate approach. If the cathode defects could be filled, the rate of water and air diffusion into the device could be reduced markedly. We have examined several coating materials to see if a simple overcoating affects the dark spot growth rate. A simple device was chosen for this study (ITO/Cupc/NPD/Alq_3/LiF-Al). Each device was coated with a different material and the growth of dark spots examined. Some of the overcoating materials we examined actually increased the rate of dark spot growth. The coatings included metal eutectic mixtures (InGa and InGaSn) and silicone. Other materials lead to marked decreases in dark spot growth rates. The relative dark spot growth rates are shown in Figure 11. The best results were obtained for carbon paste, which consisted of a mixture of silicone bath oil and carbon black.

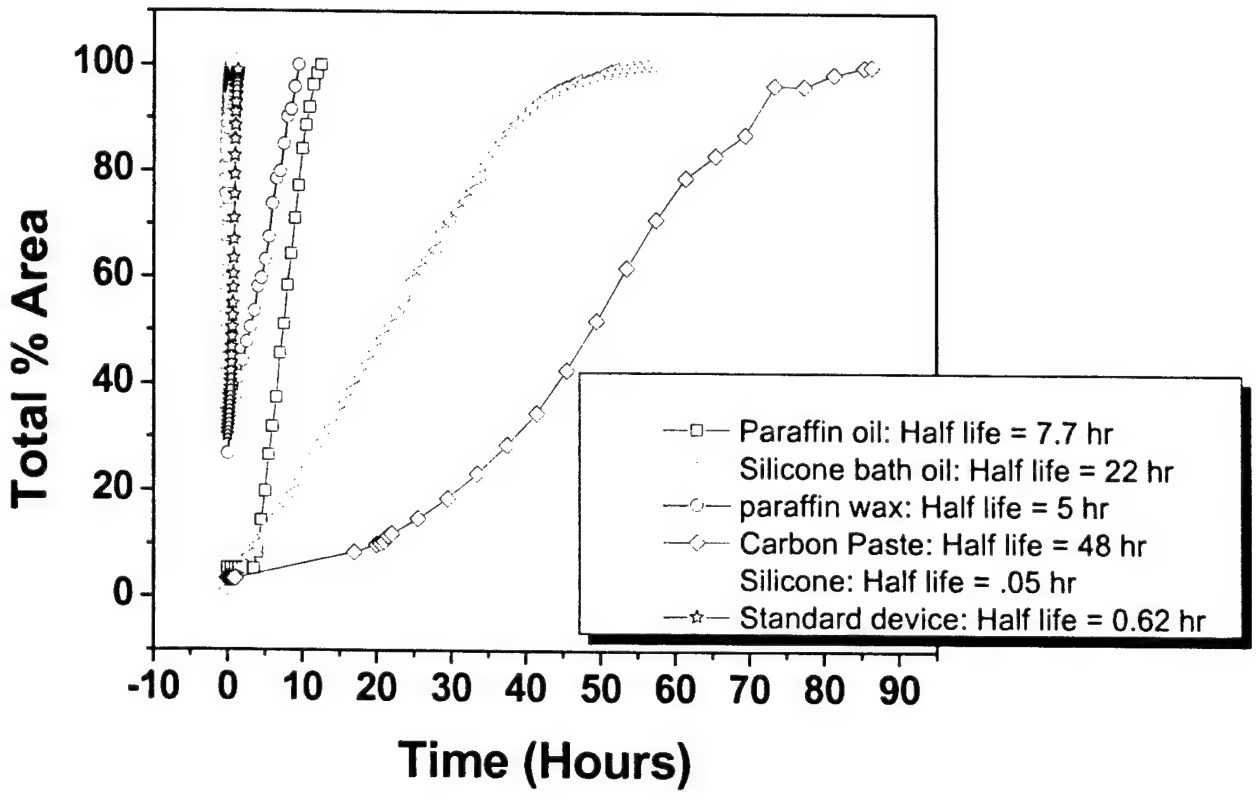

Figure 11: Relative dark spot growth rates for various OLED overcoatings.

3.5 NSOM Studies of OLED Failure

Near Field Scanning Optical Microscopy (NSOM) studies were used to investigate TOLED device failure in phosphorescence based OLEDs. The focus of this work is the investigation of dark spot formation and other aspects of device failure under a variety of conditions involving aging with or without current passing through the device and in the presence and/or absence of exposure to an ambient atmosphere. The results have clearly shown that ambient exposure is a major causative factor in dark spots. In addition, the results demonstrate that dark spots can be induced by physical damage of the electrode surface by indentation with a scanning probe microscopy tip. Most importantly, the results show, more than any other study, that initially formed dark sports are predominantly due to electrode damage rather than damage of the underlying organic emitting layer, which are surprisingly undamaged even at the interface with the electrode. These investigations have also explored physical damage to the TOLED structure that occurs late in the dark spot formation process, as the resistive heating of the device causes melting and eventually gas formation. The work on this project was completed by late 2002.

The model TOLED device structure that was investigated is shown in Figure 12. The NSOM tip was scanned over the ITO cathode. The initial morphology of the device was extremely smooth with less than 1 nm of root-mean-square (RMS) roughness. The NSOM induced phosphorescence was highly uniform on the 100 nm scale of the NSOM technique, and the phosphorescent spectrum was identical to that observed in the far field. A topographic image of the TOLED device is shown in Figure 13. Figure 14 shows an NSOM experiment on a dark spot formed by damage of the electrode induced by an electronic near-field scanning optical microscope (ENSOM) tip. Note that the dark OLED spot appears as a bright spot in the NSOM image. This is apparently due to less quenching of the phosphorescence by the cathode in the region of a dark spot. This is an interesting observation that will be explored in greater detail in future experiments since it opens the door to improved OLED efficiency. Figure 15 reveals the extreme device damage that occurs when darks spots continue to develop. This damage is probably due to resistive heating of the device. Under these conditions, the organic is heated beyond its sublimation point, allowing for organics to boil out of pin holes in the top of the electrode. This process causes volcano-like specks on the top electrode and a rippling of the entire OLED surface.

Another interesting observation in this work has been the discovery that the top electrode protects the organic layer from photo-oxidation when the device is exposed to intense radiation in an ambient atmosphere. This is probably a key factor in favoring electrode structure over organic layer destruction during the dark spot formation process.

Work is under way to prepare publications on the NSOM studies of device failure and on the use of electrically biased ENOM tips to investigate TOLED device operation.

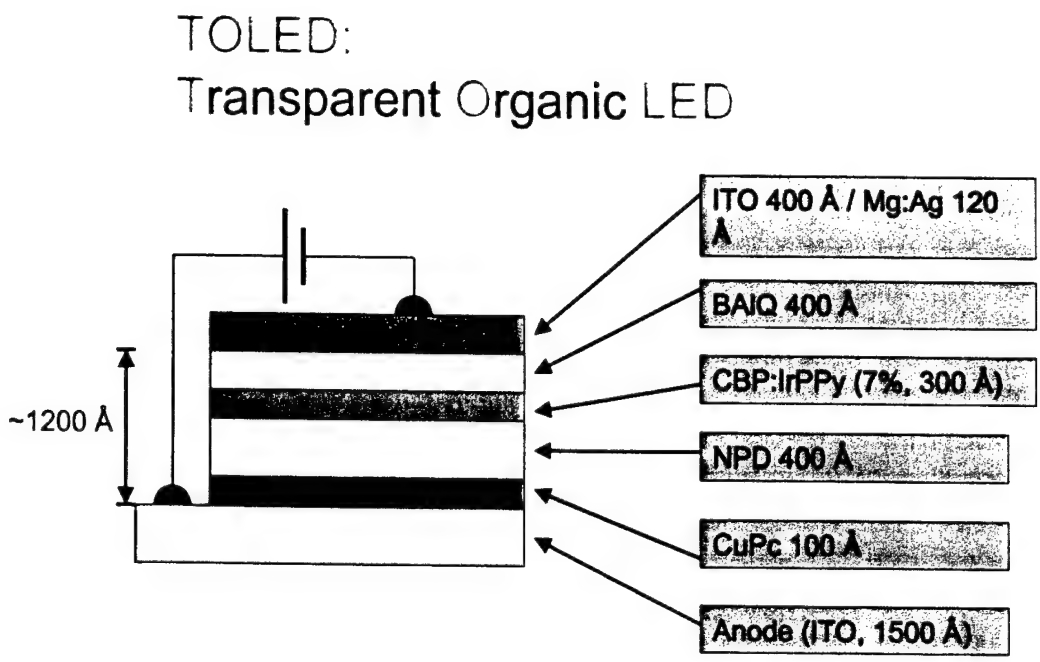

Figure 12: TOLED structure.

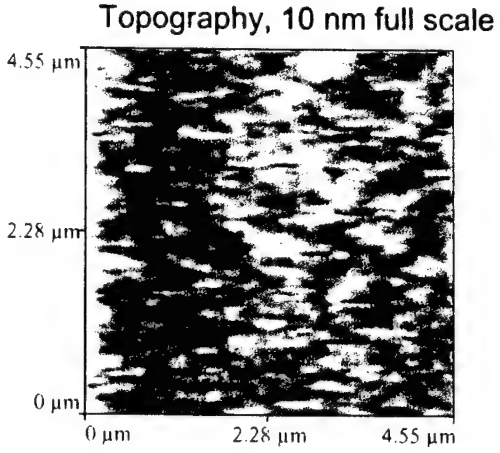

Figure 13: Topographic image of the TOLED device.

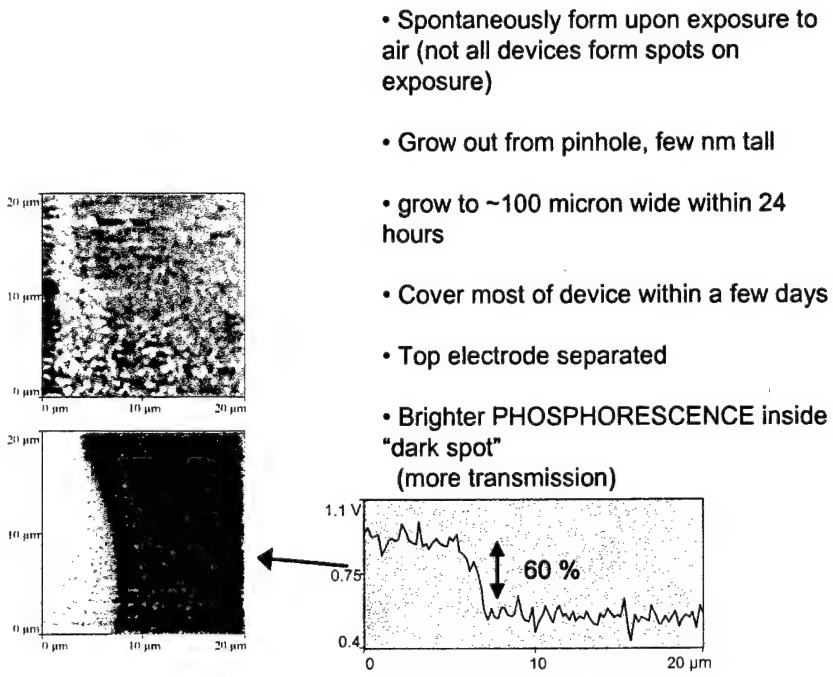

Figure 14: NSOM experiment on dark spot formed by damage of electrode induced by an NSOM tip.

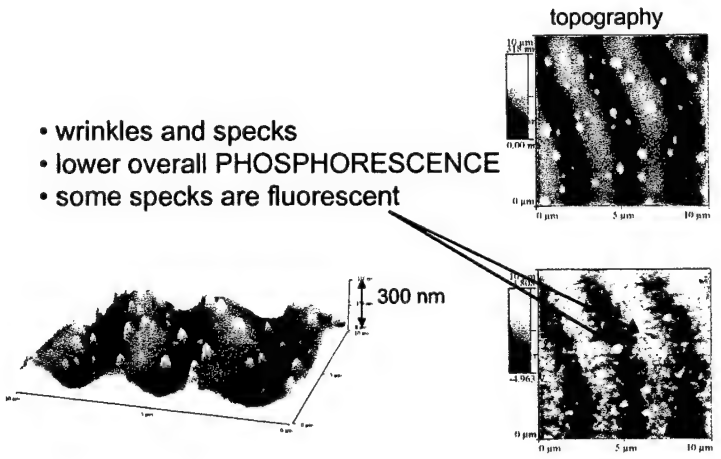

Figure 15: Extreme device damage that occurs when darks spots continue to develop.

3.6 Electrophosphorescent Device Stability

Universal Display Corporation accomplished an operational device stability study of electrophosphorescent display devices as a part of the presently reported effort. A full review of this device stability work is available elsewhere (see Kwong et al. paper listed in Appendix B).

All devices were fabricated by high vacuum (<10^{-7} Torr) thermal evaporation and are illustrated schematically in Figure 1(d). For the PHOLEDs described here that emit from the substrate surface (referred to as bottom emission), the anode electrode is ~1200 Å of ITO. For the top emission devices, the anode is comprised of a reflective stack of 160 Å ITO on silver (Ag) with a glass substrate. The organic stack is comprised of 100-200 Å thick of copper CuPc as HIL, 300-500 Å of α-NPD as the HTL, 300 Å of CBP doped with 4-12 wt% of the phosphorescent emitter as the EML, 100-150 Å of BAlq as the EML-ETL interface layer, and 300-500 Å of Alq_3 as the ETL. The cathode consisted of 10 Å of LiF followed by 1,000 Å of Al for bottom-emission devices. The cathode for the top-emitting PHOLEDs consisted of 200 Å Ca deposited by vacuum thermal evaporation, followed by 800 Å ITO by sputter deposition. For the transparent PHOLEDs, a compound cathode of 100 Å of MgAg (10:1 weight ratio of Mg to Ag) followed by 800 Å of sputtered ITO was used. The active area of all the devices was 5 mm^2. All devices, unless otherwise noted, were encapsulated with a glass lid sealed with an epoxy resin in a nitrogen glove box (<1 ppm of H_2O and O_2) immediately after fabrication, and a moisture getter was incorporated inside the package.

The reflectivities and transmissivities of various anodes and cathodes were measured with a Varian Cary 100 UV-Vis spectrophotometer. The electroluminescence was measured with a Photoresearch PR705 spectrophotometer, and the current-voltage-luminance (J-V-L) characteristics were measured with a Keithley 236 source measure unit and a calibrated Si photodiode. Device operational stabilities, measured on several identically fabricated devices, were determined to be within ±5%. All lifetests were conducted in continuous direct current (DC) drive at room temperature without any initial burn-in periods. Half-life, $T_{1/2}$, is defined as the time for the luminance to decay to 50% of the initial luminance (i.e., $0.5L_0$).

3.6.1 Bottom-Emission PHOLEDs on Glass Substrates

Green PHOLED based on *fac*-tris(2-phenylpyridine)iridium [$Ir(ppy)_3$] as the phosphorescent dopant give a $T_{1/2}$ of 10,000 hours at L_0=500 cd/m^2. In our recent effort to optimize the device, the stability of the $Ir(ppy)_3$ devices projects to $T_{1/2}$~10,000 hours at L_0=600 cd/m^2 (Figure 16). The initial luminous efficiency (LE) was 23.0 cd/A, corresponding to an external quantum efficiency (η_{ext}) of 6.5%. The drive current density of this device was 2.62 mA/cm^2 at an initial voltage of 7.6 V. After 1,000 and 5,000 hours of operation, the device luminance dropped to 88.2% and 67.4% of the initial value respectively. The Commission Internationale de l'Eclairage (CIE) coordinate of the device was (0.30, 0.63) and was essentially unchanged during lifetest. Extrapolating the lifetime at L_0=600 cd/m^2, this $Ir(ppy)_3$ PHOLED has $T_{1/2}$~10,000 hours.

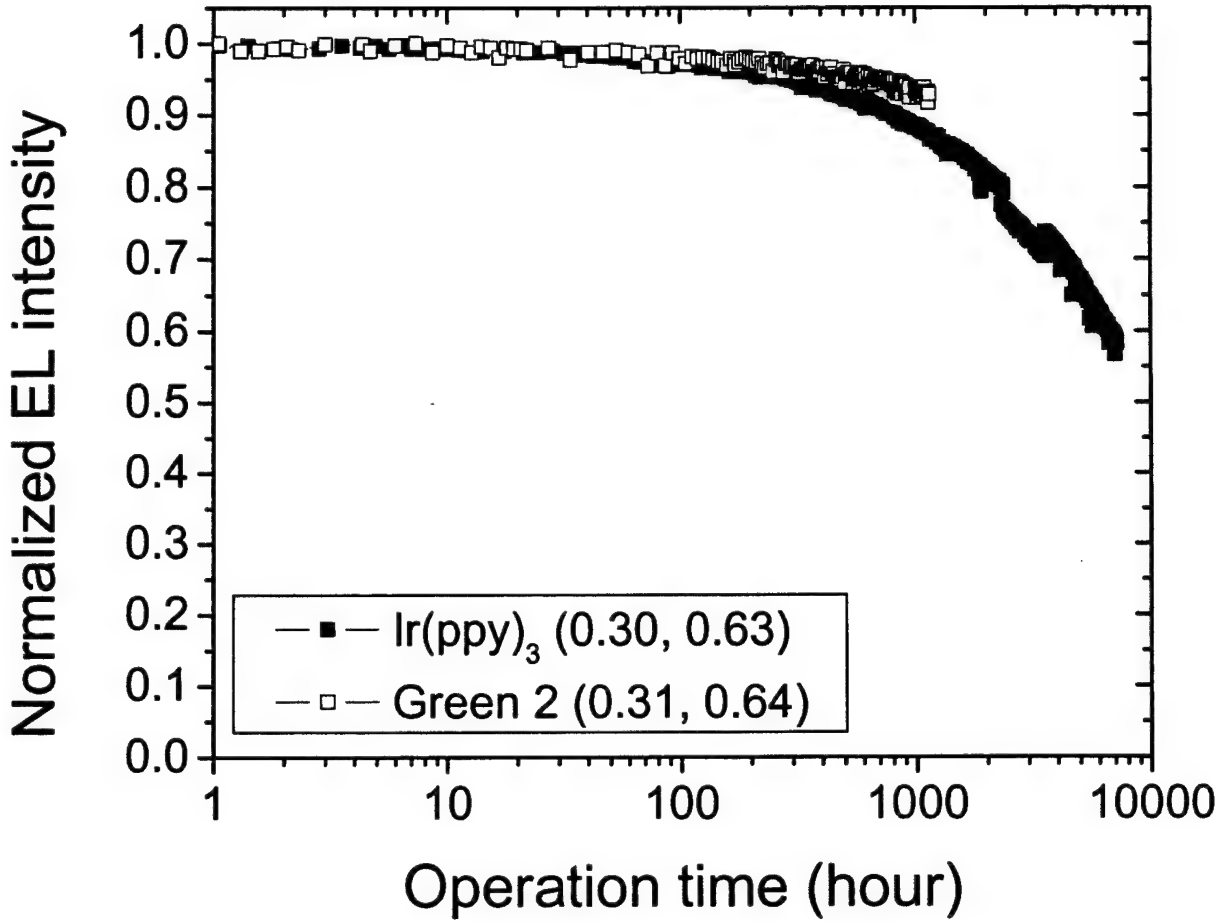

Figure 16: Lifetime of the $Ir(ppy)_3$ and Green 2 PHOLEDs at L_0=600 cd/m^2 (CIE coordinates of each device are in parentheses).

In the more recent work on improving the efficiency and stability for green PHOLEDs, we have developed a new material system with essentially the same spectral characteristics of $Ir(ppy)_3$. This new system, Dopant Green 2, has brought further improvement in both efficiency and lifetime in the green PHOLED family. At 600 cd/m^2, the initial efficiency of this green PHOLED device was 29.3 cd/A (η_{ext}=7.8%). The CIE coordinate was (0.31, 0.64), indistinguishable from the $Ir(ppy)_3$ device by the human eye. At the same initial luminance as the $Ir(ppy)_3$ device, i.e., L_0=600 cd/m^2, it can be seen that the Green 2 device is more stable (Figure 16). The drive current was 2.05 mA/cm^2 at an initial voltage of 8.0 V. After 1,000 hours of operation, the luminance dropped to 93.5% of its initial value, compared to 88.2% of the $Ir(ppy)_3$ device. We expect its $T_{1/2}$ to be ~15,000 hours.

Due to the low photopic response of the human eye to red, and the relatively large contribution of the red in brightness for a balanced white color, the red component constitutes a large portion of the total power consumption for a full color display. It is therefore critical to develop highly efficient red devices with high stabilities. We previously reported a 17.6 cd/A orange-red PHOLED based on iridium(III) bis(2-phenylquinolyl-$N,C^{2'}$)acetylacetonate [$PQ_2Ir(acac)$] as the phosphorescent emitter to have a $T_{1/2}$~5,000 hours at L_0=300 cd/m^2.

We report here more recent results on red PHOLEDs using dopants we refer to as Red 1, Red 2 and Red 3. The efficiencies of these red PHOLEDs are very high. The CIE coordinates, independent of current density, are (0.61, 0.38), (0.61, 0.39), and (0.65, 0.35), respectively. Obviously, Red 1 and Red 2 are orange-red, and Red 3 is red emitting. The luminous efficiency for devices fabricated using these three red PHOLEDs is plotted against the luminance in Figure 17. The efficiencies do not suffer from significant roll-off as observed in some platinum porphyrin red devices. One explanation is the shorter triplet exciton lifetime of the new red phosphorescent dopants (typically <5 μs), leading to reduced T-T exciton annihilation, compared to platinum porphyrins (typically >30 μs). But more importantly, the overall device composition such as the type and thickness of the charge transporting materials, electrode materials, emitter doping concentrations, etc., critically affects the efficiency roll-off, not just the exciton lifetime alone. This hypothesis is well supported by the fact that certain fluorescent small molecule and polymer OLEDs, with very short-lived singlet exciton (typically <10 ns), show the same degree of, or even higher, efficiency roll-off compared to phosphorescent OLEDs. The maximum efficiencies of the Red 1, Red 2 and Red 3 device are 23.9 cd/A at 410 cd/m^2, 18.1 cd/A at 66 cd/m^2, and 12.8 cd/A at 175 cd/m^2, respectively. At 300 cd/m^2, a typical display luminance for the red component in full color displays, the efficiencies are 23.9 cd/A, 17.0 cd/A, and 12.7 cd/A, respectively. Even at 10,000 cd/m^2, high efficiencies of 18.6 cd/A, 9.3 cd/A, and 8.0 cd/A are retained. The performance of these new red materials is summarized in Table 2. The external quantum efficiencies are greater than 10%. The relatively lower luminous efficiency of the Red 3 device is only due to the deeper red color compared to the orange-red color of the Red 1 and Red 2 devices. The outstanding performance at both low and high current drives enables their use in both active and passive modes in displays.

The operational stability of the red devices is very high. The initial luminance for stability testing was selected to be 300 cd/m^2 for all three devices. In Figure 18, the normalized luminance is plotted against the operational time. The drive current was 1.26, 1.80, and 2.36 mA/cm^2 at initial voltages of 8.8, 8.5, and 7.9 V for the Red 1, Red 2 and Red 3 devices, respectively. After 1,000 hours of continuous operation, the luminance was retained respectively at 92.5%, 99.4% and 93.3%. Again, the exact projection of the half-life at this point is difficult; however, in our experience, based on these lifetime trends, $T_{1/2}$>15,000 hours.

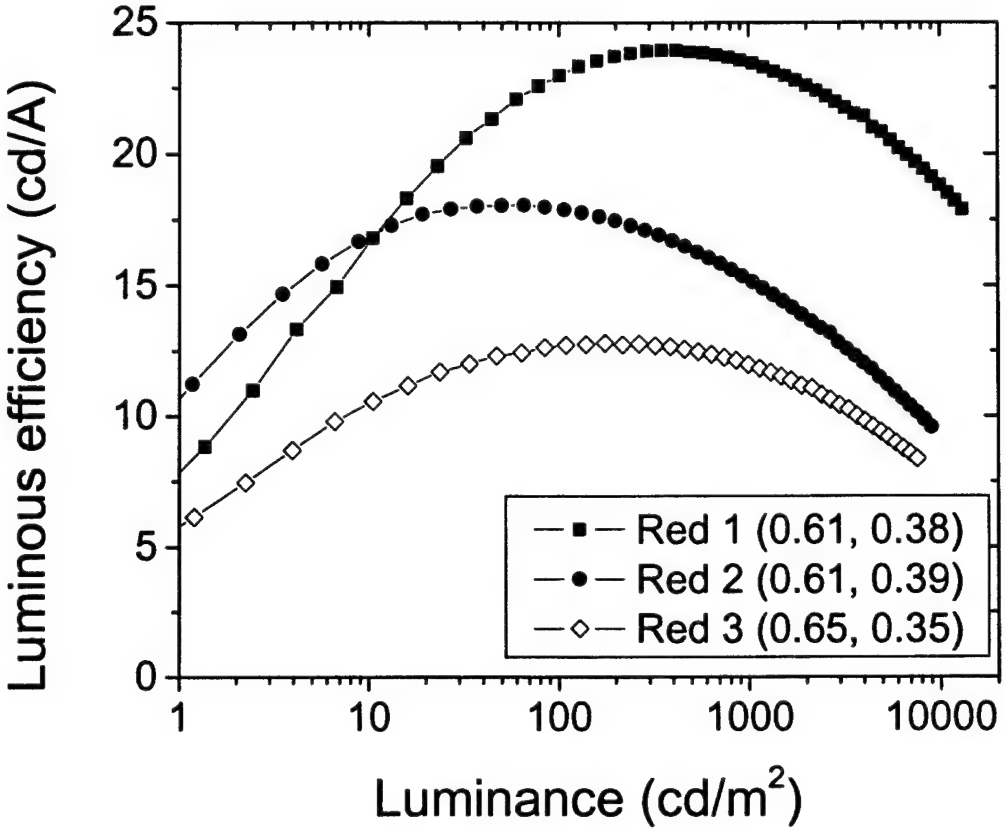

Figure 17: Luminous efficiency *vs* luminance of the Red 1, Red 2, and Red 3 PHOLEDs.

Table 2: Performance summary of Red 1, Red 2, and Red 3 PHOLEDs; efficiency and lifetime are recorded at $L_0 = 300$ cd/m^2.

PHOLED	CIE	η_{ext} (%)	LE (cd/A)	% retained at 1000 hrs
Red 1	0.61, 0.38	13.6	23.9	94.6 at 470 hrs
Red 2	0.61, 0.39	10.6	16.7	94.5
Red 3	0.65, 0.35	11.3	12.7	93.5

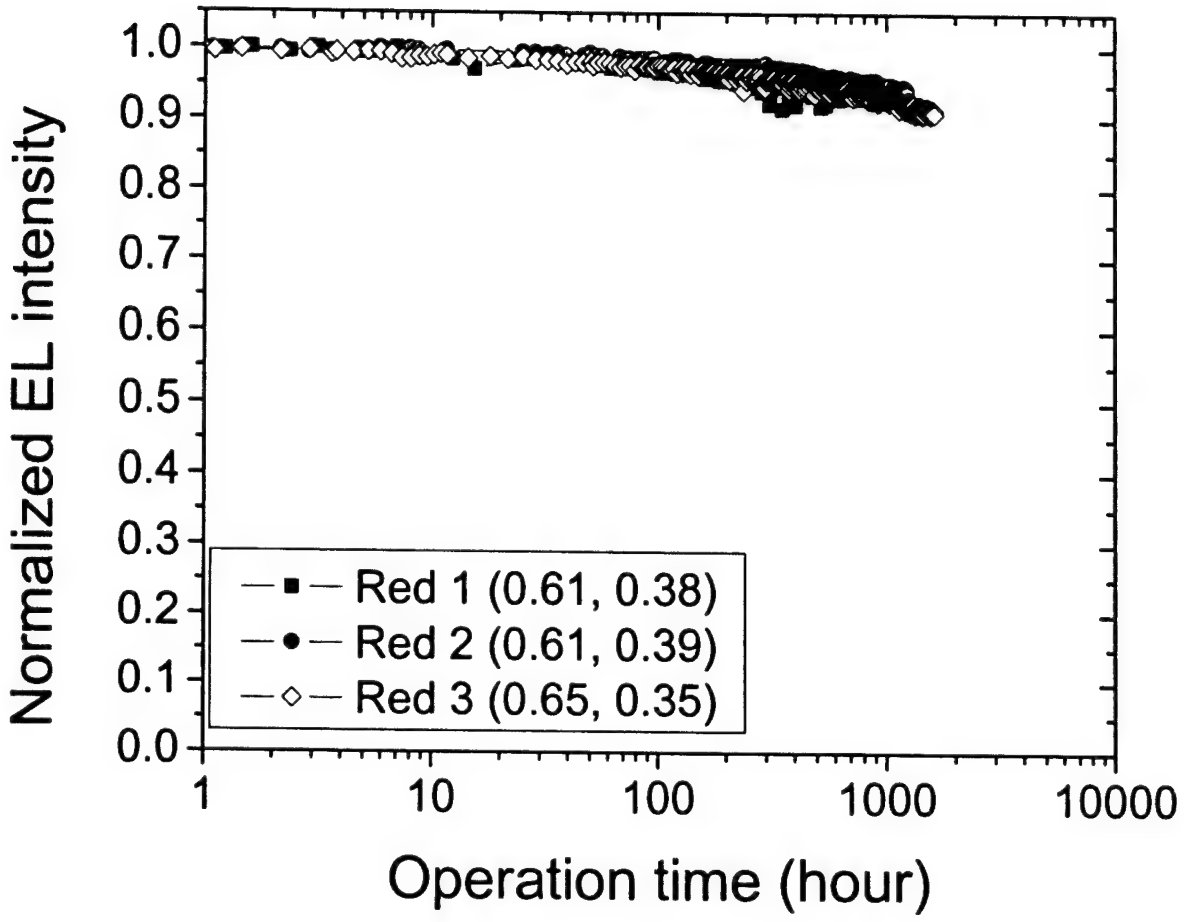

Figure 18: Lifetime of the Red 1 and Red 2, and Red 3 PHOLEDs at L_0=300 cd/m^2 (CIE coordinates of each device are in parentheses).

3.6.2 Transparent Top-Emitting PHOLEDs on Glass Substrates

Conventional OLEDs employ a bottom-emitting structure where the cathode is a reflective metal, the anode is a transparent ITO anode, and light is emitted through the anode and the glass substrate as illustrated in Figure 1(a). While this represents the most mature OLED technology, alternative electrode configurations are possible. Top-emitting OLEDs, with an opaque/reflective bottom anode and a transparent top cathode, as illustrated in Figure 1(c), have been demonstrated by Bulovic et al. in 1997. Top-emitting OLEDs are well suited in high-resolution active-matrix OLED displays where they are deposited over a planarized back-plane, thus increasing the aperture ratio over displays employing bottom-emitting OLEDs. Recently, our group has demonstrated that top-emitting OLEDs can be more efficient than corresponding bottom-emitting OLEDs due to favorable microcavity effects. Another possibility is to use a transparent cathode in conjunction with an ITO anode to make a fully transparent device as illustrated in Figure 4(c) with obvious applications in see-through displays, etc. In this section, we will review recent progress in top-emitting and transparent OLEDs which are enabled by the same transparent cathode technology.

All devices in this section used the $Ir(ppy)_3$ PHOLED standard structure. The emission intensity of top-emitting OLEDs depends strongly on the top ITO layer thickness due to microcavity effects. Both experimental data and modeling indicate that 800Å is the optimal ITO thickness for these green phosphorescent top-emitting OLEDs. The current-voltage-luminance (J-V-L) characteristics of the top and bottom emitting OLEDs are plotted in Figure 19. The J-V curves of the top and bottom emission OLEDs are identical within measurement uncertainties, while the top emission OLED has a slightly higher luminous efficiency. At 10 mA/cm^2 the luminance efficiency is 20.3 cd/A for the bottom emission and 23.1 cd/A for the top emission OLED (through the cover glass), i.e., 15% higher. The transmissivity of glass/Ca (200 Å)/ITO (800 Å) is 62.8% at λ = 515 nm [the peak of $Ir(ppy)_3$ emission], much less than the transmissivity of 89.9% for the ITO coated glass. The reflectivity of the Ag/ITO anodes is 85.5% at λ = 515 nm, again less than that of the aluminum (Al) cathodes at 88.5%. Overall, the electrodes of the bottom emission OLEDs are more reflective/transmissive than those of the top emission ones. Therefore, the enhanced luminance in top emission OLEDs can only be attributed to the more favorable microcavity structure.

The J-V-L curve of the transparent OLED is also shown in Figure 19. The current density at a given bias voltage is lower than that of the top and bottom emission OLED because of the slightly thicker organic layer used and the lower electron injection from the MgAg/ITO cathode. At 10 mA/cm^2, the luminance efficiency is 16.4 cd/A which is based on the sum of the emission from both sides. Approximately 75% of the light is emitted through the ITO anode. The luminance efficiency is lower due to the low transmission of the MgAg/ITO cathode (55% at 515 nm).

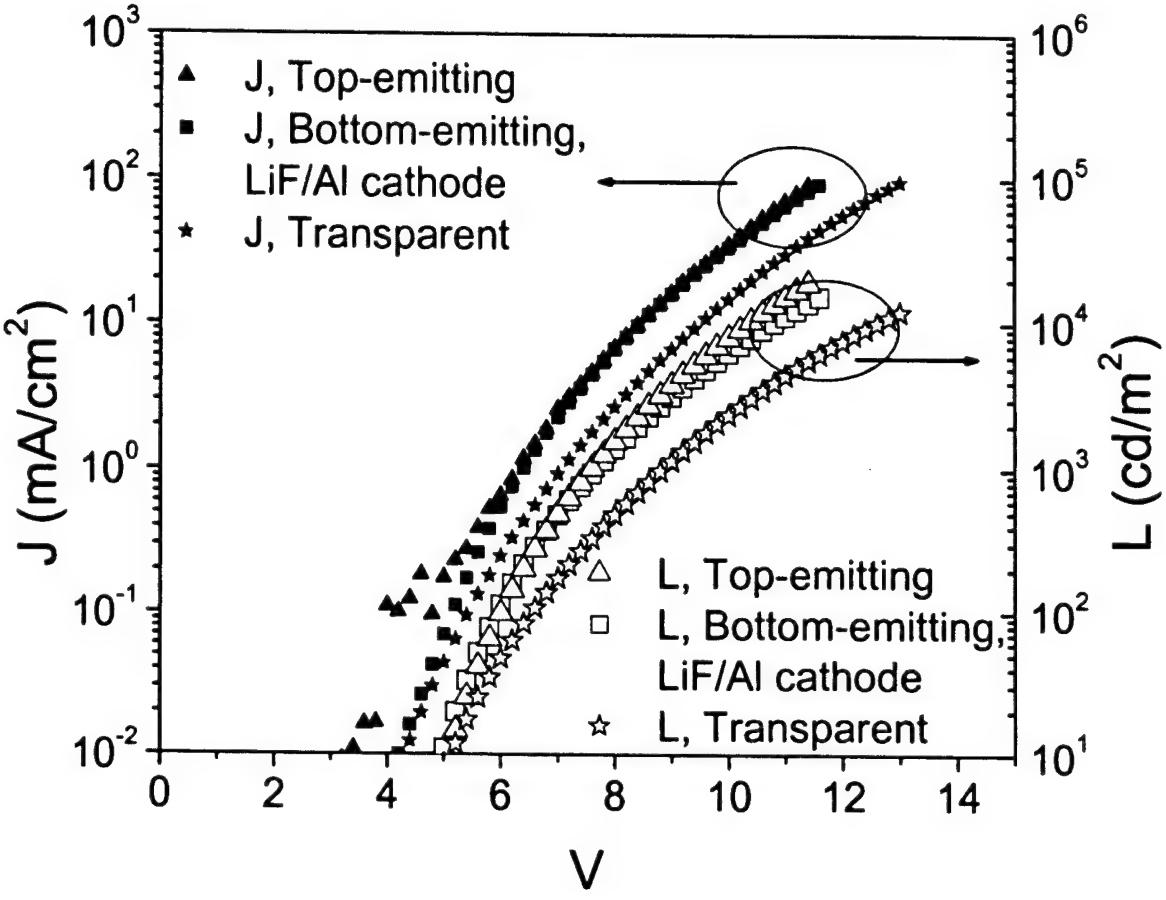

Figure 19: Comparison of J-V-L curves of top-emitting, transparent, and bottom-emitting OLEDs (luminance measured through the cover glass).

The far-field photon radiation from these devices was measured directly with a Photoresearch PR705 spectrophotometer. Due to the relative size of the devices and the focal spot of the spectrophotometer this measurement could be carried out reliably only up to a far-field angle of 60° from normal. Figure 20 shows the angular dependence of photon radiation for the top-emitting OLED (through the cover glass), the same top-emitting OLED corrected for the cover glass, and the corresponding bottom-emitting OLED. In accordance with our predictions, photon radiation is higher in these top-emitting OLEDs even uncorrected for the cover glass. There is only a weak angular dependence which indicates that the emission is approximately Lambertian in this angular range. Estimating the integrated photon flux by the formula $\Sigma I(\theta) \sin(\theta) \Delta\theta$, where $I(\theta)$ is the photon radiation at angle θ, the uncorrected and corrected top emission devices were found to emit 4.2% and 20.8% more photons than the bottom emission OLED in the forward 120° cone, respectively.

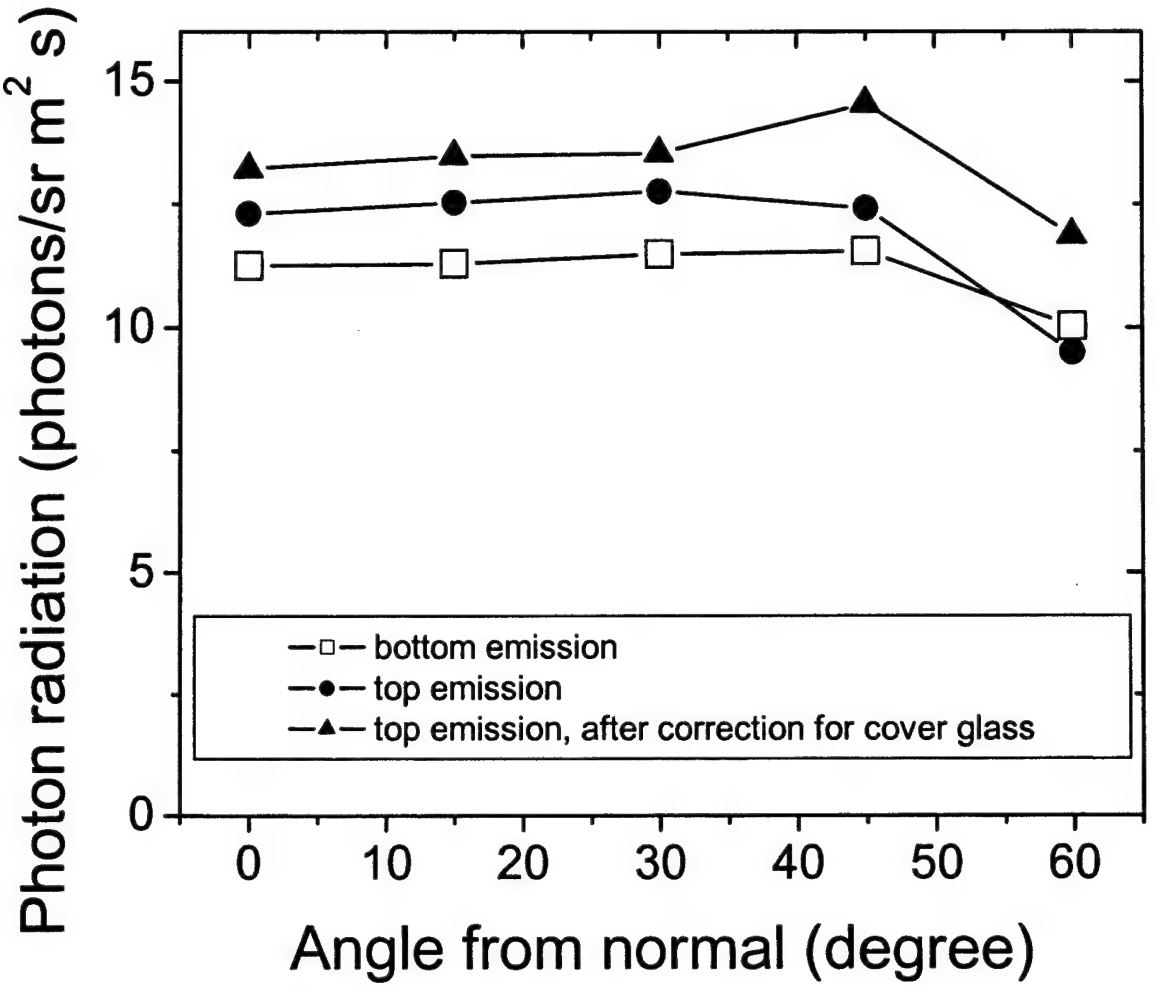

Figure 20: Photon radiation *vs* far-field angle; all data was taken at J = 10 mA/cm^2.

Figure 21 shows DC life-testing results of a typical long-lived bottom-emitting OLED and a transparent OLED with a MgAg/ITO based compound cathode. The initial luminance is 600 cd/m^2 for both devices. For the transparent OLED, it is the sum of the emission from both sides. The current density through the transparent OLED is slightly higher due to the lower external efficiency because of the absorption in the MgAg layer. The bottom-emitting OLED has a half-life of ~10,000 hours, and the transparent OLED is projected to reach over 6,000 hours. The luminance degradation is observed to be Coulombic, i.e., solely dependant upon the aggregate charge flowing through the device ($J_{OLED}\ T_{½\ OLED} \cong J_{TOLED}\ T_{½\ TOLED} \cong$ constant). This has been reported by other groups and indicates the absence of extrinsic decay mechanisms such as dark-spot formation.

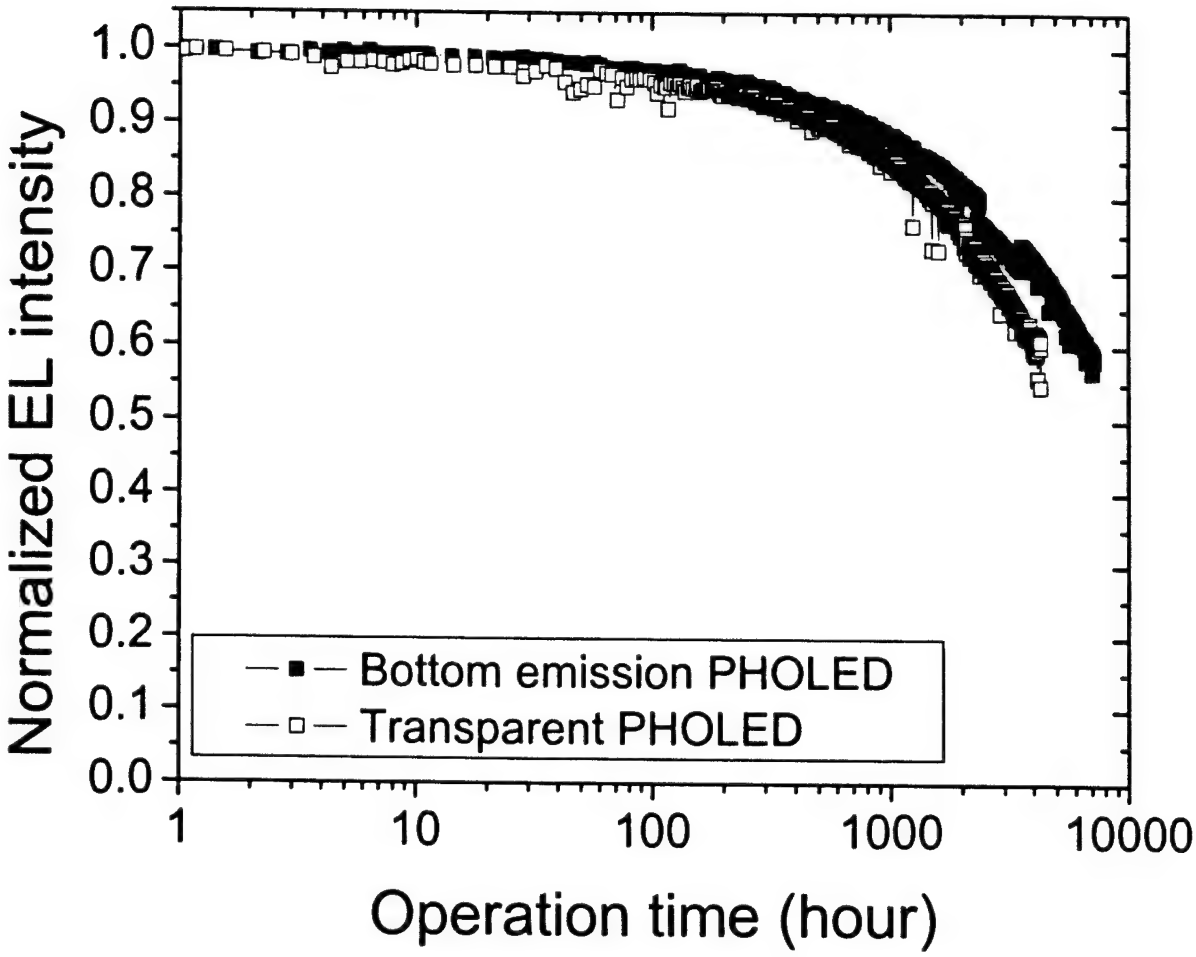

Figure 21: Lifetime of a bottom-emitting and transparent $Ir(ppy)_3$ PHOLEDs with MgAg/ITO cathode.

2.6.3 Bottom Emission PHOLEDs on Flexible Plastic Substrates

Glass substrates do not allow exploitation of the flexibility of both polymeric and small molecule OLEDs to enable new light weight, rugged, flexible displays produced by roll to roll manufacturing. Plastic substrates, however, do allow for such displays. Examples of PHOLEDs grown on flexible substrates are shown in a previous Air Force Research Laboratory report.[7] Although flexible FOLED displays on a plastic substrate have been demonstrated, conventional

[7] Michael Hack, Stephen Forrest, Mark Thompson, Tom Jackson, Robert Praino, David Huffman, ***Ruggedized, Full-Color, Flexible Displays***, Air Force Research Laboratory Technical Report AFRL-HE-WP-TR-2003-0092 (68 pp. (2003). Available from National Technical Information Service, 5285 Port Royal Road, Springfield VA 22161.

encapsulation techniques are ineffective due to moisture permeation through the substrate and long lifetimes had not been shown until recently. To enable a device lifetime of 10,000 hours, the maximum permeability of a substrate to the ingress of water can be estimated within an order of magnitude to be $5x10^{-6}$ g/m^2/day. This is an *estimated upper limit* on the requirement for the substrate and does not take into account any degradation processes at the anode/organic interface or within the organic materials themselves that may be catalyzed by water. Typically, plastic materials have a water vapor permeation rate of 10^{1} to 10^{-1} g/m^2/day at 25°C and are therefore inadequate for OLEDs. Furthermore, a leak rate below 10^{-2} g/m^2/day is difficult to achieve using inorganic barrier layers deposited at or near room temperature, due to pinholes and defects. The high surface roughness of commercially available plastic substrates exacerbates these problems.

Here we present PHOLEDs with extended operating lifetimes using a hybrid organic-inorganic multi-layer barrier coating on 175 μm thick heat stabilized polyethylene terephthalate (PET), demonstrating that suitably processed plastic substrates can be used to fabricate long-lived OLEDs. The composite barrier consists of alternating layers of polyacrylate films and an inorganic oxide. By repeating the alternating films, the polymer layers 'decouple' any defects in the oxide layers. This prevents the propagation of defects through the multilayer structure. The optical and barrier properties of the composite substrate can be tailored by varying the total number and thickness of the polymer and inorganic layers in the thin-film coating, yielding an engineered flexible substrate. The barrier-coated PET substrates exhibit moisture barrier performance below the limit of MOCON, Inc. detection instruments ($5x10^{-3}$ g/m^2/day).[8] More detailed measurements of permeability based on the corrosion of Ca are published elsewhere and indicate a permeation rate through the substrate and barriers estimated to be $4x10^{-6}$ g/m^2/day.

PHOLEDs were fabricated on the barrier coated flexible substrates to test the viability of using them to make long lived flexible displays. Onto the barrier were grown sequentially deposited layers of patterned ITO [160 nm] as the anode contact. All materials and fabrication steps were identical to the $Ir(ppy)_3$ based PHOLED described in the previous section.

The FOLED had a peak luminous efficiency of 17.5 cd/A (η_{ext}=4.8%) at 600 cd/m^2. This is slightly lower than the same device on glass, primarily because of the lower transparency and light outcoupling efficiency due to the thicker ITO and the multilayer barrier coating on the plastic substrate. (Note: more recently, the barrier coated substrates have been further optimized to enable better light outcoupling from the substrate, and plastic substrate devices have shown efficiency comparable to that of glass substrate devices). The lifetime was measured at an initial luminance of 425 cd/m^2 at a current density of 2.5 mA/cm^2. Figure 22 shows a typical plot of normalized luminance versus time for this device. A device fabricated on glass with the same organic and metal layers as the FOLED and encapsulated using the same procedures (i.e., with glass lid) is also shown for comparison. It was driven at 2.6 mA/cm^2 (L_0=600 cd/m^2). After a brief initial rise in luminance during the first 24 hours of testing, the FOLED decays to 50% of its initial luminance in 3,800 hours, as compared to 10,000 hours for equivalent devices made on glass. At 3,800 hours the PHOLED on glass is at 69% of its initial luminance. Assuming lifetime is inversely proportional to drive current, these results correspond to a lifetime of 16,000 hours at

[8] MOCON, Inc, 7500 Boone Ave. N., Minneapolis, MN 55428, (763) 493-6370, mocon@mocon.com.

100 cd/m^2 for the encapsulated plastic device. The shorter lifetime for the devices on the barrier-coated plastic substrate may be partly due to the superior barrier properties of the glass substrates. However, we note that the epoxy exhibited poorer adhesion to the barrier-coated plastic than to the glass; indeed, after ~3,000 hours a high failure rate of the plastic package due to delamination of the lid was observed. Faster diffusion of moisture through the edge seal of the flexible plastic versus glass substrate could therefore contribute to the lifetime enhancement of the glass based pixels.

The same type of multilayer barrier structure used on the PET substrate can also be applied over the PHOLED as a hermetic encapsulant. In this truly flexible (substrate and encapsulation) configuration, the PHOLED is protected on all sides from moisture ingress. Furthermore, no edge seal or glass/metal lid is required, reducing package volume and materials cost. Preliminary results indicate that the lifetime of FOLEDs encapsulated using a multilayer barrier structure approaches that of similarly encapsulated PHOLEDs on glass.

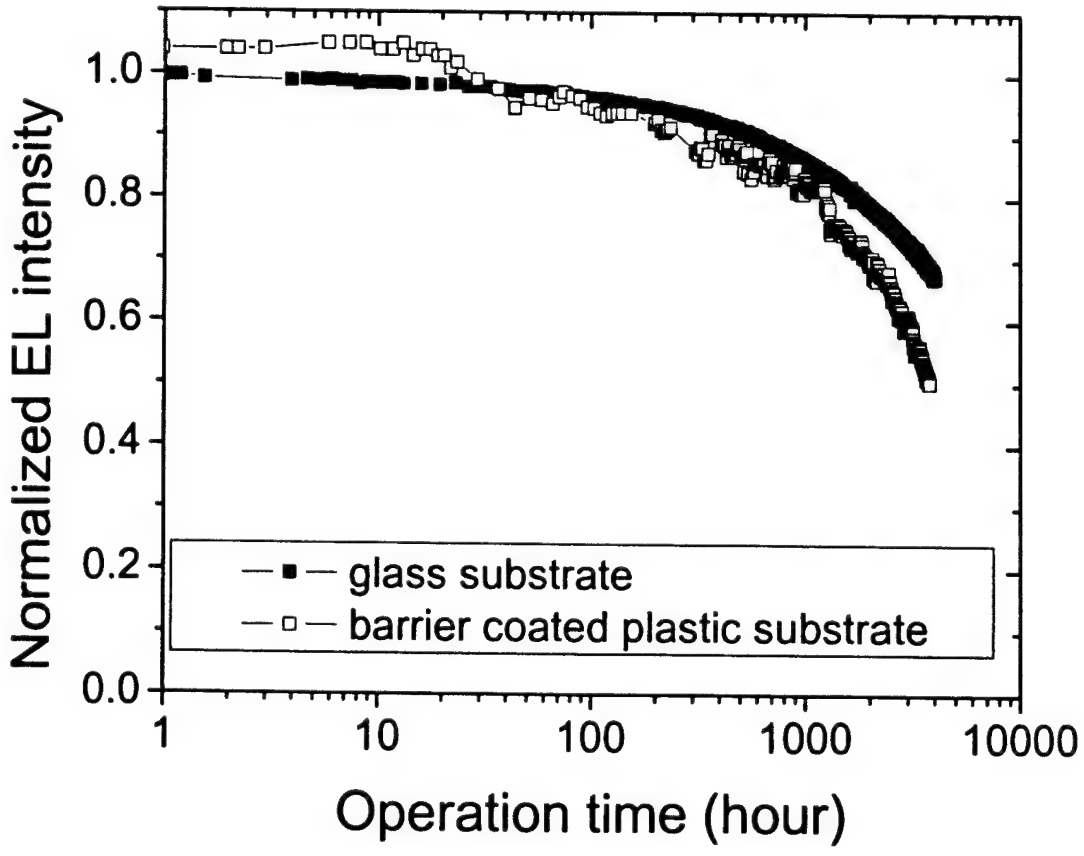

Figure 22: Lifetimes of $Ir(ppy)_3$ PHOLEDs on barrier coated PET (driven at 2.5 mA/cm^2) and ITO coated glass (driven at 2.6 mA/cm^2).

4. DISCUSSION AND CONCLUSIONS

This program has resulted in the establishment of new protocols in the understanding and improvement of OLED device reliability. During the course of this project, vast improvements in PHOLED reliability were demonstrated, with electrophosphorescent green and blue devices now meeting virtually all the demands of modern flat panel display applications. However, much further improvement is required to meet these demands for blue phosphors and fluorophores. Nevertheless, considerable fundamental progress in understanding degradation mechanisms in blue PHOLEDs, with their unique energetic properties, have been made. Finally, new direct observation methods have been developed for observing the evolution of dark spots in OLED cathodes. This work is based on the use of our proprietary transparent cathode technology in conjunction with near field scanning optical microscopy tools.

Inspection of transparent contacts employed the novel combination of NSOM and optical microscopy in conjunction with a TOLED. By microscopic observation of the development and growth of dark spots as a function of time under TOLED operation, we found that all dark spots are present upon device manufacture, and that these dark spots grow with time during operation. The dark spots are associated with dust particles on the substrate that disrupt the metal/organic interface, and leave fractures in the metal surface that permit the ingress of contaminants upon exposure to atmosphere. We have described this work in detail in an article by D. Kosolov, et al., J. Appl. Phys., **90**, 3242 (2001).

Efficient and stable bottom/top emission and flexible PHOLEDs have been demonstrated. Enabled by new phosphorescent materials, bottom emission, long-lived green PHOLEDs showed efficiencies of >29 cd/A. Two orange-red and one red devices showed efficiencies of 23.9 cd/A, 17.0 cd/A, and 12.7 cd/A respectively. All these devices have lifetimes predicted to be >15,000 hours at display brightness. Even at higher brightness, these devices retain very high efficiencies, thus suiting not only active matrix but also passive matrix display operations.

We demonstrated that top-emitting OLEDs employing identical organic layers can be more efficient than conventional bottom-emitting devices due to favorable microcavity effects. Top-emitting OLEDs based on Ag/ITO anodes and Ca/ITO transparent compound cathodes emit 20.8% more photons in the forward 120° cone than corresponding bottom-emitting OLEDs. We also fabricated long-lived transparent OLEDs with MgAg/ITO cathodes which proved that the lifetime is not limited by the sputter deposition of ITO. We expect both types of OLEDs to enable a new generation of displays.

Operational stabilities of high-efficiency green and red electrophosphorescent bottom-emission devices with various emitting dopants were been studied. Operational lifetimes of 10,000 hours or more, operated at an initial brightness of 600 cd/m^2 and 300 cd/m^2 for green and red, respectively, are reported. Operational stabilities of top-emission electrophosphorescent devices and electrophosphorescent devices built on barrier coated plastic substrates have also been studied and show lifetimes >5,000 hours and >2,000 hours, respectively, under display level luminance conditions.

For devices on plastic substrates, in order to realize the barrier properties necessary to prevent degradation of FOLEDs, a novel non-conformal multilayered film was used that reduces the permeation rate of water vapor through a flexible substrate to less than $2x10^{-6}$ g/m^2/day. Based on measurements of an epoxy sealed PHOLED package with a barrier coated PET substrate and glass lid, a $T_{1/2}$ of 3,800 hours from an initial luminance of 425 cd/m^2 was observed.

We also investigated the operational lifetime limitations presented by the HBL. We found that the morphological instabilities of bathocuproine (BCP) were one of the predominant mechanisms leading to a reduction in operating lifetime of high efficiency PHOLEDs. We doped BCP with BAlq, an alternative hole blocker that gives high stability at reduced efficiency. This work has resulted in a patent disclosure, listed in Appendix A, and full details of our results are presented in B. W. D'Andrade, et al., *Appl. Phys. Lett.*, **83**, 3858 (2003).

5. RECOMMENDATIONS

The novel technique of studying OLED devices with a simultaneous combination of NSOM and optical microscopy in conjunction with a TOLED should become a routine technique and should be further improved to increase the pace of OLED research.

Much further improvement in blue phosphors and fluorophores is needed to meet product requirements for the blue phosphorescent material.

Top-emitting structures are more efficient than the traditional bottom-emitting structures due to a quantum cavity effect. This effect should be further developed to decrease the power and increase the reliability of OLEDs in applications.

Our results represent a critical first step in the realization of plastic-based OLEDs for flexible displays. Combined with a conformal encapsulation or lamination technology, which could be based on the same hybrid multilayer stack as used in the present reliability research, flexible and rollable display technology development has been enabled.

Further work should be done on the role of various layers of the OLED structure on the operational lifetime. This study focused primarily on the electrode interfaces and the HBL. These and other layers shown in Figures 1(a) and 1(b) need to be systematically investigated—both in terms of materials and structure.

6. SYMBOLS, ABBREVIATIONS, AND ACRONYMS

AFRL	Air Force Research Laboratory (in Dayton OH)
Al	Aluminum
Alq_3	Tris(8-hydroxyquinolinato) aluminum, aka aluminum trisquinolate (electron transporting layer material; also, the emissive layer in original OLEDs)
AFM	Atomic force microscopy
AM	Active matrix (active element holds desired electrical signal for full frame time), (backplane substrate TFT array used to address AMOLED), (see passive matrix)
AMOLED	Active matrix organic light emitting display
Backplane	Electrical circuitry built on back substrate of a flat panel display to apply electrical representation of an image in a manner (driver-conditioned signals) that modulates/controls photonic emission from each picture element.
BAlq	4-biphenyloxolato aluminum(III)bis(2-methyl-8-quinolinato)4-phenylphenolate, (hole blocking layer material)
Barrier Coating	Multiple alternating layers of polyacrylate films and an inorganic oxide
BCP	2,9-dimethyl-4,7-diphenyl-1,10-phenanthroline (hole blocking layer material), aka "bathocuproine"
Brightness	Psychological dimension in which visual stimuli are ordered continuously from light to dark and which is correlated with light intensity
BSN	Iridium (III) bis(2-(1-naphthyl)benzothiazolato-N,C2') acetylacetonate
BSN*	Iridium (III) bis(2-(1-naphthyl)benzothiazolato-N,C2') 2,2,6,6-tetramethyl-3,5-heptane-dionate
BT	Iridium (III) bis(2-phenyl benzothiozolato-N,C2') acetylacetonate
btIr	A red phosphor based on Iridium
btpIr	A red phosphor based on Iridium
ca.	Calculated
CBP	N,N'-dicarbazolyl-4,4'-biphenyl (host material for emissive layer of device) 4,4'-bis(N-carbazolyl)biphenyl (alternate chemical name)
Candella	Luminous intensity of a source emitting 540 GHz radiation at an intensity of 683^{-1} w sr^{-1} in a given direction.
Cd	Candella
cd/m^2	Candella per square meter (standard unit of luminous intensity per unit area)
cd/A	Candella per Ampere (unit for measuring of luminance efficiency) (unit of energy conversion efficiency in current driven device)
CIE	Commission Internationale de lÉclairage (standard color space coordinates)
$cm^2/V\text{-}s$	Unit of charge mobility (in semiconductor materials subjected to electric field)
CMOS	Complementary metal oxide semiconductor (power-conserving circuit design)
COTR	Contracting Officer's Technical Representative
$Cp^{5}\bullet$	1,2,3,4,5-pentaphenylcyclopentadienyl radical
CRE	Color rendering index
CuPc	Copper phthalocyanine (hole injection layer material)
C^N	mono-anionic cyclometallating ligand
DARPA	Defense Advanced Research Projects Agency
DCM2	Red dye (a fluorescent material)

EBL	Electron blocking layer
EIL	Electron injection layer
EL	Electroluminescent
Electroluminescence	Luminescence resulting from application of electrical energy to a material
Electrophosphorescence	Luminescence caused by application of electrical power (current) via energy excited states similar to, or identical with, those involved in phosphorescence
EP	Electrophosphorescent (material)
EPR	Electron paramagnetic resonance.
ET	Electron transporter (layer within a device structure)
EML	Emissive layer
ETL	Electron transport layer
ETM	Electron transporter material
Firpic	Iridium(III)bis[(4,6-di-fluorophenyl)-pyridinato-$N,C^{2'}$]
Fluorescence	Radiation emitted (usu. visible) resulting from and occurring only during the absorption of radiation (e.g. ultraviolet or two-photon infrared) from some other source. The absorbed radiation (e.g. UV) is often the result of an electrical discharge, with two energy conversions occur (from electrical to UV to visible).
Fluorescent	Glowing as a result of fluorescence
FOLED	Flexible OLED
HBL	Hole blocking layer
HDS	High Definition Systems (applied research program for displays at DARPA)
HOMO	Highest occupied molecular orbital
HIL	Hole injection layer
HRL	Hughes Research Lab (in Malibu CA)
HT	Hole transporter (layer within a device structure)
HTL	Hole transport layer
HTM	Hole transporter material
IJP	Ink jet printing
Inverted OLED	Device with cathode "down" and the anode "up" (opposite to the normal sense of an OLED structure). The direction for observation of emitted light is often through the top (anode) surface.
IP	Intellectual property
Ir	Iridium (atomic element)
Ir complexes	Heavy metal complex dopant, or phosphor, based on Ir
$Ir(ppy)_3$	Iridium tris-(phenyl-pyridine). (Also sometimes written Irppy) *fac*-tris(2-phenylpyridine)iridium (alternative chemical name)
ISB	*bis*-iminostilbene-biphenyl
ISF	N,N'-iminostilbene-4,4'-fluorene
ITO	Indium tin oxide (material for fabrication of transparent, thin-film electrodes)
J-V-L	Current-voltage-luminance (characteristics)
KOH	Potassium hydroxide (etching solution used in thin-film electronics fabrication)
L_o	Initial luminance (value at t = 0 for a newly made display device)
LE	Luminous efficiency (in cd/A)

Li	Lithium
lm	Lumen
lm/W	Lumen per Watt (power conversion efficiency unit for electro-optical device)
Lumen	Unit of luminous flux equal to the light emitted in a unit solid angle by a uniform point source of one candella intensity.
luminance	Luminous intensity of a surface in a given direction per unit of projected area
luminescence	Quality or state of emitting or reflecting usu. steady, suffused, or glowing light
lumophore	luminescent molecule
LX	ancillary bidentate (ligand)
LUMO	Lowest unoccupied molecular orbital
mCP	N,N'-dicarbazolyl-3,5-benzene (a material doped to create a luminescent layer)
MLCT	Metal-ligand charge transfer
MF-TOLED	Metal-free TOLED
MOCON	Name of a company, MOCON, Inc.
MOCVD	Metal oxide chemical vapor deposition
niBr	N-2,6 dibromophenyl-1,8-naphthalimide (electron transporter film material)
α-NPD	4,4'-bis[N-(1-naphthyl)-N-phenylamino]biphenyl (an HTL material)
NPD	N,N'-diphenyl-N,N'dinapthylbenzidine (hole transporting material)
NSOM	Near-field scanning optical microscopy
OLED	Organic light emitting diode (device, display)
OVPD	Organic vapor phase deposition
O^O	diketonate ligand
PET	Polyethylene terephthalate (a plastic flexible substrate material)
PHOLED	Phosphorescent OLED (material structured to have 100% quantum efficiency)
Phosphorescence	Luminance that is caused by the absorption of radiations and continues for a noticeable time after these radiations have stopped; an enduring luminescence without sensible heat. Emission is from an excited state with forbidden direct transition to ground state (i.e. low probability direct optical transitions), (e.g. triplet excited state emissions in most materials).
Phosphorescent	Light emitted involving non-optically allowed transitions
Pixel	Picture element, smallest portion of a display device capably of producing the full range of colors, graylevels, and angular distribution function of the full display
PL	Photoluminescence
PLED	Polymer light emiting diode
PM	Passive matrix (multiplexed electrical addressing scheme involving the sequential application of signals to each pixel of the display device; no active element exists in the display screen to retain the image control signals during frame time), (perception of a complete image relies on the relatively slow chemistry in the retina of the human eye to create an illusion that the entire image is present), (OLED light emission occurs only at moment control signal is applied to pixel). is present), (requires higher peak power or current at each pixel).
PMOS	Positively-doped-channel metal oxide semiconductor
POEM	Center for Photonics and Optoelectronic Materials (at Princeton University)
PQ	Iridium (III) bis(2-phenylquinolyl-N,C2') acetylacetonate
$PQ_2Ir(acac)$	Iridium(III) bis(2-phenylquinolyl-$N,C^{2'}$)acetylacetonate (orange-red PH dopant)

ppm	Parts per million
ppy	Phenyl pyradine (a ligand molecule used in forming dopants, aka phosphors)
Pt	Platinum (atomic element)
Pt complex	Heavy metal complex dopant, or phosphor, based on cyclometalated Pt
PU	Princeton University (in Princeton NJ)
RMS	Root-mean-square
Sheet Resistance	Ratio of material resistivity to sheet thickness (in Ω/□)
Si	Silicon (atomic element)
SOI	Silicon on insulator
SOLED	Stacked OLED
$T_{1/2}$	Half-life (in hours)
T_g	Glass transition temperature
TiN	Titanium nitride
TiW	Titanium tungsten
TFT	Thin film transistor
TOLED	Transparent OLED
Torr	Unit of pressure
TCE	Trichloroethylene
tCP	1,3,5-tri-(N-carbazolyl)benzene
TPD	N,N-di-(3-methylphenyl)-N,N diphenyl-4,4-diaminobiphenyl
TPP	5,10,15,20-tetraphenylporphyrin
T-T	Triplet-triplet (annihilation)
TT	Technology Transfer (to industry), Technology Transition (to defense) application
UTA	University of Texas at Austin (in Austin TX)
UDC	Universal Display Corporation (in Ewing NJ)
UGH	Ultrawide-energy gap host
USC	University of Southern California (in Los Angeles CA)
UV	Ultraviolet
WOLED	White OLED
α-NPD	4,4'-bis[N-(1-naphthyl)-N-phenylamino]biphenyl (an HTL material)
ϕ	C_6H_5 (phenyl unit)
η_{ext}	External quantum efficiency
λ_{max}	Wavelength at which maximum light emission is observed
Ω	Ohm, standard unit of electrical resistance
□	Ratio L/W of the length, L, to the width, W, of a thin-film conductor
Ω/□	Unit of sheet resistance: ratio of material resistivity to thin-film thickness
$^1O_2$	Singlet oxygen (molecule)

APPENDIX A.
LIST OF PATENTS RESULTING FROM THIS DARPA-SPONSORED GRANT

1. 03-1990-1, Princeton University Invention Disclosure, "Doping to Extend Reliability"
Inventors: Anna Chwang, Brian D'Andrade, Stephen Forrest
Assignee: Princeton University
Application No. Serial No. 10/680,065 filed 10/6/2003

APPENDIX B.
LIST OF TECHNICAL JOURNAL PUBLICATIONS RESULTING FROM THIS DARPA-SPONSORED GRANT

(cumulative, chronological, including papers in press or planned)

1. "Direct observation of structural changes in organic light emitting devices during degradation," D. Kolosov, D. S. English, V. Bulovic, P. F. Barbara, S. R. Forrest and M. E. Thompson, *J. Appl. Phys.*, **90**, 3242 (2001).

2. "Extremely efficient red electrophosphorescent devices," Raymond C. Kwong, Matthew Nugent, Tan Ngo, Kamala Rajan, Lech Michalski, Yeh-Jiun Tung, Julie J. Brown, Proceedings of the 21st International Display Research Conference in conjuction with the 8th International Display Workshops (2001), 1774.

3. "Bis-Cyclometallated Ir(III) Complexes as Efficient Singlet Oxygen Sensitizers," Ruomei Gao, David G. Ho, Billy Hernandez, Matthias Selke, Drew Murphy, Peter I. Djurovich, Mark E. Thompson, *Journal of the American Chemical Society,* **2002**, *124(50),* 14828-14829

4. "1,8-Napthalimides in Phosphorescent Organic LED's: The Interplay Between Dopant, Exciplex, and Host Emission," Dmitry Kolosov, Vadim Adamovich, Peter Djurovich, Mark. E. Thompson, and Chihaya Adachi, *Journal of the American Chemical Society*, **2002**, *124(33)*, 9945-9954.

5. "High operational stability of electrophosphorescent devices," R. C. Kwong, M. R. Nugent, L. Michalski, T. Ngo, K. Rajan, Y-J Tung, M. S. Weaver, T. X. Zhou, M. Hack, M. E. Thompson, S. R. Forrest, and J. J. Brown, *Appl. Phys. Lett.*, **81**, 162 (2002).

6. "Blue organic electrophosphorescence using exothermic host-guest energy transfer," R. J. Holmes, S. R. Forrest, Y.-J. Tung, R. C. Kwong, J. J. Brown, S. Garon and M. E. Thompson, *Appl. Phys. Lett.*, **82,** 2422 (2003).

7. "Efficient deep blue organic electrophosphorescence by guest charge trapping," R. J. Holmes, B. W. D'Andrade, S. R. Forrest, X. Ren, J. Li and M. E. Thompson, *Appl. Phys. Lett.*, **83**, 3818 (2003).

8. "Operational stability of electrophosphorescent devices containing *p* and *n* doped transport layers," B. W. D'Andrade, S. R. Forrest and A. B. Chwang, *Appl. Phys. Lett.*, **83**, 3858 (2003).

9. "Current Status of Electrophosphorescent Device Stability," Raymond C. Kwong , Michael S. Weaver, M.-H. Michael Lu, Yeh-Jiun Tung, Anna B. Chwang, Theodore X. Zhou, Michael Hack, and Julie J. Brown, *Organic Electronics* **4**, 155-165 (2003).

10. A. B. Chwang, M. A. Rothman, S. Mao, R. Hewitt, M. S. Weaver, J. A. Silvernail, K. Rajan, M. Hack, J. J Brown, X. Chu, L. Moro, T. Krajewski, N. Rutherford, *Applied Physics Letters* **83** (3), 413-415 (2003).

APPENDIX C.
LIST OF PROFESSIONAL PERSONNEL ASSOCIATED WITH THIS EFFORT

Persons who contributed to technical work on this effort are listed by institution below.

Princeton University
Steve Forrest, Department of Electrical Engineering, Principal Investigator
Russel Holmes, Department of Electrical Engineering, Research Assistant
Brian D'Andrade, Department of Electrical Engineering, Research Assistant
Jiangeng Xue, Department of Electrical Engineering, Research Assistant
Shashank Agashe, Department of Electrical Engineering, Research Assistant
Marc Baldo, Department of Electrical Engineering, Research Associate

University of Southern California
Mark Thompson, Department of Chemistry, Subcontractor Principal Investigator
Peter Djurovich, Department of Chemistry, Research Associate
Steve Cordero, Department of Chemistry, Research Associate
Dmitry Kolosov, Department of Chemistry, Research Assistant
Azad Hassan, Department of Chemistry, Research Assistant
Vadim Adamovich, Department of Chemistry, Research Assistant
Simona Garon, Department of Chemistry, Research Assistant
Xiaofan Ren, Department of Chemistry, Research Assistant
Drew Murphy, Department of Chemistry, Research Assistant

University of Texas at Austin
Paul Barbara, Department of Chemistry and Biochemistry, Subcontractor Principal Investigator
Doo Young Kim, Department of Chemistry and Biochemistry, Research Assistant
Jason McNeill, Department of Chemistry and Biochemistry

Universal Display Corporation
Julie Brown, Chief Technology Officer, Subcontractor Principal Investigator
Yeh Tung, Research Engineer
Ray Kwong, Research Engineer
Anna Chwang, Research Engineer

APPENDIX D.
LIST OF ADVANCED DEGREES AWARDED
FOR RESEARCH ACCOMPLISHED UNDER THIS GRANT

Advanced degrees awarded in association with research sponsored under this grant are listed below by institution in the following format: (date, recipient, type of degree, thesis title).

Princeton University:
none.

University of Southern California:

2001, Dmitry Kolosov, "1,8-Napthalimides as Novel Materials for Phosphorescent Organic Light Emitting Devices and Degradation Studies of Transparent Light Emitting Devices."

2002, Vadim Adamovich, Ph.D., "Novel Materials and Techniques of Fabrication for Organic Light Emitting Diodes."

University of Texas at Austin:
none.

APPENDIX E.
JUNE 11, 2003 FINAL REVIEW MATERIALS

Investigations of the Operational Lifetime and Modes of Failure of Organic Light Emitting Devices

Final Program Review
June 11, 2003

Princeton **University**/USC/Universal Display Corp./UT

DARPA/W-P Reliability Program Final Review

Place: Princeton University
Date: June 11, 2003
Time: 9 am-12:30 pm

9:00-9:15: Overview of OLEDs and Program Objectives (Forrest)
9:15-9:40: Reliability and photophysical degradation of PHOLEDs and conductivity doped PHOLEDs (D'Andrade)
9:40-9:55: Issues with blues
10:00-10:45: Environmental effects (Thompson)
10:45-11:30: Long term reliability of blue PHOLEDs and FOLEDs (Brown)
11:30-12:00 Tools and visualization of cathode degradation (Barbara)
12:00-12:30: Discussion (All)

Objectives

- To develop methods for the determination of long term failure modes of OLEDs
- To determine the primary sources of OLED failure
- To eliminate or reduce failure mechanisms active in OLEDs

Programmatic Details

- Start date: April 1, 2001
- End Date: June 1, 2003
- Program Total: $700,000
- Contract No.: MDA972-01-1-0032

(UDC contract expired January 1, 2003)

Team

- Princeton University: Steve Forrest (PI)
  - Russel Holmes
  - Brian D'Andrade
  - Jiangeng Xue
  - Shashank Agashe
  - Marc Baldo (post-doc)
- USC: Mark Thompson
  - Peter Djurovich
  - Dmitry Kolosov
- Universal Display Corp.: Julie Brown
  - Yeh Tung
  - Ray Kwong
  - Anna Chwang
- University of Texas: Paul Barbara
  - Doo Young Kim
  - Jason McNeill

Methods for Investigating OLED Failure

- Lifetime ≡ $(\tau_{1/2})_{EL}$
- Failure Modes :

1. Mechanical : cathode delamination
2. Thermal : device heating, molecular bond breaking
3. Electrical : current leading to heating, charge imbalance (OLEDs)
4. Chemical : unstable excited species, reaction with air

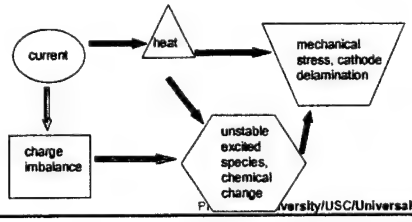

Methods

- Choose model system (blue PHOLEDs, conductivity doped PHOLEDs)
- Standardize OLED fab. processes
- Measure photophysical degradation
- Measure electrically induced degradation
  - Hole only and electron only devices
- Change chemical compositions in systematic fashion to solve problems
  - Dopants, blockers, hosts
- Use NSOM for examination of cathode and other physical defects and effects on lifetime using TOLED platform

The blue difference

- Endothermic vs. exothermic energy transfer
- Non-blocking structures
- New chemistry

Energy transfer rates and directions

Forward (exothermic) transfer

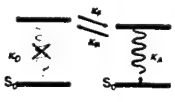

- Donor energy > Acceptor energy
- $\kappa_F \sim \kappa_A > \kappa_R, \kappa_D$
- Radiative rate determined by κ_A
- Route for red and emission

Reverse (endothermic) transfer

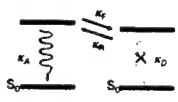

- Acceptor energy ~ Donor energy
- $\kappa_F \sim \kappa_R > \kappa_A > \kappa_D$
- Radiative rate determined by κ_A, κ_R
- Route for and blue emission

Baldo & Forrest, PRB 62, 10958 (2000)

Exothermic energy transfer: Reduced Temperature Dependence

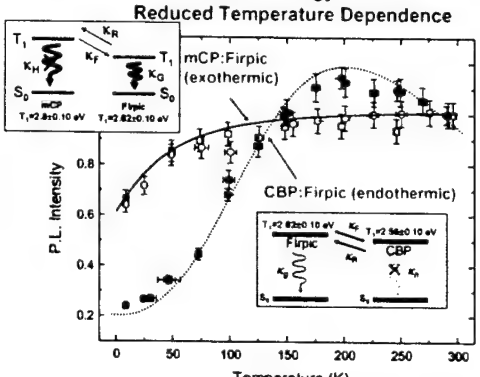

Princeton Accomplishments

- Developed methods to observe photophysical degradation in new dopants and structures.
  - Transferred to UDC
- Developed use of TOLEDs for visualizing dark spot evolution (USC, UT).
- Developed blocker doping to improve stability (UDC).
- Investigated new blocker/dopant combinations to achieve charge balance in blues (USC).
- Developed high power efficiency conductivity doped PHOLEDs and investigated operational lifetime for first time.
- Worked closely with all partners to integrate results and conclusions

p-i-n devices

- Low voltage devices with high power efficiency
- Low voltage inverted structures
- Ultra-thin emissive layers (50Å)
- *p* and *n* doped organic layers
  - low contact resistance
  - high conductivity

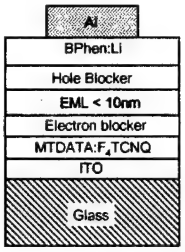

POEM

PIN device characteristics

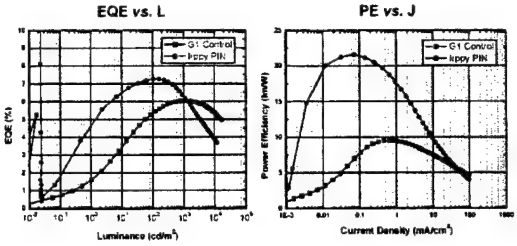

PIN device characteristics

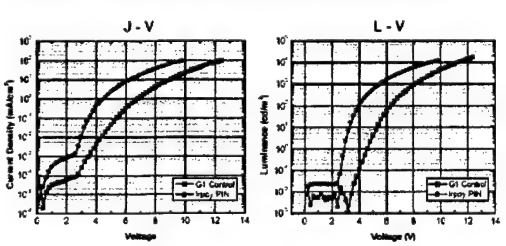

POEM

p-i-n devices

Stability issues with *p-i-n* device

- BPhen phase change
  Note: BPhen:Li/Cs is the best combination for n-doped organic
- Li diffusion
- Confinement of excitons and charge in thin EML

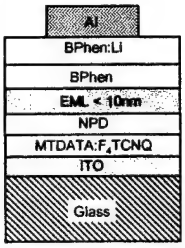

POEM

BPhen Crystallization

Si substrate / BPhen

Si substrate / BPhen:Li / BPhen

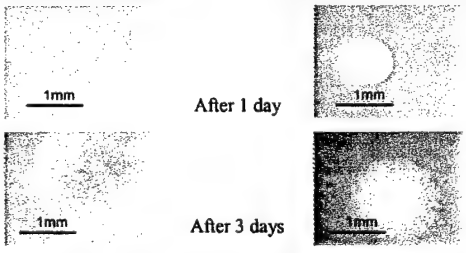

After 2 weeks, substrates completely covered

POEM

BPhen Crystallization

Si substrate / BPhen

Si substrate / BPhen:Li

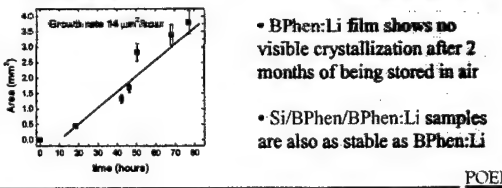

- **BPhen:Li film shows no visible crystallization after 2 months of being stored in air**
- **Si/BPhen/BPhen:Li samples are also as stable as BPhen:Li**

POEM

The glass transition temperature

- T_g of a thin film can be modified by mixing

$$\frac{1}{T_g} \approx \frac{w_a}{T_{g,a}} + \frac{w_b}{T_{g,b}}$$

BPhen (Tg = 62°C)+ BAlq (Tg = 92 °C)

- Modification of molecular structure of material
  Incorporate bulky constituents on parent structure

POEM

Mixed HBL, BPhen:BAlq

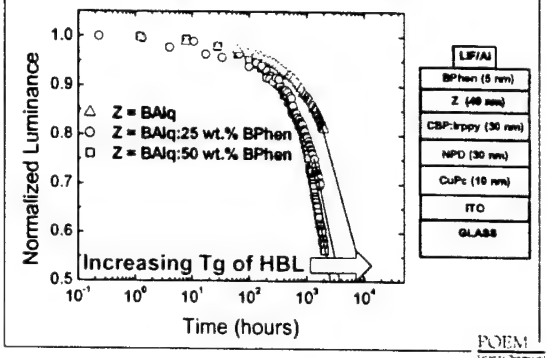

POEM

Mixed HBL, BPhen:BAlq

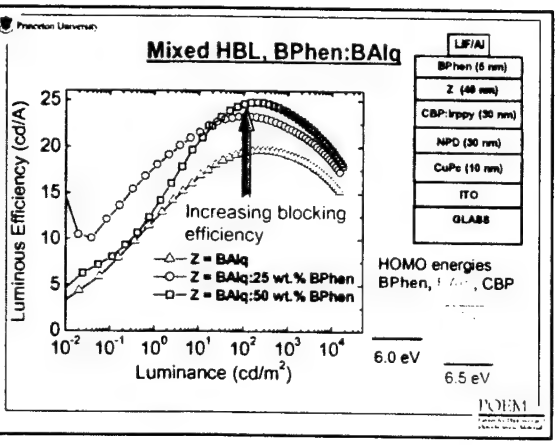

POEM

No change in J-V with mixed HBL

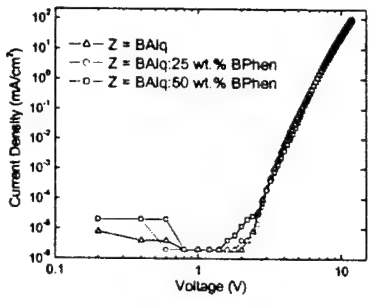

POEM

Figure 2 D'Andrade et al

Structures of derivatives of 4,7-diphenyl-1,10-phenanthroline

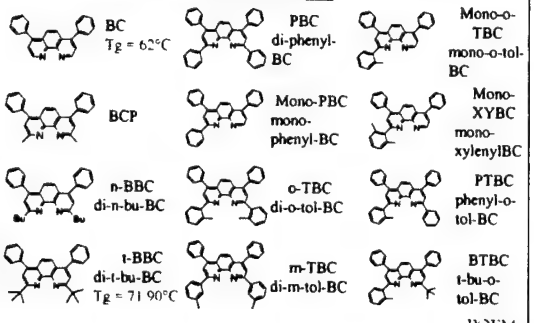

POEM

Tg of derivatives of 4,7-diphenyl-1,10-phenanthroline

Compound name	BCP	n-BBC	t-BBC	PBC	Mono-PBC	o-TBC
T_g(°C)			71.90		93.24	80.36
T_m(°C)	287	140	178	332	240	221
Compound Name	m-TBC	Mono-oTBC	Mono-XYBC	PTBC	BTBC	
T_g(°C)	90.52	83.47	99.33	50.26	70.18	
T_m(°C)	235			206		

POEM

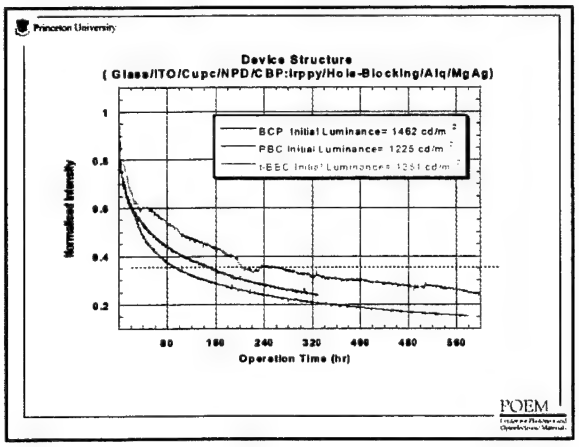
Princeton University
Device Structure
(Glass/ITO/Cupc/NPD/CBP:Irppy/Hole-Blocking/Alq/MgAg)
BCP Initial Luminance= 1462 cd/m
PBC Initial Luminance= 1225 cd/m
Normalized Intensity
Operation Time (hr)
POEM

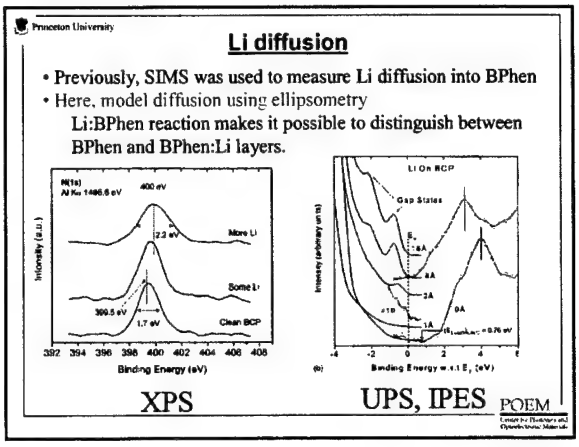
Princeton University
Li diffusion
• Previously, SIMS was used to measure Li diffusion into BPhen
• Here, model diffusion using ellipsometry
Li:BPhen reaction makes it possible to distinguish between BPhen and BPhen:Li layers.
More Li
Some Li
Clean BCP
Binding Energy (eV)
Li On BCP
Gap States
XPS
UPS, IPES
POEM

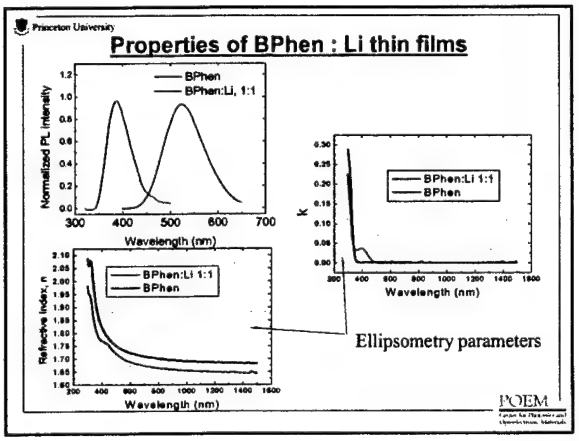
Princeton University
Properties of BPhen : Li thin films
BPhen
BPhen:Li, 1:1
Normalized PL Intensity
Wavelength (nm)
BPhen:Li 1:1
BPhen
Refractive Index, n
k
Ellipsometry parameters
POEM

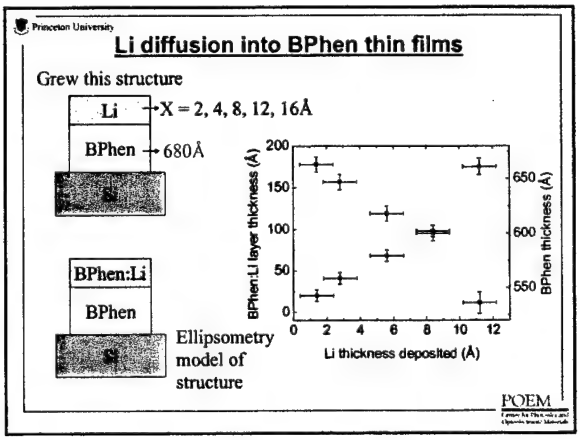
Princeton University
Li diffusion into BPhen thin films
Grew this structure
Li
X = 2, 4, 8, 12, 16Å
BPhen
680Å
BPhen:Li
BPhen
Ellipsometry model of structure
BPhen:Li layer thickness (Å)
BPhen thickness (Å)
Li thickness deposited (Å)
POEM

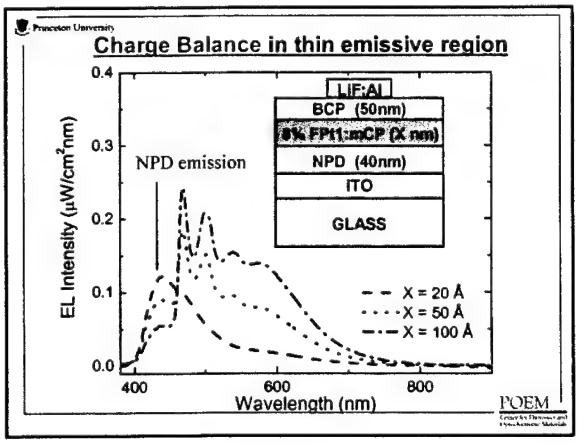
Princeton University
Charge Balance in thin emissive region
LiF:Al
BCP (50nm)
5% FPt1:mCP (X nm)
NPD (40nm)
ITO
GLASS
NPD emission
EL Intensity (μW/cm²nm)
X = 20 Å
X = 50 Å
X = 100 Å
Wavelength (nm)
POEM

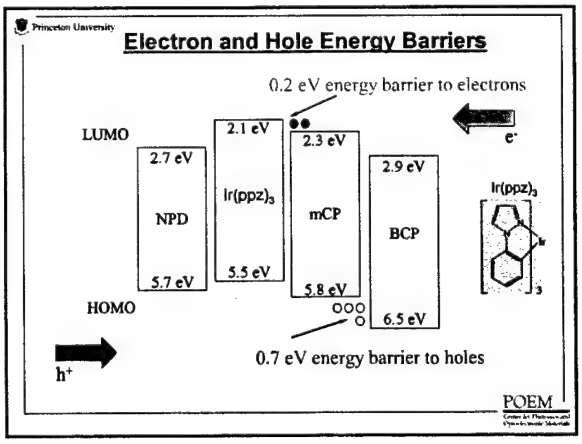
Princeton University
Electron and Hole Energy Barriers
0.2 eV energy barrier to electrons
LUMO
HOMO
2.7 eV
NPD
5.7 eV
2.1 eV
Ir(ppz)3
5.5 eV
2.3 eV
mCP
5.8 eV
2.9 eV
BCP
6.5 eV
e⁻
h⁺
0.7 eV energy barrier to holes
POEM

Electron Blocking Layer

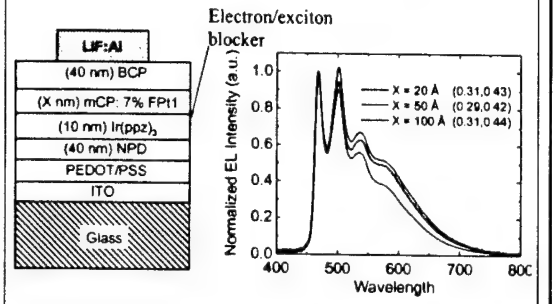

POEM

Theory

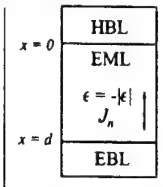

Approximations:
- Constant electric field within EML
- Rate of generation of excitons is primarily dependent on the concentration of electrons

$$\frac{k_B T}{q}\mu_n \frac{d^2 n}{dx^2} - |F|\mu_n \frac{dn}{dx} - \frac{n}{\tau_n} = 0, \quad 0 < x < d$$

Boundary Conditions:

$$J_n^{inj} = -q\mu_n n(0)|F| + k_B T \mu_n \left.\frac{dn}{dx}\right|_{x=0} \quad at\ x = 0$$

$$-q\mu_n n(d)|F| + k_B T \mu_n \left.\frac{dn}{dx}\right|_{x=d} = -q\mu_n n(d)|F|\theta \quad at\ x = d$$

Solve for n:

$$n(x) = n_1 \exp(-x/L_1) + n_2 \exp(x/L_2)$$

POEM

Electron Density within EML

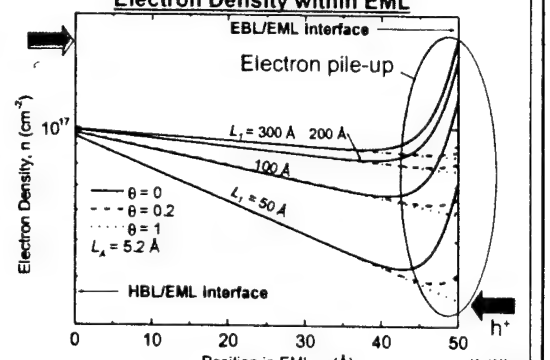

POEM

Voltage versus EML thickness

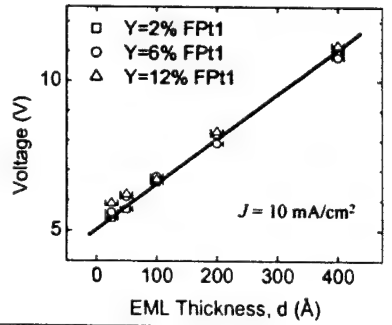

POEM

EQE versus EML thickness

- Lines are fits to theory
- Optimal conc. of dopant
- Confinement of charge and excitons <100%

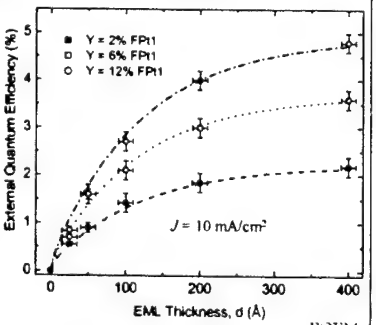

POEM

p-i-n Device Stability

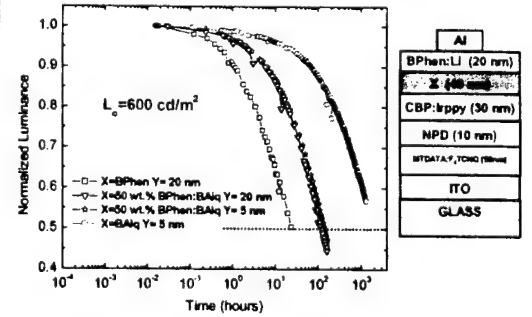

POEM

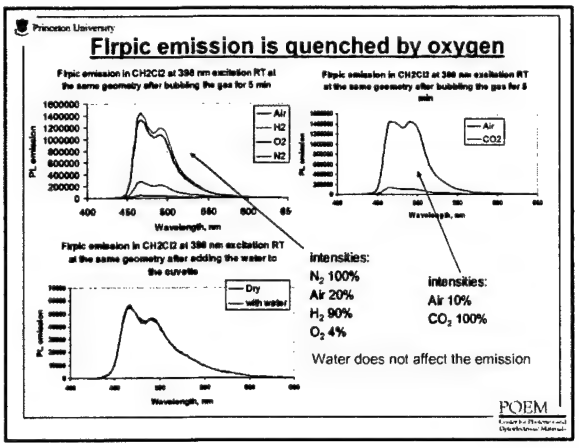
Princeton University
FIrpic emission is quenched by oxygen
FIrpic emission in CH2Cl2 at 398 nm excitation RT at the same geometry after bubbling the gas for 5 min
Air
H2
O2
N2
FIrpic emission in CH2Cl2 at 398 nm excitation RT at the same geometry after bubbling the gas for 5 min
Air
CO2
FIrpic emission in CH2Cl2 at 398 nm excitation RT at the same geometry after adding the water to the cuvette
Dry
with water
Wavelength, nm
intensities:
N2 100%
Air 20%
H2 90%
O2 4%
intensities:
Air 10%
CO2 100%
Water does not affect the emission
POEM

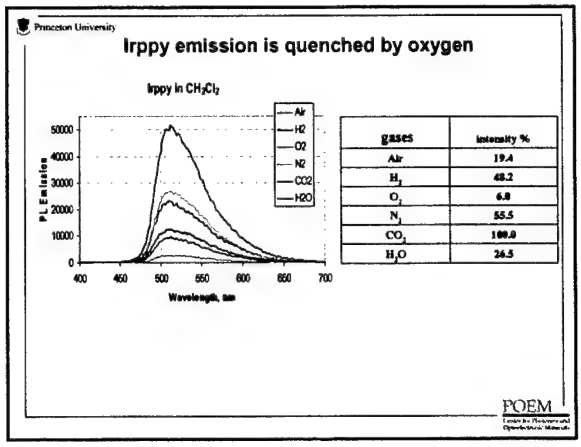
Princeton University
Irppy emission is quenched by oxygen
Irppy in CH2Cl2
Air
H2
O2
N2
CO2
H2O
PL Emission
Wavelength, nm
gases | intensity %
Air | 19.4
H2 | 48.2
O2 | 6.8
N2 | 55.5
CO2 | 100.0
H2O | 26.5
POEM

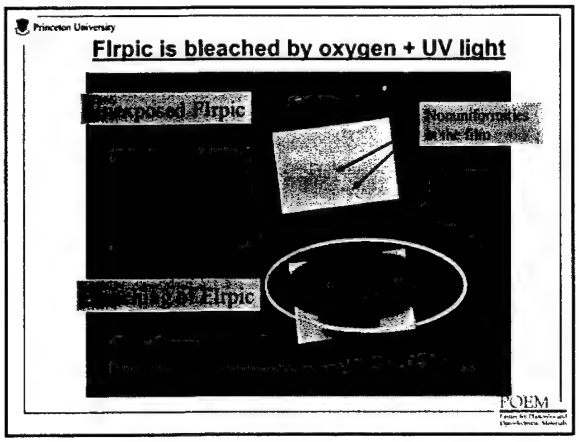
Princeton University
FIrpic is bleached by oxygen + UV light
Unexposed FIrpic
Nonuniformities in the film
Exposed FIrpic
POEM

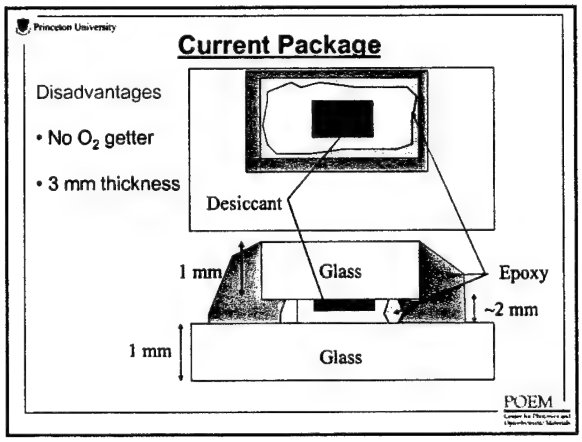
Princeton University
Current Package
Disadvantages
• No O2 getter
• 3 mm thickness
Desiccant
1 mm
Glass
Epoxy
~2 mm
1 mm
Glass
POEM

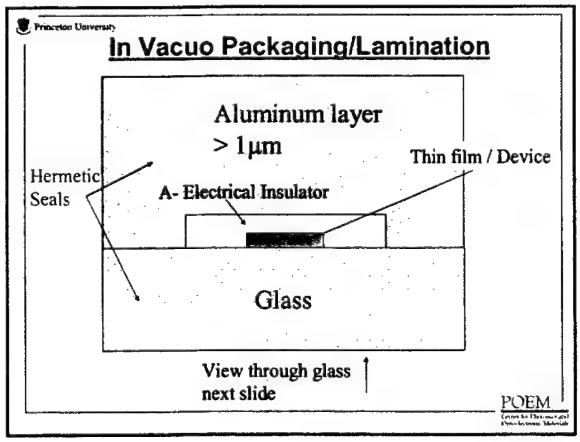
Princeton University
In Vacuo Packaging/Lamination
Aluminum layer
> 1μm
Thin film / Device
Hermetic Seals
A- Electrical Insulator
Glass
View through glass
next slide
POEM

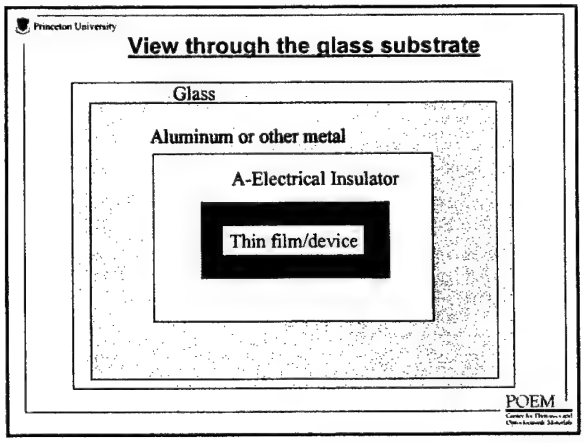
Princeton University
View through the glass substrate
Glass
Aluminum or other metal
A-Electrical Insulator
Thin film/device
POEM

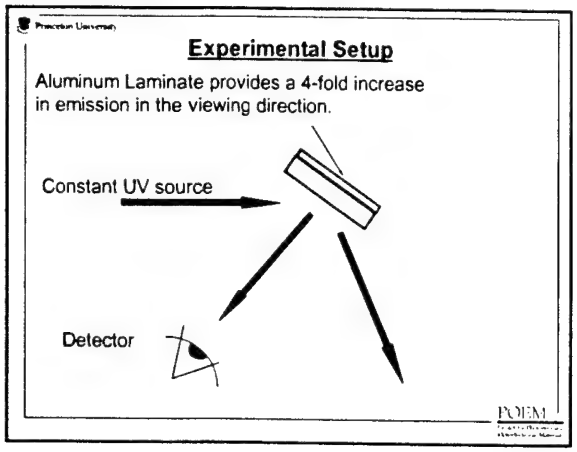

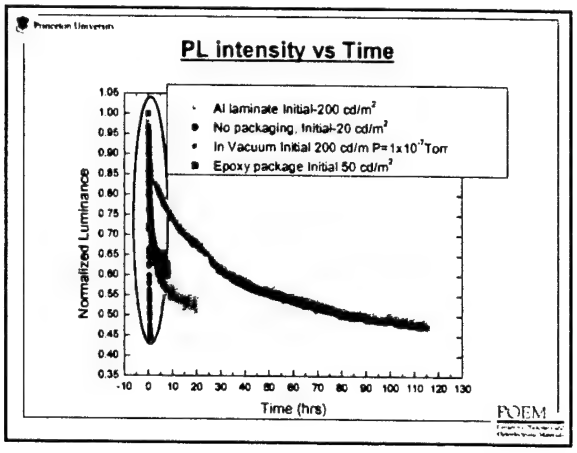

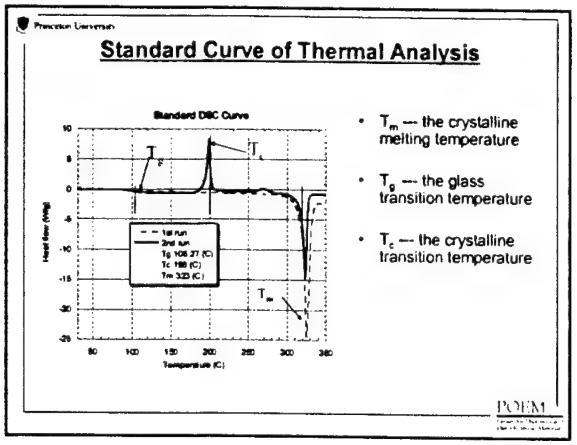

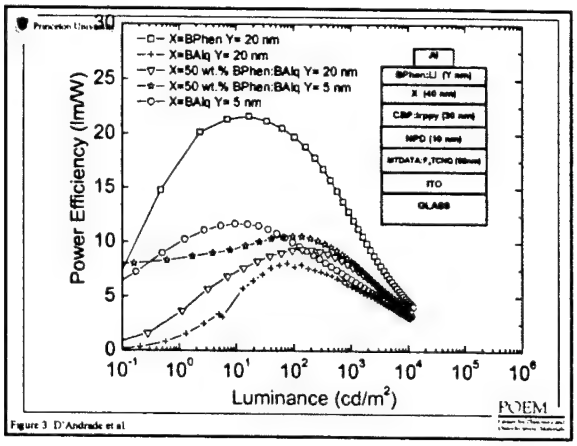

Figure 3 D'Andrade et al.

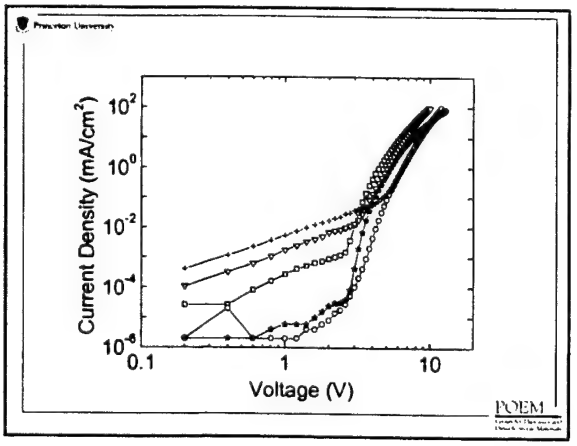

High Efficiency, Deep Blue OLEDs – Guest Charge Trapping for Improved Charge Balance

R.J. Holmes and Prof. S.R. Forrest
Department of Electrical Engineering, Princeton University
X. Ren, J. Li and M.E. Thompson
Department of Chemistry, University of Southern California
June 11, 2003

Outline

- Host-guest energy transfer vs. guest charge trapping in OLEDs
- Progress to date in achieving efficient blue electrophosphorescence
- What is charge balance in OLEDs?
- Deep blue, hole-trapping emitters and wide energy gap hosts
- Device performance of deep blue OLEDs
- Evidence of guest charge trapping vs. host-guest energy transfer
- Conclusions

Routes to Efficient Phosphorescence

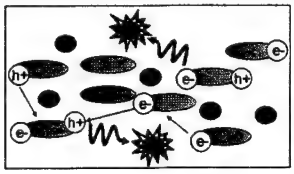

Host-Guest Energy Transfer:

Injected carriers form excitons at host molecular sites

Excitation is transferred nonradiatively to guest molecules, where radiative recombination takes place

Guest Charge Trapping:

Injected charge is trapped by guest molecules, allowing for carriers to form excitons on guest molecules

Radiative recombination takes place on guest molecules

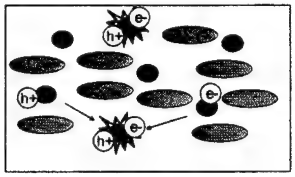

Blue Organic Electrophosphorescence

- Efficient blue electrophosphorescence based on exothermic host-guest energy transfer has been previously demonstrated during this study (Holmes et al. Appl. Phys. Lett. 82, 2422, 2003)
  - External quantum efficiency >7%, CIE co-ords (0.16, 0.37)
  - Problem: Emission is not blue enough, *devices are unreliable*
  - Device instability is partially the result of the buildup of charge in the emissive layer of the device, ***poor charge balance***
- Current study examines blue electrophosphorescence by means of direct charge trapping on guest molecules
  - High efficiencies are still reachable, alleviate some of the charge buildup in the emissive layer
  - Direct trapping allows ***control over charge balance*** in the emissive layer of the device by varying the doping concentration

What is Charge Balance in Phosphorescent OLEDs?

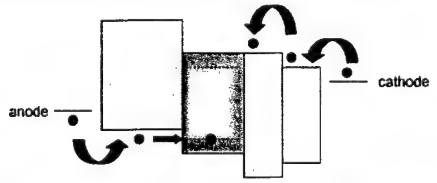

- Overall carrier injection is balanced, one electron is injected for every hole into the device as a whole
- Injection into the emissive layer may still be unbalanced, as a result of the different potential barriers, mobilities or traps that each carrier experiences
- Results in a buildup of charge at interfaces, leading to poorer overall device operation (i.e. quantum efficiency) and also to less reliable devices
- Above, holes reach the emissive layer at a faster rate than electrons, leading to a surplus of holes and a charge imbalance

Deep Blue Electrophosphorescence by Charge Trapping

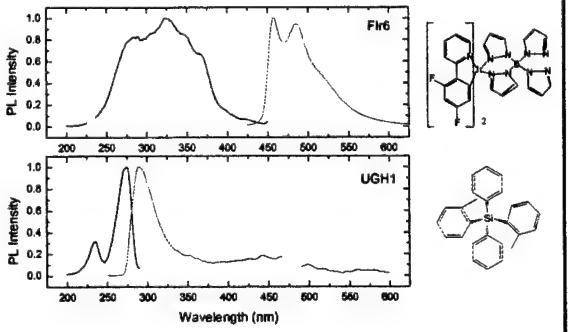

Blue Electrophosphorescence by Charge Trapping

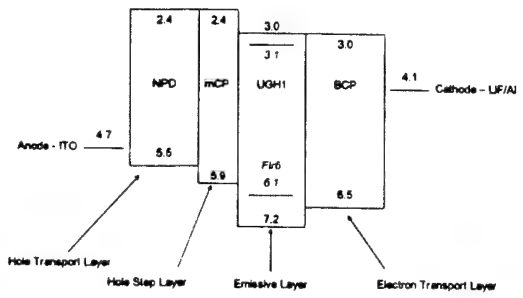

Blue Electrophosphorescence by Charge Trapping

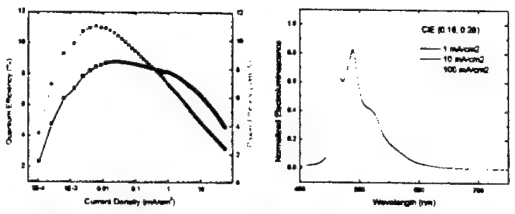

Host UGH1 and dopant Flr6 (10%) yield a high device efficiency of almost 9% at an operating current of 0.03 mA/cm², a luminance of 3300 cd/m² and a voltage of 5.7 V.

Question is as follows: The host UGH1 has a large energy gap on which it is likely difficult to form exctions.

What is the dominant means of exciton formation and light emission in this device?

Based on the energetics of Flr6 and UGH1, suspect that charge trapping on Flr6 is responsible for the high efficiencies

Neat Flr6 Devices

Test Flr6 in a neat film device. If Flr6 is to conduct charge efficiently in a doped device, it should also behave reasonably efficiently in neat device:

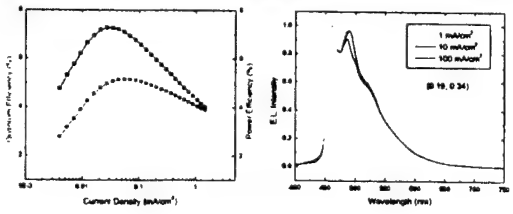

Flr6 is extremely efficient in neat film devices with an efficiency of 5.1% at 0.06 mA/cm² and 5.3 V.

Flr6 is a conductor and can efficiently transport charge and form excitons on its own

Neat UGH1 Devices

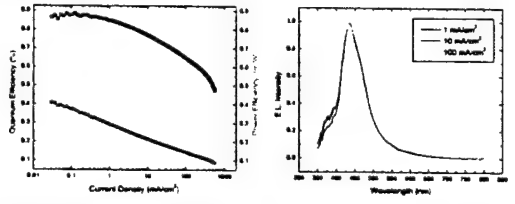

•Dopantless, neat UGH1 device exhibits very poor device characteristics, no pure emission from the host is observed.

•Without Flr6, UGH1 behaves as a hole blocker, forcing exciton formation to occur in the NPD transport layer instead of in the wide energy gap UGH1

UGH1 is a good electron conductor but is a very poor hole conductor, making exciton formation on UGH1 difficult

Operating Voltage vs. Flr6 Concentration

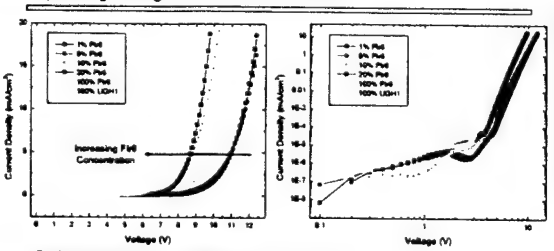

•Devices relying on energy transfer between host and guest should have driving voltages that are independent of dopant concentration

•A dependence of driving voltage on dopant concentration suggests that the dopant is playing a role in charge transport

•Current for neat UGH1 device is made up of both a recombination current from NPD as well as an electron current transported by UGH1 across the device

Emission Spectrum vs. Flr6 Concentration

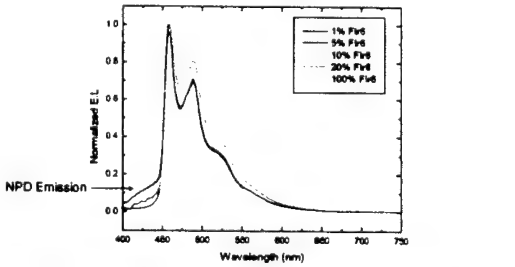

•In addition to the observed decrease in operating voltage with increasing Flr6 concentration, NPD emission is observed for very low concentrations of Flr6 in UGH1

•Both results support the theory that Flr6 behaves as a low resistance pathway for holes into the emissive layer, consistent with a charge trapping view of device operation

Step Layers and Charge Balance – Remove Step Layer

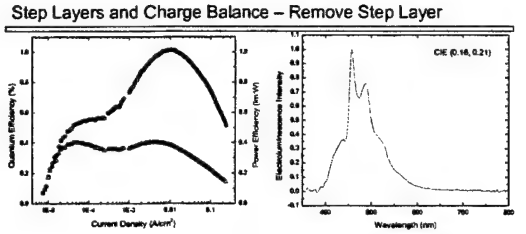

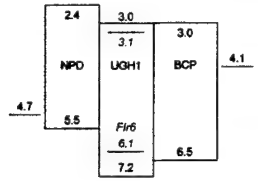

- Devices missing the step layer are very poor, resulting in significant NPD emission
- Poor behavior suggests need for mCP step layer to aid hole injection into the emissive layer and help confine excitons in the emissive layer
- By increasing hole injection into the emissive layer, charge balance is also expected to increase

Controlling Charge Balance

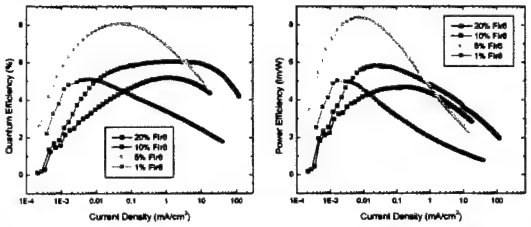

- The shape change observed for a plot of quantum efficiency vs. current density as a function of concentration suggests that charge balance in the emissive layer can be optimized by varying the dopant concentration
- This is only the case because the system in question relies on guest charge trapping and not energy transfer from host to guest
- Here, optimum charge balance occurs for a concentration between 5 and 10% Flr6

Conclusions

- Demonstrated efficient, deep blue electrophosphorescence based on charge trapping and exciton formation directly on the guest molecules of Flr6 in a system of UGH1 and Flr6
- Optimized the device for maximum charge balance by adjusting dopant (Flr6) concentration and hence, the ease with which electrons and holes can enter and transport through the emissive layer of the device
- Suspect that by using a dopant that traps charge, and that by regulating charge flow into the emissive region with the help of step layers and varying dopant concentrations, charge buildups can be reduced or eliminated in the emissive region
- The elimination of such charge buildups should ultimately lead to more reliable devices since regions of charge buildup seem to generally compromise device stability by exploiting any instabilities to excess charge present at the molecular scale in the emissive species

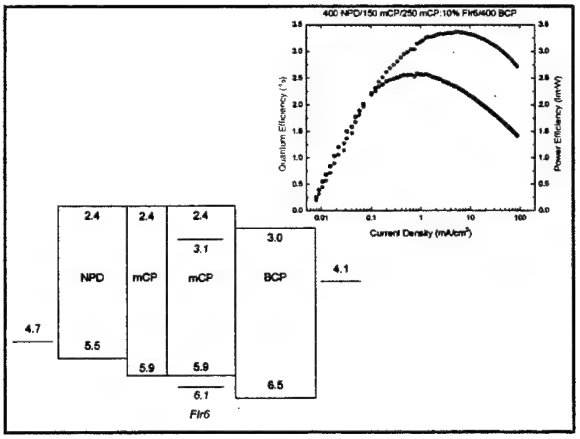

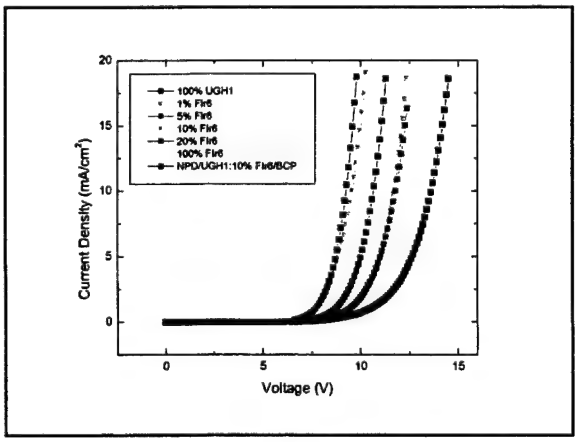

Failure Modes in Organic Light Emitting Devices

Mark Thompson – University of Southern California
Steve Forrest – Princeton University
Paul Barbara – University of Texas
Julie Brown – Universal Display Corporation

Modes of OLED Decay

Long term "intrinsic" decay in electroluminescence intensity
- uniform loss of efficiency over the device emitting area

Growth of local non-emissive areas or dark spots, "extrinsic decay"
- shorter time scale
- inert atmosphere greatly reduces rate of dark spot formation and growth
- flexible substrates show rapid dark spot formation
- changes in cathode topography observed, thought to fall above the dark spots

Extrinsic Degradation studies of OLEDs (dark spot growth)

- Unpackaged devices degrade very rapidly
  - hours to days for complete failure
- Devices die by formation and growth of dark spots
- Degradation has been correlated with the environment and operating parameters
  - e.g. drive power, humidity and oxygen levels
- An understanding of dark spot growth will enhance stability toward environmental contaminants
  - Devices with a greater environmental resistance require less stringent packaging for long life operation
- Unpackaged devices (esp. TOLEDs) allow the use of surface techniques to probe devices during degradation, in situ studies

Experimental Setup for TOLED Study

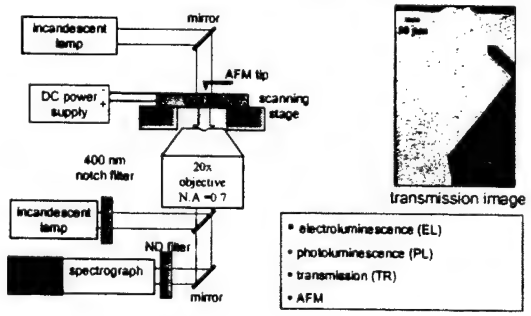

D. Kolosov, *et. al., J. Appl. Phys.*, 2001

Correlated AFM and EL at Early Stages of Degradation

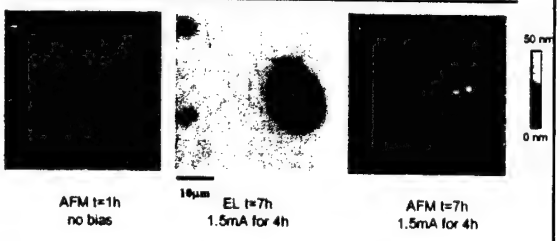

- Surface mapped by AFM before running device (RMS roughness = 3 nm).
- No initial topographic features/defects exist in the dark spot areas.
- No topographic differences between EL dark spot and EL active areas.
- PL and TR images are featureless, no difference between EL active and inactive areas

D. Kolosov, *et. al., J. Appl. Phys.*, 2001

Changes in Devices After Extended Time Periods

92 h in ambient, run at 1.5 mA for 58 h

92 h in ambient, no applied bias

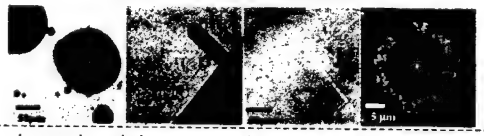

analogous degradation processes in stressed and control devices

Questions to be resolved in Dark Spot Formation/Growth

- What other factors or materials choices affect the rate of dark spot growth?
- Is it possible to prevent or retard diffusion of water and oxygen into the OLED without using epoxy sealed or hermetic packages?

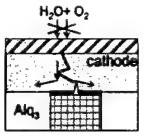

We need an efficient method to evaluate the distribution of dark spots and their growth rate as a function of the environment, materials, device architecture, *etc.*

USC/PU/UT/UDC

Environmental control of dark spot formation and growth

- Independent control of O_2 and H_2O is important to determine the role each plays in dark spot growth
  - System allows the control of:
    relative humidity 0 – 100% (± 3%)
    oxygen 0 – 100% (± 0.5%)
- Devices will be run in a controlled environment and monitored as a function of humidity and oxygen levels
  - number *vs.* time gives nucleation rate
  - size *vs.* time gives the rate of growth
- High humidity is needed to accelerate dark spot growth

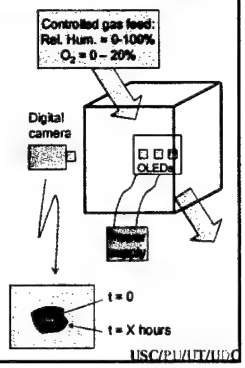

USC/PU/UT/UDC

Controlled environment OLED testing box

Power Supply

Environmental Chamber

Humidity Controller

Digital Camera OLED

Optical Microscope

USC/PU/UT/UDC

mpeg movie of a dying device

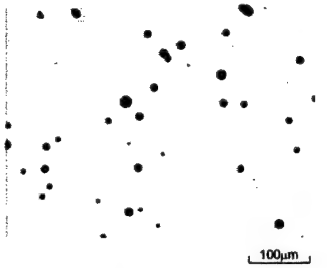

- OLED structure:
  NPD(400Å)/Alq_3(500Å)/
  LiF(10Å)/Al(1000Å)
- Conditions:
  Nitrogen
  Humidity 80%
  T=22°C
  Constant current 20mA
  7000-8000 Cd/m²
- Area shown:
  600 x 450 μm²

Nucleation rate: within 1 hour all dark spots are visible. No new dark spots form.
Dark spots are the result of defects built into the device.

USC/PU/UT/UDC

Dark spot density and growth rate

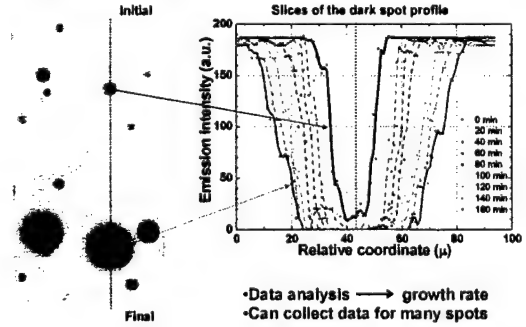

- Data analysis ⟶ growth rate
- Can collect data for many spots

USC/PU/UT/UDC

Dark spot growth rate as a function of cathode material and humidity

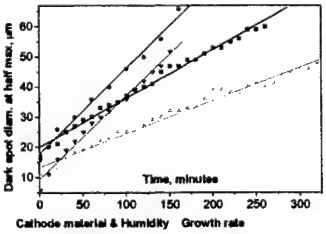

Cathode material & Humidity	Growth rate
LiF/Al 30% humidity	0.16μm/min
LiF/Al 80% humidity	0.28μm/min
Mg:Ag/Ag 30% humidity	0.11μm/min
Mg:Ag/Ag 80% humidity	0.28μm/min

OLED structure:
ITO
NPD(400Å)
Alq_3(500Å)
Cathode (LiF/Al or Mg:Ag/Ag)

Conditions:
Nitrogen
Humidity 30% and 80%
T=22°C
Constant current 20mA

USC/PU/UT/UDC

Does the nature of the cathode/ETL interface affect dark spot growth?

How interface-layers can affect the dark spot growth. Do spots grow from the inside?

ITO/NPD/Alq_3/IF (100 Å)/LiF-Al, IF = BCP, L_2IrX, ORG_x

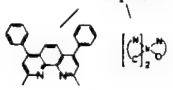

- Environmental conditions are all the same:
  Nitrogen, 80% rel. humidity, 22°C

USC/[illegible]/LT/[illegible]

Do dark spots grow faster on working or non-working devices?

OLED was on at 5 mA for 256 min | OLED was off for 256 min

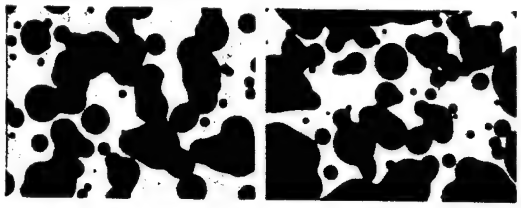

Total dark spot areas of the driven and undriven devices are very similar

USC/[illegible]/LT/[illegible]

Do the different organic interface layers affect the growth rate of the dark spots? (ITO/NPD/Alq3/**IF (100 Å)**/LiF-Al, **IF** = BCP, L_2IrX, ORG_x)

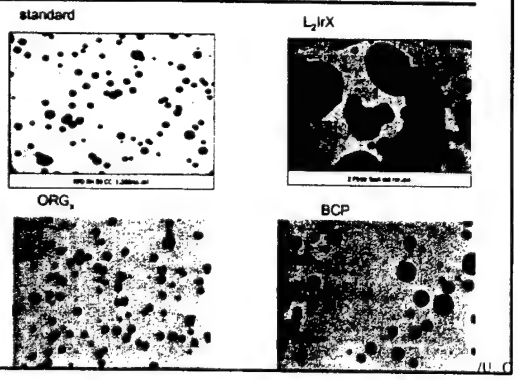

/U C

Total dark area plot: ORG_x, FIrpc and BCP interface

- FIrpic clearly gives very high dark spot growth rates
  - multiple slopes have to do with the increase in current density as the device areas is decreasing
- BCP looks slower than it really is
  - halo region is largely counted as bright

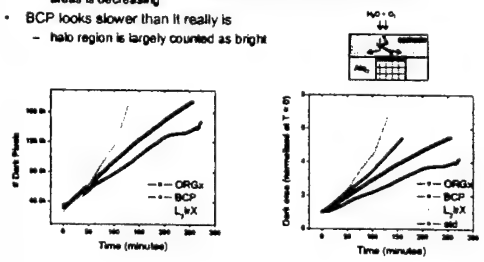

USC/[illegible]/LT/[illegible]

ORG_x EIL affects OLED performance

ORG_x used as EIL enhances the QE and the brightness

For the device with 80 Å of ORG_x up to 20 000 Cd/m²

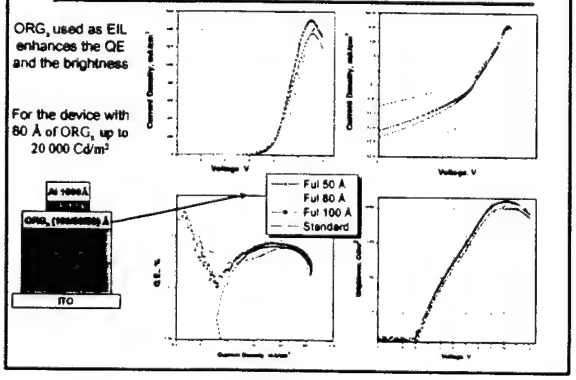

Thicknesses of EIL affects the rate of *Dark Spot Growth*

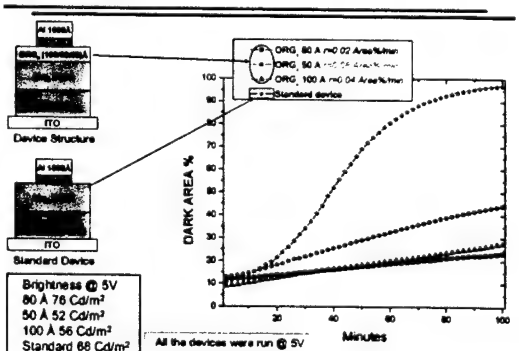

Brightness @ 5V
80 Å 76 Cd/m²
50 Å 52 Cd/m²
100 Å 56 Cd/m²
Standard 68 Cd/m²

All the devices were run @ 5V during degradation studies

USC/[illegible]/LT/[illegible]

Why does ORG_x help prevent Dark Spots Growth?

- When operating the device at constant voltage (5V), the dark spot growth follows a linear law: DS(t) = 0.05t

- Due to high field under the operating conditions used, water reduction occurs:

$2\ H_2O + 2\ e^- \rightarrow H_2 + 2\ OH^-$ -0.82V

Schaer et al. Adv. Func. Mat. (2001), 11, 116-121

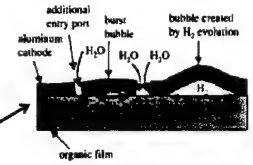

- ORG_x used as barrier for water penetration prevents from hydrogen formation since the reduction of ORG_x occurs easily

$ORG_x + e^- \rightarrow ORG_x^-$ -0.44V

- Alternatively: Alq_3^- reacts rapidly with H_2O, hydrolyzing the ligands, forming Al_2O_3 or other insulting phase, ORG_x^- is stable to water

Devices with ORG_x did not show any bubble formation during the environmental life-test study: no H_2 formation.

USC/PU/UT/UDC

Effect of Hole Injectors on the Degradation of OLEDs

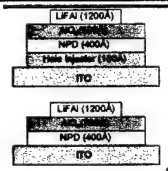

Devices run at a constant current, initial brightness = 700 Cd/m²

- Some dark spots grow at irregular rates. Often linked to the merging of dark spots: merged spots grow faster.
- "necking often occurs prior to merging.

Total Area vs Time At Constant Current

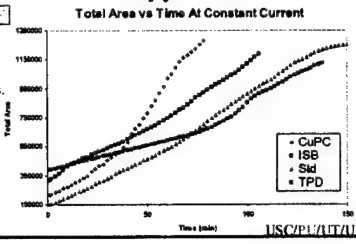

At Constant Current

- Hole Injectors can either stabilize or destabilize OLEDs.
- Growth Rate
  - CuPC: 0.83 %Area/min
  - ISB: 0.17 %Area/min
  - Std: 0.62 %Area/min
  - TPD: 0.30 %Area/min

USC/PU/UT/UDC

Effect of Hole Injectors on the Degradation of OLEDs

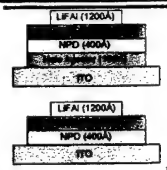

Devices run at a constant current, initial brightness = 700 Cd/m²

- Some dark spots grow at irregular rates. Often linked to the merging of dark spots: merged spots grow faster.
- "necking often occurs prior to merging.

Total Area vs Time At Constant Current

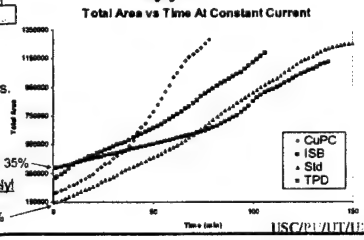

At Constant Current

- Hole injectors can either stabilize or destabilize OLEDs.
- Growth Rate

Handling time was too long!!
It takes time to pretest OLED
Degradation starts immediately!

35%

15%

USC/PU/UT/UDC

Removable package for OLEDs

- The device must be tested and run under an inert environment prior to degradation testing.
- Package needs to be removed while the device is in the desired environment
- We must be able to remove the trap form outside the
- Solution: a vacuum chuck

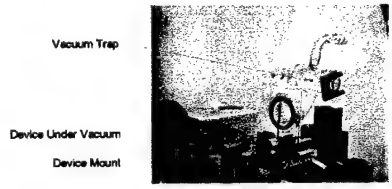

USC/PU/UT/UDC

Removable package for OLEDs

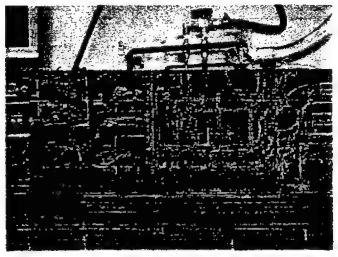

USC/PU/UT/UDC

Effect Of Hole Injectors On The Degradation Of OLED's

Total Area vs Time

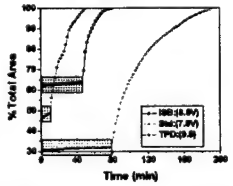

- The Standard Device has the Longest Lifetime.
- The Presence of Hole Injectors Destabilizes The Devices.
- Total Growth Rate:
  - ISB: 1.16 %Area/min
  - Std: 0.51 %Area/min
  - TPD: 0.91 %Area/min

USC/PU/UT/UDC

UDC prepared and packaged OLEDs

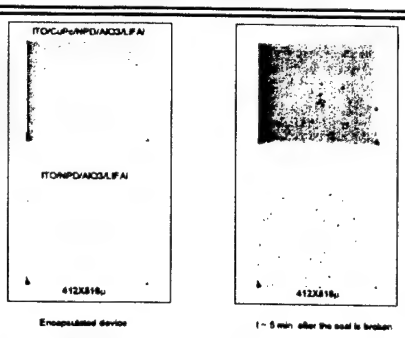

- Dark spots can be seen as soon as the seal is taken off of an encapsulated device.

USC/[illegible]/LCT/UDC

Degradation of devices with very low T = 0 dark spot area

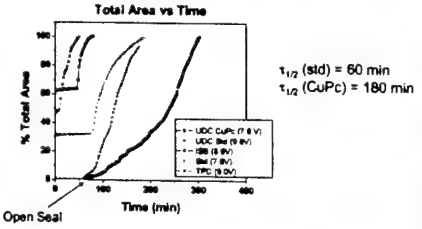

$\tau_{1/2}$ (std) = 60 min
$\tau_{1/2}$ (CuPc) = 180 min

- Devices that have very few spots to begin with, degrade slowly because of the steady slow rate of degradation.
- Devices that are already 30% or more degraded degrade faster due to merging of spots. This gives rise to Stair-Case Effect
- Standard devices (ITO/NPD/Alq_3/LiF-Al) fabricated in the Clean Room are less stable than devices with a Cupc hole injector.

USC/[illegible]/LCT/UDC

Effect of Hole Injectors on the Degradation of OLEDs

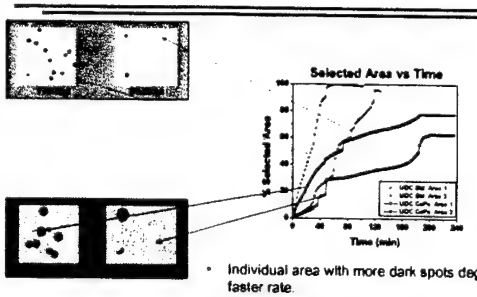

- Individual area with more dark spots degrade at a faster rate.
- Standard device prepared in the clean room is less stable than the device with CuPc and has a shorter life span.

USC/[illegible]/LCT/UDC

Sources of dark spots

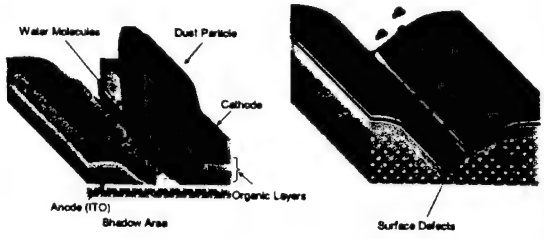

Dust particle based defect
Should not be prevalent in cleanroom prepared devices

Cathode defect
May be a pinhole or grain boundry. Expected in all devices.

USC/[illegible]/LCT/UDC

Devices Made In UDC Clean room

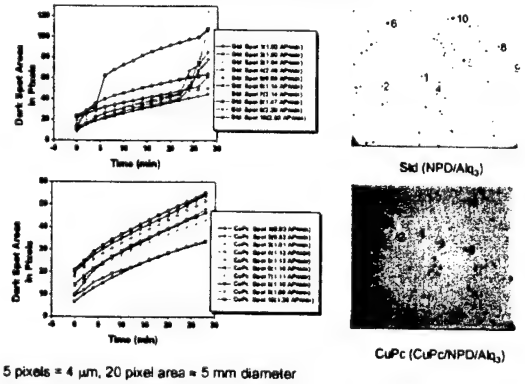

5 pixels = 4 μm, 20 pixel area = 5 mm diameter

Devices Made In The Lab

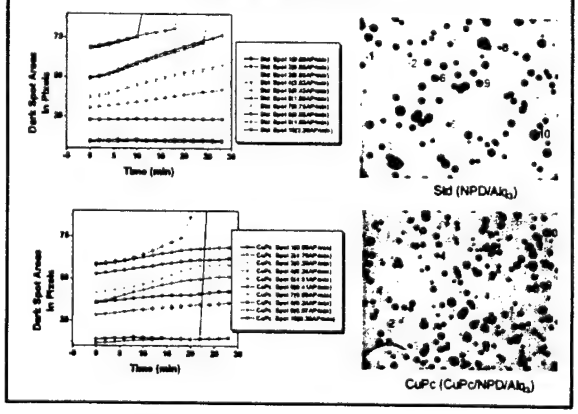

Can Liquid Metals (Eutectics) Be Used To Stop The Growth Of Dark Spots?

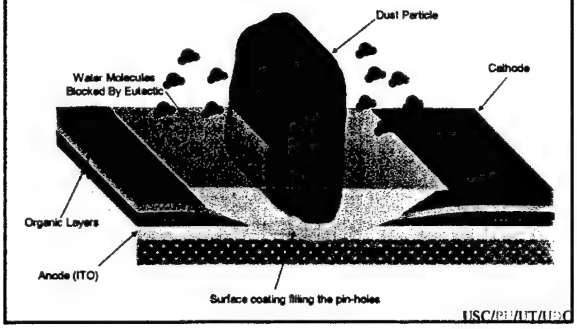

USC/PU/UT/UDC

Cathode Surfaces Of Undegraded Device Before And After Applying The Ga-In-Sn Eutectic

Before The Application Of The Ga-In-Sn Eutectic

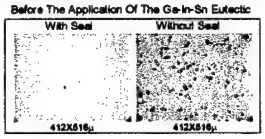

After The Application Of The Ga-In-Sn Eutectic

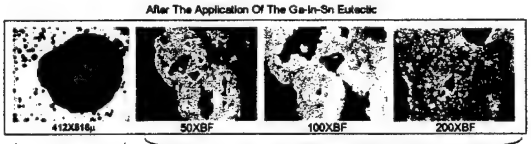

- The Ga-In-Sn eutectic does adhere to the cathode surface
- The device becomes non-emissive in treated areas.

USC/PU/UT/UDC

Effect of Silicone on the Degradation of OLEDs

Total Area vs Time

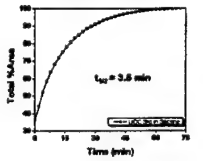

- Silicone grease fails to slowdown the rate of dark spot growth

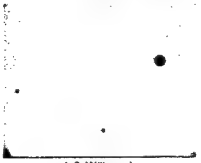
t=0: With seal

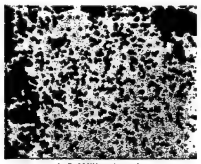
t=0: Without seal

USC/PU/UT/UDC

Effect of Paraffin Wax and Paraffin Oil on the Degradation of OLEDs

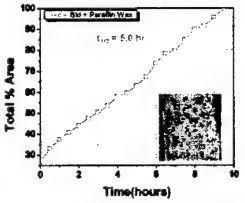

- The dark area does not grow for 3.5 hours.
- After the induction period of 3.5 hours the rate rapidly increases with a half life of 4.17 hours.

- Paraffin wax increases the life expectancy of a badly degraded device.

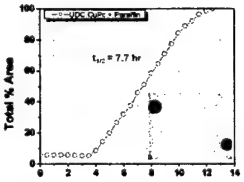

USC/PU/UT/UDC

Effect of Silicone Bath oil on the Degradation of OLEDs

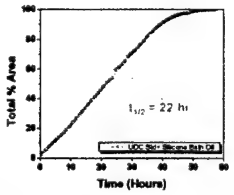

- Silicone bath oil slows down the growth rate of dark spots
- Silicone oil is more effective than paraffin oil

USC/PU/UT/UDC

Effect of Carbon Paste on the Degradation of OLEDs

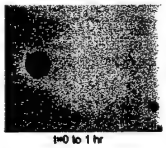
t=0 to 1 hr

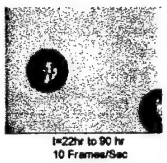
t=22hr to 90 hr
10 Frames/Sec

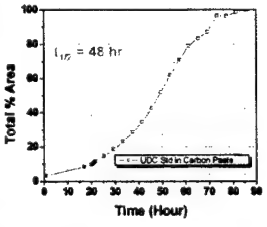

- Carbon paste decreases the rate of dark spot growth

USC/PU/UT/UDC

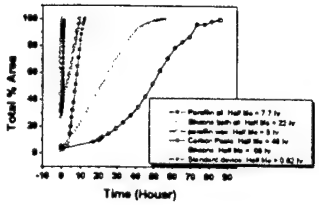

- All measurements were taken at 6.0V (constant voltage)
- Ga-In-Sn eutectic and Silicone Grease cannot slow down the dark spot growth
- Silicone oil, paraffin oil, and Carbon paste decelerate the growth rate of dark spots

Increase in efficiency ⟶

Paraffin wax < Paraffin oil < Silicone oil < Carbon paste

Summary

- Dark spots are the result of atmospheric exposure
  - The growth rate is not affected by device driving conditions
  - Metal over coating (Ag) does not affect the growth rate of dark spots
- Growth rate is accelerated by spot merger
- The identity of the compound in contact with the electrodes affects the growth rate of dark spots
  - L_2IrX accelerates the rate of growth, ORG_x decreases it
  - Cupc retards dark spot growth – planarizes the substrate, cuts down particulates
- Dark spot growth rate appears constant for differing spot sizes
- Over coating with organic materials can significantly decrease the growth rate
  - Need to look at affect of coating on long term lifetime

Is the hole transporter stable?

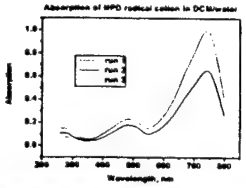

- NPD solution was oxidized to give $NPD^{+\bullet}$
- Solution is stable for hours under anaerobic conditions
- Addition of water leads to rapid bleaching of the $NPD^{+\bullet}$ signal
  - $[H_2O] = 1\ \%$
  - Final spectrum above is 2.5 minutes after addition of water
  - Similar reactivity is observed for most triarylamines
- Can we come up with other hole transporters that are stable in water in both their neutral and cationic forms? Metal complexes!!

Characterization of *fac*-Co(ppz)3 complex

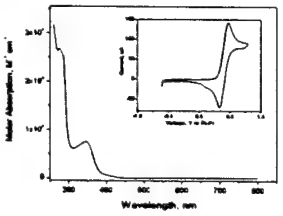

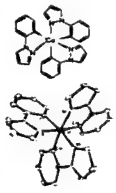

UPS data:
5.3 eV for HOMO energy

- $Co(ppz)_3$ is colorless and has reversible electrochemistry
- Makes a stable glass, T_g > 150°C
- HOMO energy is lower than NPD

Device structure: ITO/HTL(500Å)/Alq(500Å)/LiF/Al

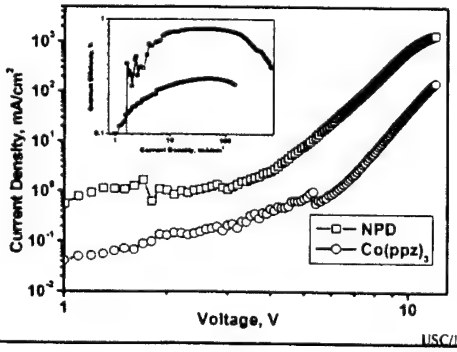

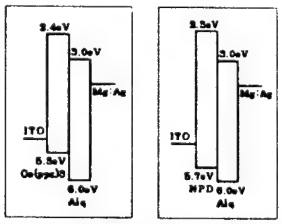

*A 0.7 eV energy offset between the HOMOs of *fac*-$Co(ppz)_3$ and Alq_3.
*Such large energy offsets are expected to lead to an increased barrier for migration of holes from the HTL to Alq_3
*Poor carrier recombination is a likely loss mechanism in *fac*-$Co(ppz)_3$ devices.

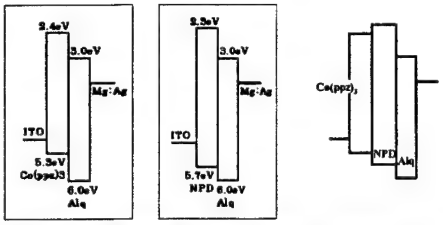

*A 0.7 eV energy offset between the HOMOs of *fac*-Co(ppz)$_3$ and Alq$_3$.
*Such large energy offsets are expected to lead to an increased barrier for migration of holes from the HTL to Alq$_3$
* Poor carrier recombination is a likely loss mechanism in *fac*-Co(ppz)$_3$ devices.
* Inserting an NPD layer lowers the hole barrier and increases the electron barrier

USC/PU/UT/UDC

NPD interface layer gives efficient device

Device structure: ITO/Co(ppz)$_3$(400Å)/NPD(100Å)/Alq(500Å)/LiF/Al

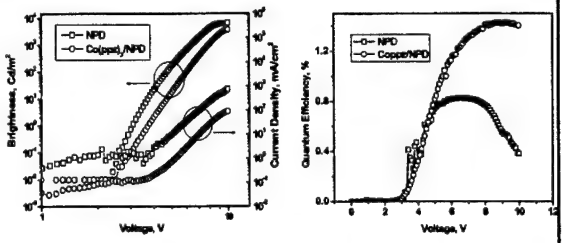

NPD layer effectively prevents electron injection into Co(ppz)$_3$

USC/PU/UT/UDC

Stability study: ITO/Co(ppz)$_3$/NPD/Alq$_3$/LiF/Al

Co(ppz)$_3$

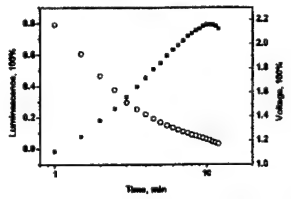

Co(ppz)$_3$ vs. Co(ppy)$_3$

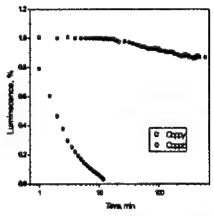

- Co(ppz)$_3$ degrades very rapidly, leading to high voltage operation.
- Co(ppy)$_3$ gives a stable device

USC/PU/UT/UDC

Stability study: ITO/Co(ppz)$_3$/NPD/Alq$_3$/LiF/Al

Co(ppz)$_3$ vs. Co(ppy)$_3$

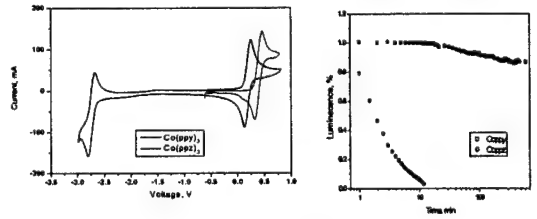

- Co(ppz)$_3$ degrades very rapidly, leading to high voltage operation.
- Co(ppy)$_3$ gives a stable device
  - Co(ppy)$_3$ is significantly easier to oxidize than Co(ppz)$_3$
  - more stable cation

USC/PU/UT/UDC

Chemical oxidation of *fac*-Co(ppz)3

Oxidation reagent: (4-BrPh)$_3$N-SbCl$_6$ (E1/2 = + 0.7 V vs Fc/Fc+)

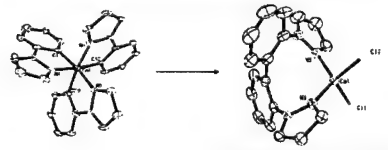

Product is not Co(ppz)$_3$$^+$!!!

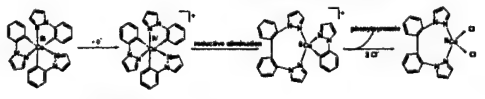

In the device the complex will stop at the cationic state, trapping charge permanently.

USC/PU/UT/UDC

Singlet Oxygen production by Phosphorescent Materials

$$^3M^* + {}^3O_2 \longrightarrow {}^1M + {}^1O_2$$

- Triplet excited states can be quenched by oxygen to form singlet oxygen
  - process analogous to T-T annihilation
- Singlet oxygen reacts spontaneously and vigorously with organic materials
  - could be a source of device degradation
- Questions:
  - Do the phosphors react with $^3O_2$ in their excited states?
  - Do the excited phosphors form $^1O_2$?
  - Does this contribute to dark spot formation?

USC/PU/UT/UDC

Oxygen Quenching of Phosphorescence

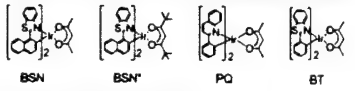

BSN BSN* PQ BT

- Four compounds were chosen that have appreciable absorbance at 355 and 532 nm
  - these are the laser wavelengths used for measurement
  - all show substantial quenching of phosphorescence in air
- Stern-Volmer Analysis allows us to determine the quenching rate constants
  - $^3M^*$ + O_2 → quenched
  - $^3M^*$ → phosphorescence

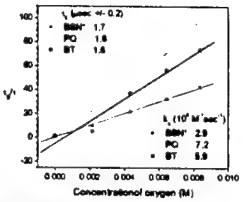

$\frac{\tau_0}{\tau} = 1 + \frac{k_q}{k_r}[oxygen]$ k_q = second order rate constant for $^3M^* + O_2$

all compounds examined are near diffusion controlled

USC/[illegible]/LCT/[illegible]

Singlet Oxygen Production

$$^1M \xrightarrow{\text{excite } \lambda \text{ nm}} {}^3M^* + {}^3O_2 \longrightarrow {}^1M + ?$$

- We have demonstrated quenching, but does the system make $^1O_2$?
  - quenching could involve other processes
  - quenching via electron transfer and exciplex has been demonstrated for phosphors and fluorophors
  - oxygen has ample oxidizing strength to oxidize the excited phosphor

USC/[illegible]/LCT/[illegible]

Singlet Oxygen Production

$$^1M \xrightarrow{\text{excite } \lambda \text{ nm}} {}^3M^* + {}^3O_2 \longrightarrow {}^1M + {}^1O_2 \quad (h\nu = 1268 \text{ nm} \rightarrow {}^3O_2)$$

- Singlet oxygen emission intensity is recorded and compared to a reference to determine the quantum efficiency for singlet oxygen production (Φ_Δ).

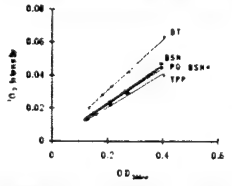

	λ (nm)	Φ_Δ	$k_q(^1O_2)$ (10^8 M^{-1} s^{-1})
BSN	355	0.59±0.07	6.3 ± 0.2
	532	0.89±0.02	
BSN*	355	0.60±0.06	4.0 ± 0.3
	532	0.77±0.08	
PQ	355	0.62±0.05	1.0 ± 0.2
	532	0.89±0.07	
BT	355	0.86±0.07	0.5 ± 0.2
	532	1.00±0.07	

M. Selke, *et. al.*, Cal. State Los Angeles

USC/[illegible]/LCT/[illegible]

Singlet Oxygen and Lifetime

$$^3M^* + {}^3O_2 \longrightarrow {}^1M + {}^1O_2 \quad (h\nu = 1268 \text{ nm} \rightarrow {}^3O_2)$$

- Solutions can be irradiated for > 60 min (generating $^1O_2$) with no loss in activity
  - the phosphor itself is very stable toward singlet oxygen
  - all phosphors show very low singlet oxygen quenching rates
- Do green and blue emissive dopant show the same efficiencies for singlet oxygen production? Will be tested soon.
- Many fluorescent molecules also generate singlet oxygen, e.g. TPP, so the problem may affect all OLEDs and not just electrophosphorescent ones.
- Exothermic transfer shows minimal impact of exposure to O_2, endothermic shows a strong impact. Related to the lifetime of the exciton.
- Devices need to be packaged to avoid atmospheric degradation and oxygen affects seem weak in fabricated devices.
  - cathode prevents free diffusion of oxygen into the film and oxygen must encounter phosphor in its excited state
  - Device lifetimes of OLEDs run in air or oxygen are similar to those under nitrogen

USC/[illegible]/LCT/[illegible]

Total dark area plot, for low and high current densities

- dark spots grow slowly at low current densities
- High current densities lead to rapid dark spot growth
  - as the device area shrinks the current density goes up and the dark spot growth rate goes up

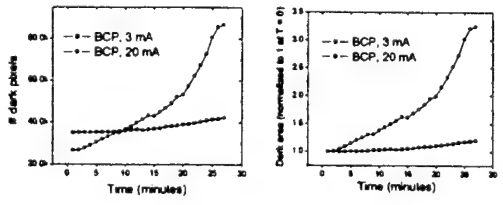

USC/[illegible]/LCT/[illegible]

Devices held at constant current (1 – 1.3 mA, 700 Cd/m²)

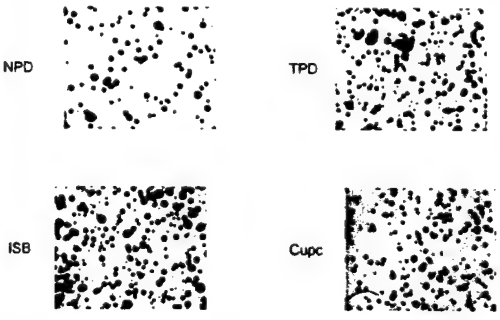

USC/[illegible]/LCT/[illegible]

Investigations of PHOLED Stability
Program Review, 6-11-03

UNIVERSAL DISPLAY CORPORATION™

UDC Subcontract: 6-1-01 to 11-30-02

Program Focus Areas

- Understanding the parameters that affect OLED Device Lifetime Performance
  - Extrinsic device parameters
- Understanding the parameters that affect PHOLED Device Lifetime Performance
  - Intrinsic device parameters
- Improving PHOLED Performance
  - Efficiency
  - Lifetime
- Summary

Device Stability Interacting Factors

Intrinsic:
1. **Electrochemical (oxidation, reduction)**
2. **Thermal (T_g, T_m, T_d)**
3. **Interfacial (cathode delamination, etc.)**
4. **Photochemical**
5. **Carrier Balance**
6. **Material Impurities**

Extrinsic:
1. **Encapsulation (H_2O, O_2, etc.)**
2. **Fabrication environment (dust, etc.)**
3. **Substrate (roughness, etc.)**
4. **Operating conditions**
5. **Storage conditions**

PHOLED Reliability Study

- **Material Purity**
  - ✓ Blocking Layer
  - ✓ Host
  - ✓ Dopant
- **Substrate Process**
  - ✓ ITO Spec/Pretreatment
  - ✓ Edge Insulator
- Package Design
  - ✓ Mechanical
  - ✓ Materials
  - ✓ Process
- **Device Structure Design**
  - ✓ Blocking Layer
  - ✓ Doping Concentration
  - ✓ Layer Thickness
  - ✓ Materials

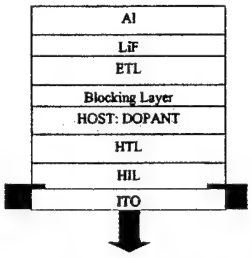

Typical OLED Display Package

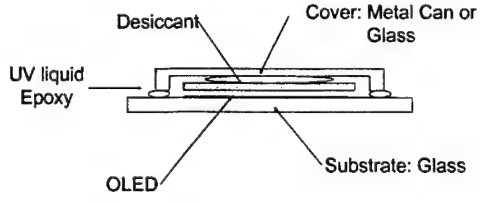

OLED Panel Fabrication Cost

The display cost makes up 22% of the module cost

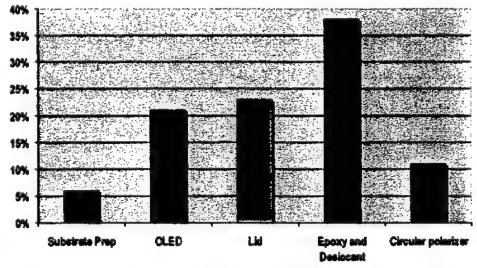

*2002 Display Search Factory Cost Model

Green PHOLED Package Stability

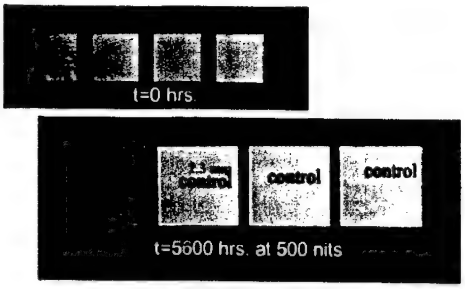

Pixel shrinkage and dark spot growth observed

Importance of Package Volume

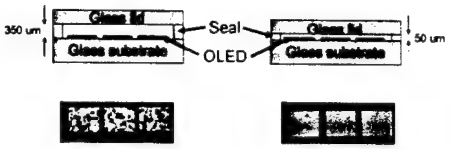

Pictures taken after 94 hours in 60 °C/85% RH chamber

Package with Adhesive Seal

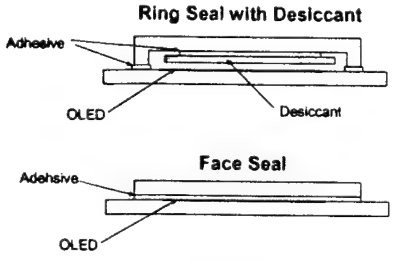

Adehsive Material Processing

- Perimeter adhesive ring – 2 mm wide, 1.5 mils thick
- Apply adhesive to cover glass
- Remove release layer and attach cover glass to substrate
- UV cure

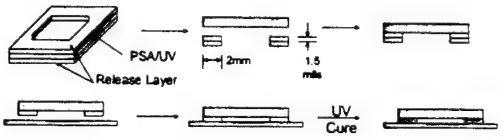

Adhesive Advantages

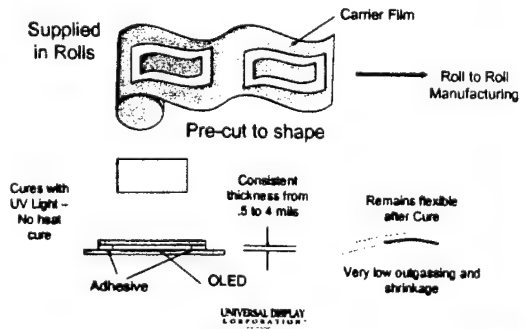

Ring Seal - UV Epoxy vs. Adhesive

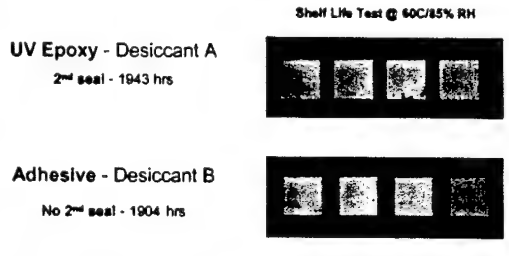

Encapsulation With Adhesive and Desiccant

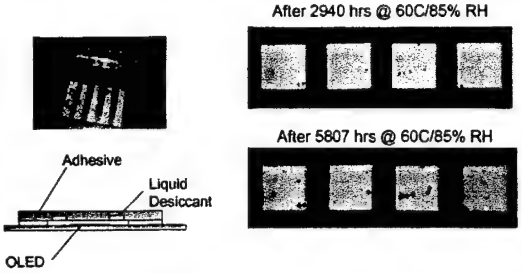

UNIVERSAL DISPLAY CORPORATION

Pixel Shrinkage Solved By:

Packaging, Process, and Device Design

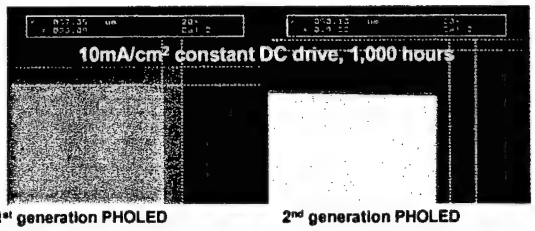

UNIVERSAL DISPLAY CORPORATION

Status of Packaging

- Developed a rugged package that does not limit the present PHOLED lifetime
- Significantly improved pixel shrinkage and dark spot growth
- Ongoing work
  - Advanced packaging to reduce materials and manufacturing process cost
  - Monolithic encapsulation to reduce the stringent requirements for inert packaging process
  - Encapsulation design for high T operation

UNIVERSAL DISPLAY CORPORATION

PHOLED Reliability Study

- **Material Purity**
  - ✓ Blocking Layer
  - ✓ Host
  - ✓ Dopant
- **Substrate Process**
  - ✓ ITO Spec/Pretreatment
  - ✓ Edge Insulator
- **Package Design**
  - ✓ Mechanical
  - ✓ Materials
  - ✓ Process
- Device Structure Design
  - ✓ Blocking Layer
  - ✓ Doping Concentration
  - ✓ Layer Thickness
  - ✓ Materials

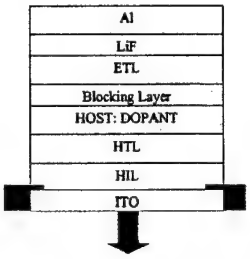

UNIVERSAL DISPLAY CORPORATION

Green PHOLED Lifetime: Program Start

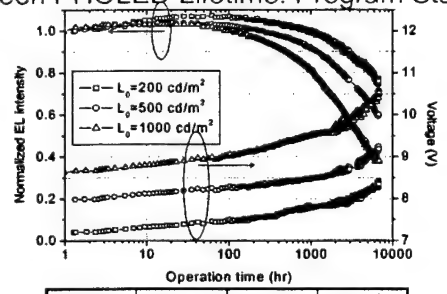

0-3000 hrs	200 cd/m²	500 cd/m²	1000 cd/m²
% retained	88	75	57
dV/dT(mV/hr)	0.26	0.24	0.41

UNIVERSAL DISPLAY CORPORATION

GD29 PHOLED Performance

CIE: (0.30,0.63), EQE Max = 6-7%

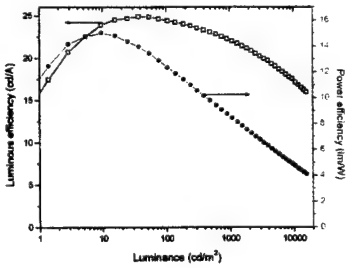

UNIVERSAL DISPLAY CORPORATION

Green PHOLED Efficiency Performance

ITO/HIL/HTL/HOST/Green Dopant/BL/ETL/LiF/Al

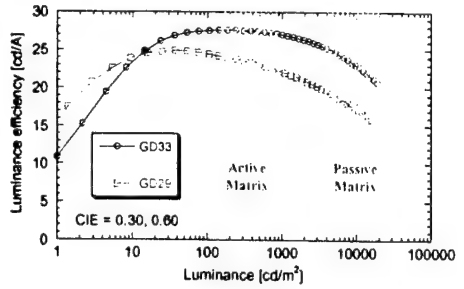

Green PHOLED Lifetime Performance at L_0=600nits (room temperature)

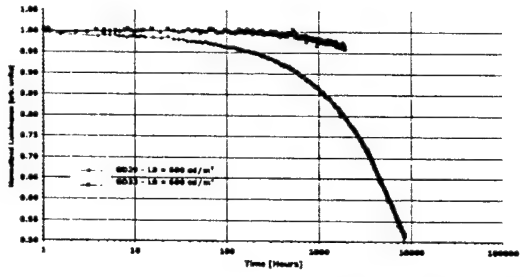

Green PHOLED lifetime

GD33 vs GD29 at 70°C, L_0=600nits

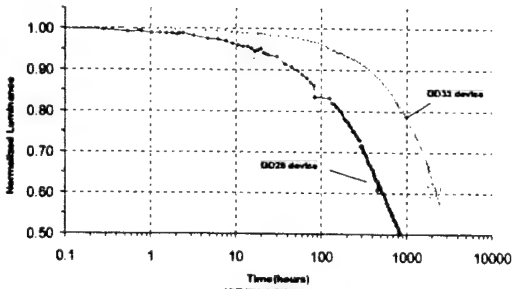

Green PHOLED Performance

Shelf and Driven Lifetest at t=7,300 hours

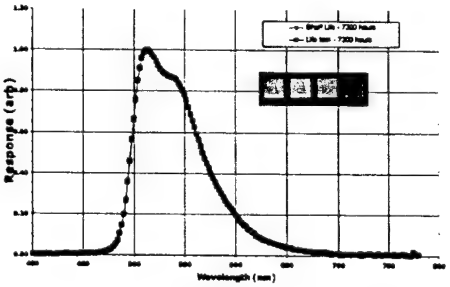

Emission Layer Design Optimization

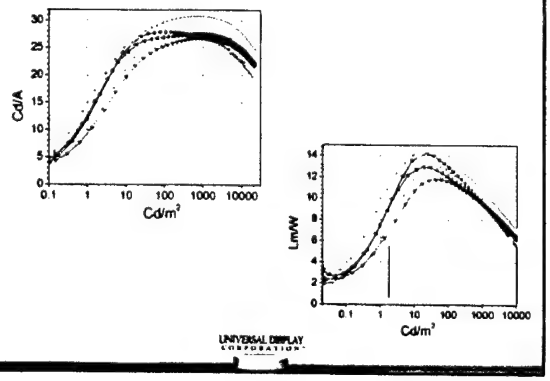

Lifetime @ 70°C, 600 nits

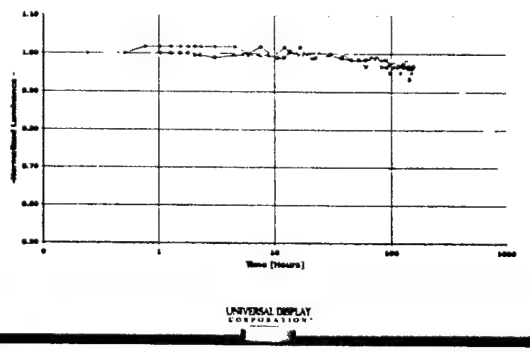

Status of Green PHOLED Lifetime

- Lifetime-Efficiency Improved
  - From 20 cd/A, 10,000 hrs at 600 nits
    - 800 hours at 60 C, 600 nits
  - To 30 cd/A, 30,000 hrs at 600 nits
    - 3,000 hours at 60 C, 600 nits
- Ongoing work
  - Further device optimization of Gen 2
  - Building on materials development for long lifetime at RT and Elevated T, Gen 3 Under development

UNIVERSAL DISPLAY CORPORATION

RED PHOLED Lifetime: Program Start

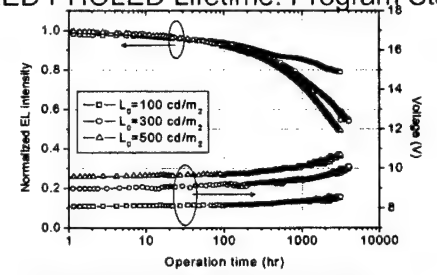

0-3000 hrs	100 cd/m²	300 cd/m²	500 cd/m²
% retained	79	59	50
dV/dT(mV/hr)	0.16	0.26	0.36

UNIVERSAL DISPLAY CORPORATION

RD07 PHOLED Performance

CIE: (0.65,0.35)

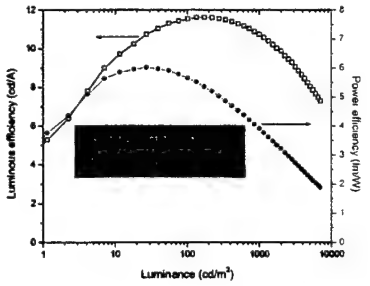

UNIVERSAL DISPLAY CORPORATION

Red PHOLED™ Performance Summary

Dopant	CIE x	CIE y	Max EQE % (@cd/m²)	Max cd/A (@cd/m²)	Max Lm/W (@cd/m²)
RD81	0.570	0.430	14.5 (200)	29 (200)	13 (100)
RD06	0.595	0.401	14.2 (200)	28 (200)	12 (50)
b	0.609	0.387	10 (400)	17.5 (400)	6.8 (70)
RD61	0.611	0.384	13.7 (400)	24.2 (400)	9.4 (55)
d	0.614	0.382	8.5 (800)	14 (800)	4.7 (70)
e	0.637	0.358	9.8 (80)	11.8 (80)	5.4 (12)
RD07	0.649	0.347	12.5 (300)	14 (300)	6.3 (45)
g	0.653	0.342	10.5 (60)	11.4 (60)	4.9 (10)
h	0.698	0.298	8.3 (10)	3.1 (10)	1.4 (2)

UNIVERSAL DISPLAY CORPORATION

Red PHOLED Performance

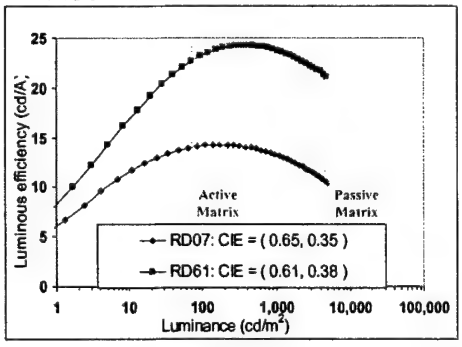

UNIVERSAL DISPLAY CORPORATION

RED PHOLED: Lifetime Progress By Manufacturing Scale-up of Materials

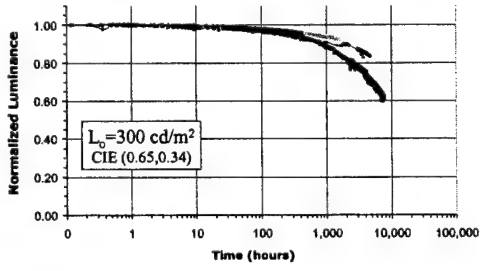

UNIVERSAL DISPLAY CORPORATION

Red PHOLED Lifetime Performance at L_0=300nits (room temperature)

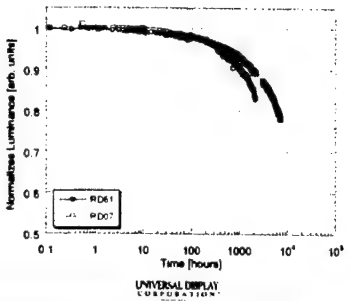

Red PHOLED Lifetime Performance at L_0=300nits (room temperature)

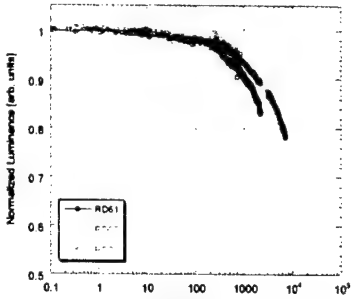

RD07 Red PHOLED, 14 cd/A

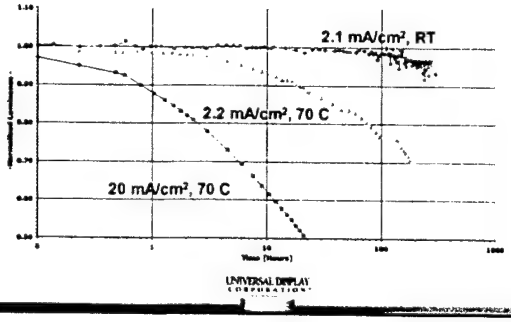

RD07 PHOLED Performance

Spectral Response

Shelf and Driven Lifetest at t=7,800 hours

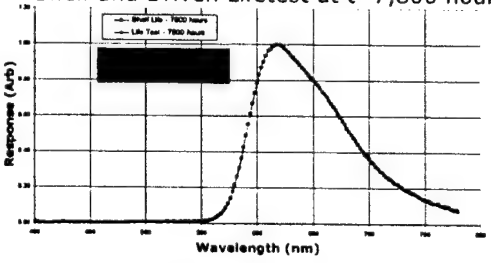

Status of Red PHOLED Lifetime

- Lifetime-Efficiency Improved
  - From 11 cd/A, 15,000 hrs at 300 nits
    - ?
  - To 14 cd/A, 25,000 hrs at 300 nits
    - 3,000 hours at 70 C, 300 nits
- Ongoing work
  - Further device optimization of Gen 2
  - Building on materials development for long lifetime at RT and Elevated T, Gen 3 Under development

High Efficiency Blue PHOLED

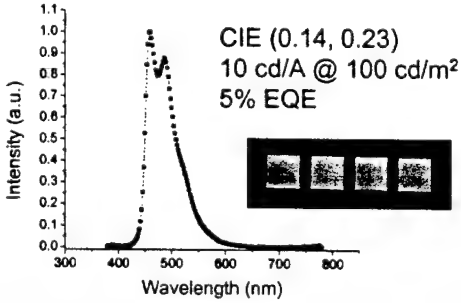

CIE (0.14, 0.23)

10 cd/A @ 100 cd/m²

5% EQE

Blue PHOLED: Very Recent Progress

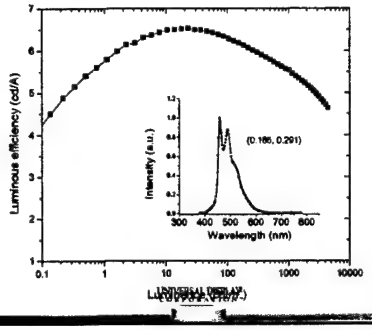

Blue PHOLED: Very Recent Progress

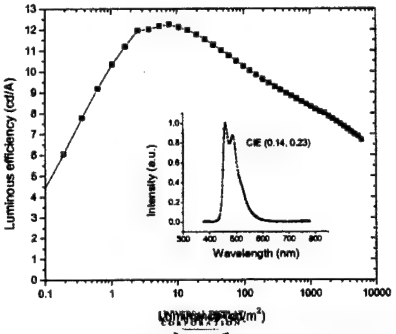

Blue PHOLED: Very Recent Progress

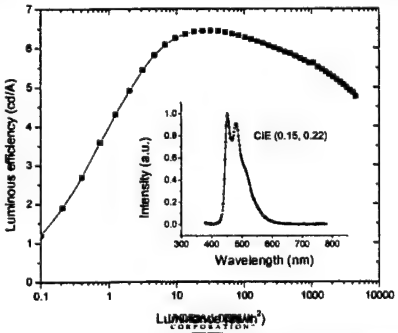

Blue PHOLED: Lifetime Understanding

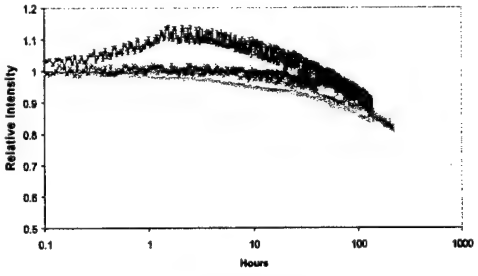

Phosphorescent OLED Status

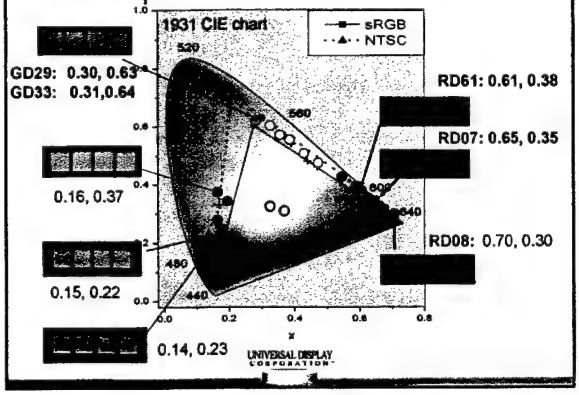

PHOLED Lifetime Progress

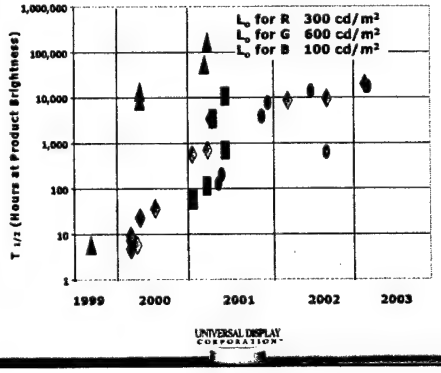

Summary

- **Development of blue continues**
  - New deep blue dopants and wide gap hosts
  - New charge injection layers for blue PHOLED
  - Improved understanding of blue reliability
- **Progress in red and green**
  - New dopants with higher efficiencies, long lifetimes
- **New OLED packaging technologies promising**
  - Ongoing investigation of alternative packaging technologies

UNIVERSAL DISPLAY CORPORATION

Samsung SDI
2.2" Full-color Display using UDC PHOLEDs

Diagonal size	2.2inch
No. of pixels	176 (H) x RGB x 220 (V)
Pixel pitch(mm)	86 x 198
Resolution	128 ppi
Panel size (mm^2)	41.976(H) x 56.232(V)
Aperture ratio	약 32%
휘도(w/o polarizer)	200 Cd/m^2 Peak : >300 Cd/m^2
White 좌표	(0.31,0.32)

➢**REPORTED SID 2002**

UNIVERSAL DISPLAY CORPORATION

Current Requirement for Fluorescent RGB

	Red color	Green color	Blue color
Panel brightness (cd/m^2)	90	150	60
Original OLED brightness (cd/m^2)	628	1047	419
Current density (mA/cm^2)	26.38	44.0	10.45
Current requirement (μA)	5.12	8.5	2.03

- All calculation is based on peak brightness 300 cd/m^2, sub-pixel size 171x264 μm.

UNIVERSAL DISPLAY CORPORATION AU Optronics, UDC SID 2003

Red PHOLED Performance

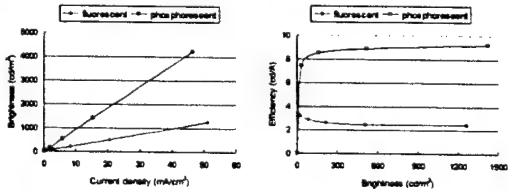

- Much higher efficiency was obtained in the case of red PHOLED.
- Under same brightness, less current is needed for PHOLED.

UNIVERSAL DISPLAY CORPORATION AU Optronics, UDC SID 2003

a-Si AMOLED Development in AUO

	Cebit (3/15/02')	SEMI EXPO(5/27/02')	LCD/PDP 2002(10/30/02')	SID 2003	4" LCD
Max. brightness	38	63	300	300	162
CIE	(0.28, 0.33)	(0.27, 0.33)	(0.29, 0.34)	(0.33, 0.32)	-
Contrast	15	50	>250	>300	150
Power consumption (Video mode)	250 mW	400 mW	1.15 W	670mW	1.8 W (backlight)

LCD driver IC

Red fluorescent material *Red phosphorescent applied*

UNIVERSAL DISPLAY CORPORATION AU Optronics, UDC SID 2003

Power Consumption

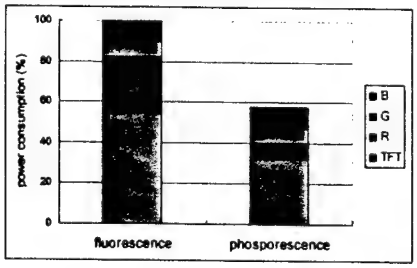

UNIVERSAL DISPLAY CORPORATION AU Optronics, UDC SID 2003

Specifications of a-Si AMOLED Display

Item	Spec
Resolution Wxh (dot	160(RGB) x 234
Dimension WxHXD (mm)	37 96.0 x 76.0 x 1.5
Pixel size (mm) x mm)	0.171 (xRGB) x 0.264
Color saturation	65.3 %
Pixel arrangement	delta
Response time (ms)	< 5
View angle	> 170 degree
Color	262K (6 bit)
Max brightness (cd/m²)	300
Operation voltage (V)	< 15
Contrast ratio	> 300 : 1
Module thickness	1.5 mm
Weight (g)	22

UNIVERSAL DISPLAY CORPORATION **AU Optronics, UDC SID 2003**

The OLED Landscape

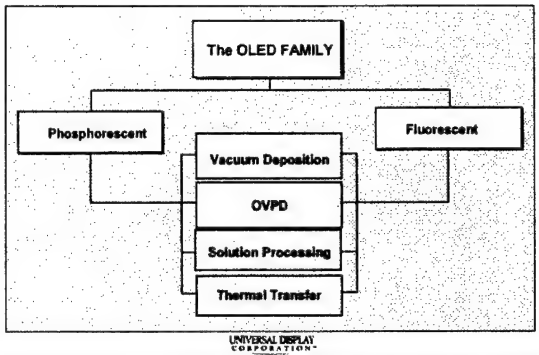

UNIVERSAL DISPLAY CORPORATION

THANKS!

- To our university collaborators
- To the entire UDC Team

- And of course thanks to you for your support (interest and $$)

UNIVERSAL DISPLAY CORPORATION

Near Field Scanning Optical Microscopy Studies of TOLED Degradation

Paul F. Barbara
Doo Young Kim
Jason McNeill
Jiangeng Xue
Stephen R. Forrest
Mark E. Thompson

Near Field Scanning Optical Microscope

- 50 nm spatial resolution
- optical and topographic image
- fiber probe is movable electrode

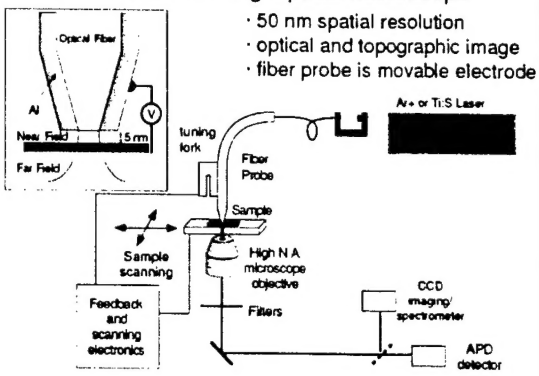

Organic Thin Films From Molecules to Materials Structure/Properties/Function

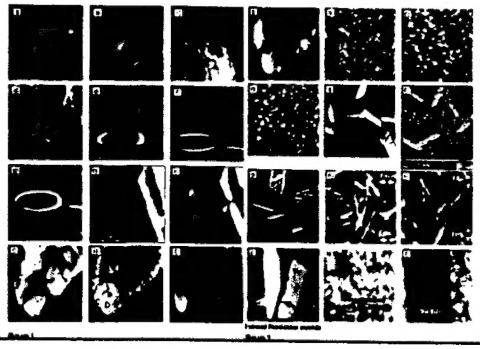

ION TRAP FROM SHARP ELECTRODE

Contour plot of probe potential

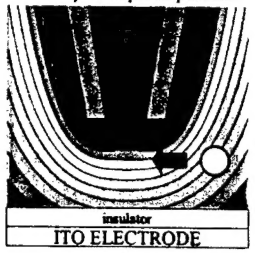

○ = HOLE POLARON (RADICAL CATION)

} ORGANIC THIN-FILM

Trap holds about 100 charges

Principles of field-induced fluorescence modulation NSOM

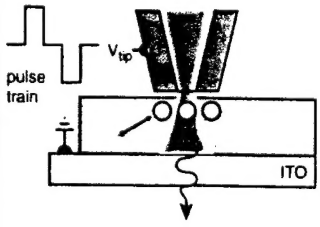

- Scan near field probe on sample
- Photo-Carrier injection at ITO
- Carrier detection by fluorescence quenching
- **Apply voltage to attract or repel carriers**

More modulation with insulating layer!

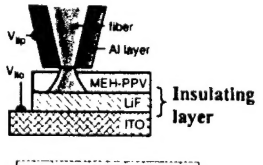

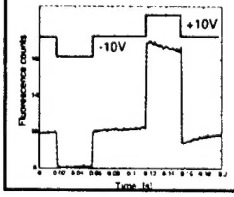

- More modulation: **70%**
- Indicates more carriers
- ~100 hole polarons
- ~1 charge per polymer molecule
- Recombination at ITO is blocked

TOLED: Transparent Organic LED

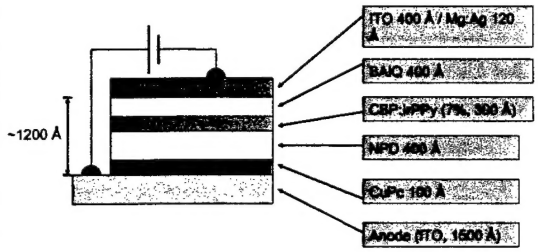

Experimental Setup for TOLED Study

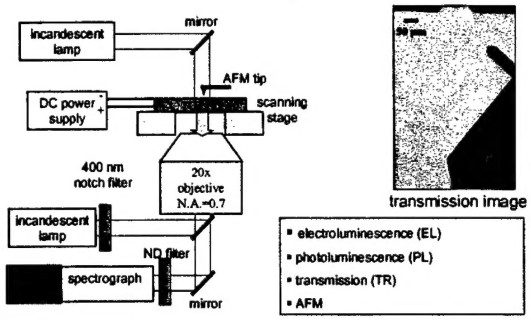

Forrest, Thompson, Barbara *and co-workers J. Appl. Phys.*, 2001

Correlated AFM and EL at Early Stages of Degradation

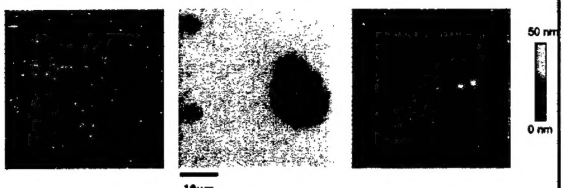

- Surface mapped by AFM before running device (RMS roughness = 3 nm).
- No initial topographic features/defects exist in the dark spot areas.
- No topographic differences between EL dark spot and EL active areas.
- PL and TR images are featureless, no difference between EL active and inactive areas

Forrest, Thompson, Barbara *and co-workers J. Appl. Phys.*, 2001

Changes in Devices After Extended Time Periods

92 h in ambient, run at 1.5 mA for 58 h

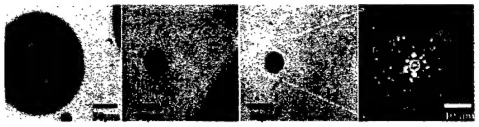

92 h in ambient, no applied bias

analogous degradation processes in stressed and control devices

NSOM of burned-out device

- wrinkles and specks
- lower overall PHOSPHORESCENCE
- some specks are fluorescent

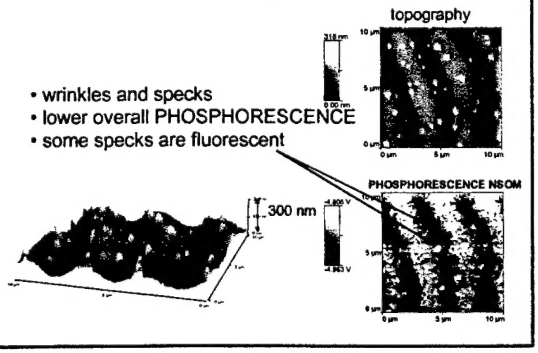

Thermal Breakdown

- Device temperature increases to above organic sublimation point in places due to resistive heating
- Organics boil out of pinholes in top electrode
- Leave behind volcano-like specks of organics

Topography and PHOSPHORESCENCE of Bum

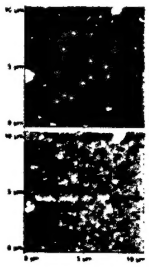

Device A, spent

- Bumps a few microns wide, 3-5 nm tall.
- Same PHOSPHORESCENCE intensity over bumps (within 5%)

"Photobleaching" depends on O_2

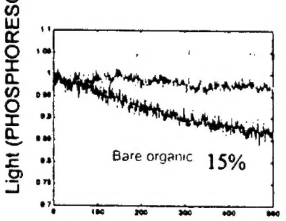

Photobleaching increases in presence of O2

Top electrode blocks O2

Larger Spots

Device B, exposed to air

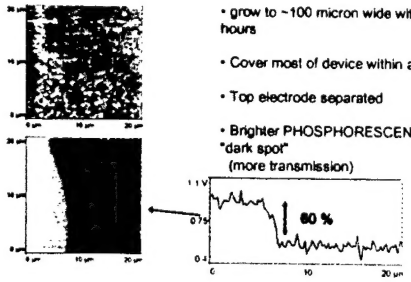

- Spontaneously form upon exposure to air (not all devices form spots on exposure)
- Grow out from pinhole, few nm tall
- grow to ~100 micron wide within 24 hours
- Cover most of device within a few days
- Top electrode separated
- Brighter PHOSPHORESCENCE inside "dark spot" (more transmission)

Induced Dark Spots

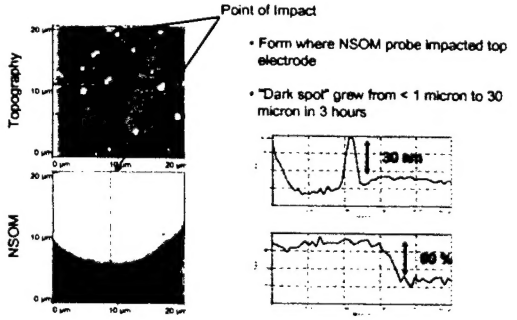

- Form where NSOM probe impacted top electrode
- "Dark spot" grew from < 1 micron to 30 micron in 3 hours

Light Quenched by Charge Carriers

- 3.2% quenching
- quenching increases with excitation intensity (photodriven)
- quenching increases with exposure time (photodriven)
- similar, but less quenching for areas with top electrode (0.5%)

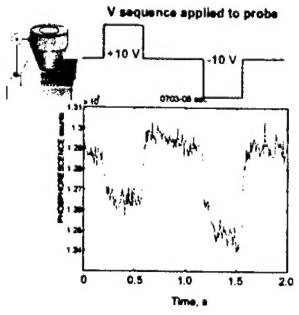

Key Concept – Hole Polaron

- Hole Polaron is a localized positive charge on the polymer
- Hole Polarons quench or thermalize singlet excitons by energy and/or electron transfer
- Hole Polarons and Singlet Excitons are Funneled to low energy sites in organic materials

Tetracene doped with pentacene

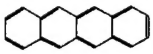

- Crystalline solid

Tetracene Doped with Pentacene

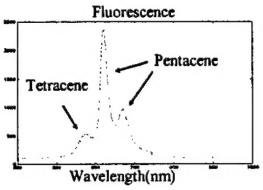

- 100 ppm pentacene in tetracene
- Efficient energy transfer from tetracene to pentacene

Field-modulation NSOM

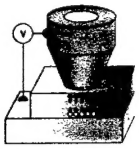

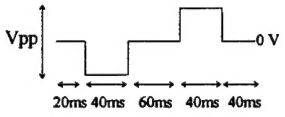

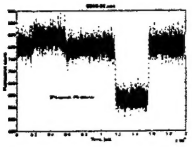

Vpp = 5V, quench = 27%

- Efficient quenching by polarons
- Instrument-limited response
- Calculated response time: subpicosecond to picosecond

Fluorescence Spectrum Changes with Voltage

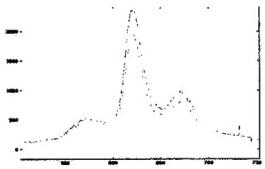

Wavelength (nm)

Tetracene fluorescence: small effect (~1%)

Pentacene fluorescence: large effect (20%)

Difference Spectrum

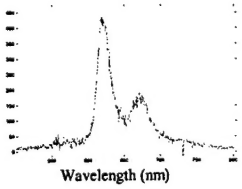

Wavelength (nm)

- Only pentacene fluorescence is quenched.
- Holes trapped on pentacene

Conclusions

- Exposure to air causes the formation of "dark spots" which are regions where separation of the top electrode occurs.
- The presence of O2 and light or electrical excitation in the organic layers can also lead to destruction of the organic semiconductor material (photobleaching).
- Dark spots were seen to grow from mechanically damaged spot
- Brighter PHOSPHORESCENCE inside "dark spot" indicates oxidation of metallic electrode